ON THE ROLE OF UNCERTAINTIES IN THE SEISMIC RISK ASSESSMENT OF HISTORIC MASONRY TOWERS

Dissertation

submitted to and approved by the

Department of Architecture, Civil Engineering and Environmental Sciences
University of Braunschweig – Institute of Technology

and the

Department of Civil and Environmental Engineering
University of Florence

in candidacy for the degree of a
Doktor-Ingenieurin (Dr.-Ing.) /
Dottore di Ricerca in Civil and Environmental Engineering[*)]

by
Silvia Monchetti
born 29/05/1987
from Firenze, Italy

Submitted on	20 February, 2018
Oral examination on	08 May, 2018
Professorial advisors	Prof. Klaus Thiele
	Prof. Gianni Bartoli

2018

*) Either the German or the Italian form of the title may be used.

To my dear grandfather Angiolo,
who always wondered
what was the aim of all that study.

ON THE ROLE OF UNCERTAINTIES IN THE SESIMC RISK ASSESSMENT OF HISTORIC MASONRY TOWERS

"we have not succeeded in answering all of our problems.
The answers we have found only serve
to raise a whole set of new questions.
In some ways we feel we are as confused as ever
but we believe we are confused on a higher level
and about more important things"

Posted outside the mathematics reading room,
Tromsø University (Norway)

ACKNOWLEDGMENTS

I could not have accomplished this research without the encouragement, guidance and support of Prof. Gianni Bartoli, Prof. Klaus Thiele, Prof. Michele Betti and Eng. Antonino Maria Marra. Thank you for the confidence. I could not have better mentors.

Thanks to Francesco, my soul mate, for the unconditional support and for the unceasing patience.

Thanks to my family, mamma Laura and babbo Oliviero in particular, who always believe in me.

Thanks to Ilaria. Since many years, she finds always the right words!

Thanks to Laura, *my little black cloud*, and to Giulia, *who has always a funny drama*, for each hilarious adventure shared together. Thanks to Davide, Tommaso, Giovanna, Sara, Laura, Luca, Lorenzo, Antonio, Francesco, Chiara and Chiara, the others wonderful *partners in crime.*

Thanks to Braunschweig for the unexpected rains and uncommon sunny days.

PhD is a journey. Keep calm and enjoy.

ABSTRACT

The research activity developed in the present work achieved both technical and scientific results on the seismic risk assessment of masonry towers. It provided semi empirical formulations for the main frequency estimation based on a wide database of historic masonry towers and a novel framework for the seismic risk assessment starting from the Bayesian model updating using dynamic experimental data.

The recent Italian earthquakes have dramatically highlighted the vulnerability of historic masonry constructions and the need to improve the knowledge on their seismic response. Due to this fact, the challenging issue of obtaining a reliable structural model has become increasingly relevant to the scientific community, promoting the employment of sophisticated tools of analysis and the need of numerical models to be set up. However, the significant lack of knowledge on historical structures (*e.g.*, material properties, geometry, construction techniques, boundary conditions), still makes their numerical modelling difficult. The knowledge of the seismic response of this structural typology, taking into account uncertain parameters, represents a critical issue and the main scientific question to which this work aimed to answer.

The framework proposed in this research started with the Finite Element (FE) model updating of masonry towers through Bayesian approach; the prior distribution of relevant uncertain model parameters was converted into the posterior one by using experimental dynamic data. Nonlinear static analyses were employed to estimate the uncertainties in the seismic response of masonry towers. Taking into account both the modelling and the measurement uncertainties, fragility curves were defined related to different towers damage levels. Eventually, the seismic hazard was considered thus leading to the seismic risk assessment of masonry towers.

The idea of this work started from the necessity of obtaining a better awareness of the uncertainties involved in the seismic capacity prediction of historic constructions, and their effect on the overall reliability.

Although the proposed results are based on the application to a real case study, the procedure may be used for other similar structures and may represent an effective and alternative tool for the seismic risk quantification of historic masonry constructions.

ZUSAMMENFASSUNG

Die vorliegende Doktorarbeit stellt teilempirische Formulierungen zur Verfügung, die mittels einer umfangreichen Datenbasis von historischen Türmen aus Mauerwerk und einer neuen auf dem Modell von Bayes basierenden Methode das Erbebenrisikos unter Nutzung der dynamischen Messwerte bewertet.

Der Bedarf nach einer solchen verbesserten Bewertung der Gefährdung von historischen Mauerwerkstürmen zeigte sich insbesondere nach den jüngsten seismischen Ereignisse Italiens bei der Frage der Beurteilung der Gefährdung der Türme der Toskana, z.B. in San Gimignano. Die wissenschaftliche Aufgabe besteht darin, das in vorhandenen Datenbanken vorhandene, aber in technischer Hinsicht begrenzte Wissen zum Strukturverhalten der Türme mit Hilfe eines Modells für eine möglichst zuverlässige Vorhersage der Strukturantwort zu verwenden. Der noch große Mangel an Kenntnissen über historische Baustrukturen, ihrer baustofflichen Eigenschaften, Geometrie, Bautechniken und Randbedingungen ermöglicht bisher keine ausreichende Beurteilung. Die Erforschung der seismischen Reaktion dieser Strukturtypologie unter Berücksichtigung der unbestimmten Parameter stellt das entscheidende Thema und die hauptwissenschaftliche Frage dar, welche diese Arbeit beantworten möchte.

Das in dieser Forschungsarbeit vorgestellte Framework beruht auf einem Finite Element Modell (FEM) der Türme aus Mauerwerk, dessen Parameter durch die *Bayes'sche Methode* an Datenbankangaben kalibriert werden. Aus einer auf statischen Überlegungen basierenden Priori-Verteilung von wesentlichen unbestimmten Modell-Parametern wird dabei unter Verwendung von experimentell ermittelten Daten eine Posteriori- Verteilung ermittelt. Die Unsicherheit der daraus folgenden Berechnungsergebnisse der Erdbebenantwort wurde mit Hilfe nichtlinearer statischer Auswertung bewertet. Aus den ermittelten Unsicherheiten sowohl der Modellierungsparameter als auch der zugrunde liegenden Messungen wurden „fragility curves" bezüglich der verschiedenen Schadenniveaus von Türmen definiert. Mit der Hilfe dieser Kurven wurde schließlich die Erdbebengefährdung für Türme aus Mauerwerk beurteilt.

Die in dieser Arbeit vorgestellte Methode verbessert die Beurteilung von seismischer Gefährdungseinschätzung, da eine Bewertung der in die Einschätzung einfließenden Unsicherheiten für die Ergebnisse möglich ist. Auch wenn die Methode am Beispiel der historischen Mauerwerkstürme durchgeführt wurde, ist sie für andere Bauwerke in gleichem Maße anwendbar..

Table of contents

Chapter 1

Introduction

1.1. Research topic and motivations

The frequency of the recent seismic events which hit Italy and the intensity of some of them (Abruzzo 2009, Emilia Romagna 2012, Central Italy 2016) have again highlighted the need of improving the knowledge of the seismic response of existing structures. The relevance of the problem, especially in Italy, derives from the significant number of non-engineered masonry constructions, including historic masonry buildings and monuments. These structures were built to withstand only vertical loads and, in many cases, cannot guarantee sufficient seismic resistance. Indeed, during the recent earthquakes a large number of fatalities and injuries were reported in old masonry structures showing the need of preserving their value and their content. In the last years, scientific community is increasingly focusing on the seismic assessment of historic masonry buildings underlining the weak points of the cultural heritage: the difficulties related to the lack of knowledge in the building process, the uncertainties in the structural parameters definition (material properties, geometry, boundary conditions, etc.) and the limitations of the different seismic analyses.

Among the typologies of historic monumental buildings, masonry towers embody an important heritage to preserve. Indeed, these structures represent a hallmark of many Italian city centres and are widely diffused also in the European territory. Due to the high slenderness and mass, the seismic risk assessment of masonry towers is a growing concern, as also demonstrated in the

figures below (Figure 1.1) which show the partial or total collapse of some towers during the recent Italian earthquakes.

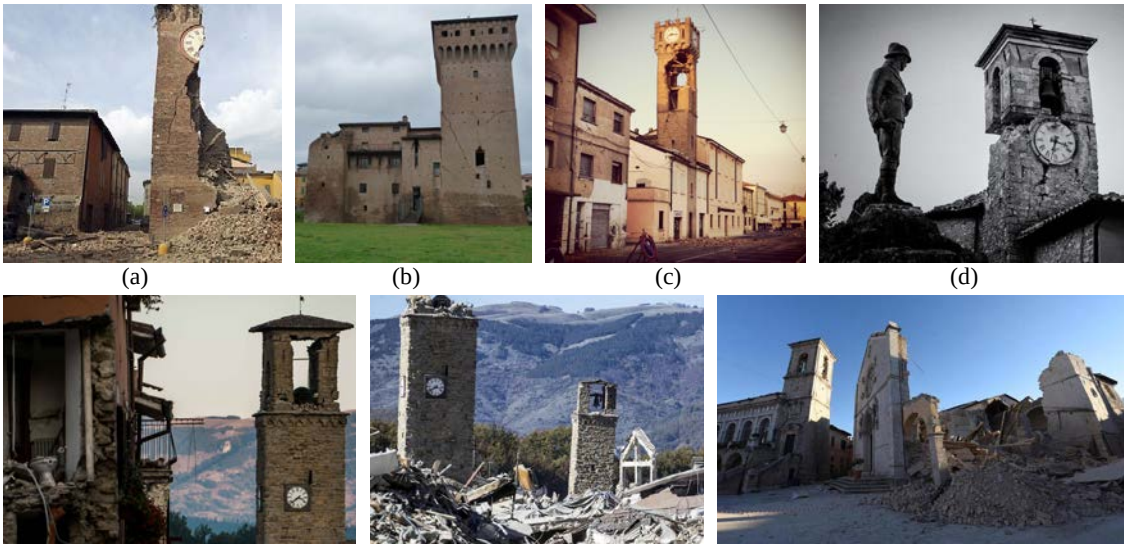

Figure 1.1 - Damages of masonry structures during the recent Italian earthquakes: a) Civic tower and b) Estense castle of Finale Emilia (MO), May 2012; c) Clock tower of Novi di Modena (MO), May 2012; d) Bell tower of San Pellegrino di Norcia (PG), August 2016; e) Civic tower of Amatrice (RI), August 2016; f) City centre of Amatrice (RI), October 2016; g) San Benedetto church of Norcia (PG), October 2016.

The idea which has motivated this work was the necessity of obtaining a better awareness on the uncertainties involved in the seismic risk assessment process of historic masonry towers and their effect on the overall reliability. This work takes advantage of the studies developed on the towers of San Gimignano (Italy) during the RiSEM project (Seismic Risk of Historic Buildings, 2011-2013) which was aimed at developing and testing expeditious and innovative methodologies (*i.e.* without direct contact with the masonry construction) to assess the structural properties needed for the seismic risk assessment. The availability of both geometric data and experimental measurements has made the towers of San Gimignano (Figure 1.2) a significant case study for the development of this research project.

Figure 1.2 – San Gimignano (SI), Tuscany, Italy.

1.2. Outline of the work

The present dissertation is organized in seven chapters; for each of them, a brief introduction is here reported.

Chapter 2 describes the scientific background of this work through an analysis on the main involved topics. It starts with a review of the seismic risk assessment procedures for masonry buildings and the case studies on historic towers are here analysed in depth. In addition, the Bayesian approach is carefully treated and some of its application in civil engineering field are reported. This chapter ends with a discussion on the open issues underlying the innovative contribution of this work.

In *Chapter 3*, a wide database from the scientific literature is collected, summing up the mechanic and geometric characteristics of 43 different masonry towers together with the experimental measurements of natural frequencies. The database is used to identify the main physical parameters influencing the dynamic behaviour of slender masonry towers and to propose semi empirical formulations for estimating the main frequency of slender masonry towers accounting for different level of knowledge on the structure.

Chapter 4 reports the proposed methodology for the FE-Model updating of masonry towers based on the Bayesian approach by using experimental measurements of natural periods. The identification of the main physical parameters influencing the dynamic behaviour of slender masonry towers, developed in the previous chapter, is herein employed to select the parameters to update. The procedure gives an alternative way to define the key parameters of the FE-Model taking into account the uncertainties involved in the measurement of the natural frequencies as well as the uncertainties inherent in the modelling of the linear dynamic behaviour of the structure. The role played by the different assumptions (prior distribution, measurement errors, modelling errors) is evaluated through the sensitivity analyses of the posterior distribution.

In *Chapter 5*, a novel approach for the definition of the seismic fragility curves for masonry towers is proposed. The procedure is based on nonlinear static analyses of a three-dimensional FE-Model. A preliminary sensitivity analyses have allowed to point out the parameters affecting the seismic response assessment of the structure. The fragility curves are herein derived by calculating the probability of failure for each considered seismic demand, in terms of peak-ground acceleration (PGA). The procedure includes the Bayesian FE-Model updating, developed in the previous chapter, and the uncertainties related to the mechanical parameters which characterized the nonlinear behaviour of the masonry.

Using the results of the previous chapters, the comprehensive evaluation of the seismic risk of this structural typology is discussed in *Chapter 6*. In this manner, the assessment of the seismic

fragility curves, which include the effect of the uncertain key structural parameters, is herein connected to the variability of the seismic hazard, considering the occurrence probability of an earthquake in a certain geographic area.

Eventually, some conclusions and future developments are reported at the end of the present work.

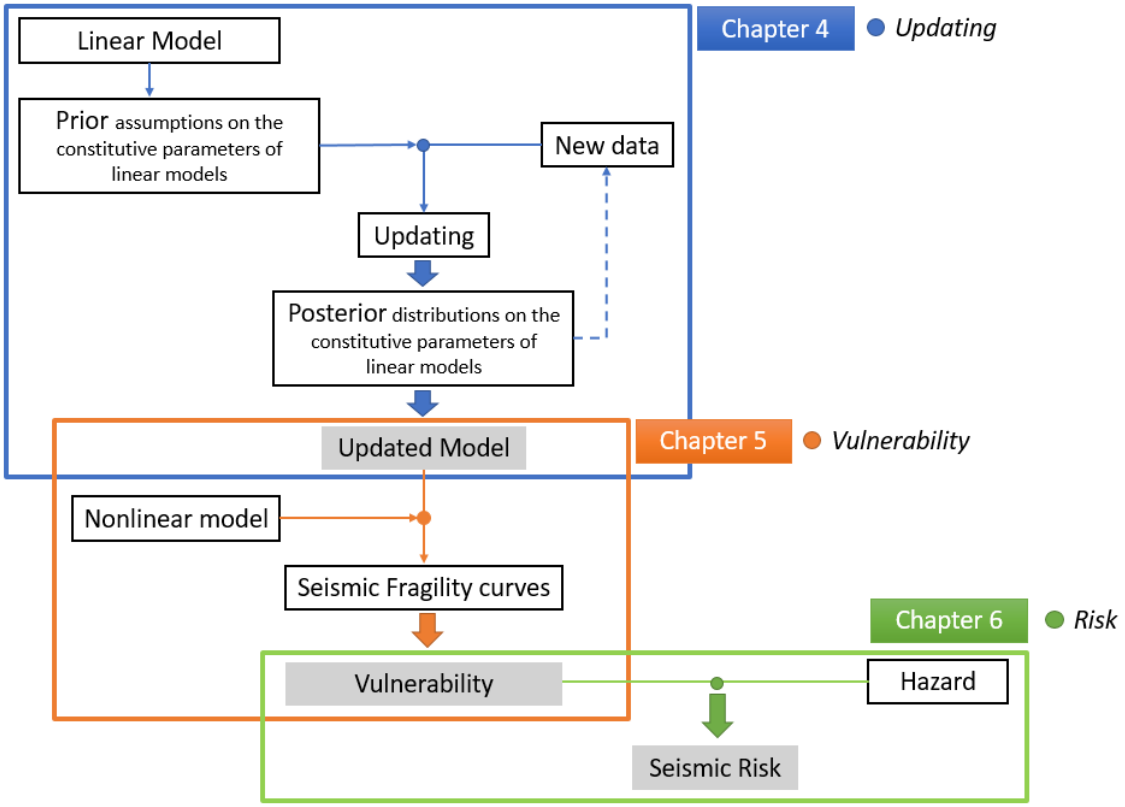

Figure 1.3 - Scheme of the thesis.

1.3. Contributions of the work

The research activity developed in the present work provides a contribution in the historic towers preservation and, more in general, in the seismic engineering research field. The knowledge of the seismic response of this structural typology, accounting for the uncertain key parameters, represents a critical issue and the main scientific question to which this work aims to answer. Although many research works are dedicated to the seismic risk assessment of slender masonry towers and many others to the application of Bayesian approach in civil engineering, a specific research which combines these two fields is still missing. In this respect, the extensive review of the scientific literature (Chapter 2) has allowed to draw the main objective which the present dissertation aims to reach: the definition of a general procedure for the seismic risk assessment of

masonry towers, starting from the Bayesian model updating using dynamic experimental data, in order to underline the role of the uncertainties in each step of the seismic risk framework.
In detail, the contents of this dissertation can be summarized as follow:

- *Wide database* containing experimental data, mechanic and geometric characteristics of different masonry towers, useful to identify the main physical parameters influencing their dynamic behaviour. This database can represent the starting point for further comparisons and qualitative analyses.
- *Novel formulations for a more reliable prediction of the main frequency of masonry towers* accounting for different level of knowledge on the structure. The proposed formulations are derived by manipulating the theoretical expression for a simple cantilever beam with a hollow square section and by retaining parameters with a clear physical soundness. If compared with the prediction capability of other existent formulations, it leads to significant improvement.
- *Bayesian FE-Model updating*. The procedure provides a useful and alternative way to the usual approach in the use of experimental dynamic data, in order to improve the knowledge on the numerical model.
- *Definition of the robust seismic fragility curves* through a procedure based on nonlinear static analyses of a three-dimensional FE-Model which allows to consider the effect of the uncertain parameters involved in the modelling of the masonry in addition to those updated through a Bayesian approach.
- *General framework for the seismic risk assessment of masonry towers* which completes the course of this thesis and adds the variability of the seismic hazard to the structural key parameters already considered as uncertain.

The results are herein presented through the application to real case studies, however the proposed procedures are general and easily applicable to similar structures, due to this fact, other researchers may benefit from this work.
This thesis work required numerous hypotheses that represent one of the possible choices among many other valid alternatives. However, the main purpose of the work was to provide a general procedure for masonry towers with the aim to improve their seismic assessment, both including different sources of uncertainties and all the available information, in a probabilistic framework.
Therefore, making choices was necessary to complete the procedure, despite knowing that those assumptions were not the only one possible.

Chapter 2

State of the art

The conservation, the monitoring and the structural safety assessment of historic masonry buildings pose important challenges to the scientific community. Nevertheless, the uncertainties involved in assessment process still make these goals difficult.
Due to this fact, the present dissertation deals with two main topics, which are introduced in this chapter through a review of the scientific literature. The first is related to the seismic risk assessment of historic masonry constructions, with particular reference to the masonry towers; the second regards the application of the Bayesian procedure as useful tool to improve the current knowledge of the system with all the available information.

2.1. Seismic risk assessment of cultural heritage

In recent years, the study of ordinary and monumental masonry buildings gained ever more attention on the part of researchers in the structural engineering field. Such increased interest is due, on the one hand, to the need to preserve the cultural heritage and, on the other, to the peculiar mechanical properties of these structures. Indeed, masonry buildings include a wide variety of structural arrangements which are often very complex and present widely varying mechanical characteristics. Moreover, these features depend on the constituent elements of the masonry and the employed building techniques [1]. Therefore, a comprehensive structural evaluation may be based on a deep knowledge of: the history of the structure and its evolution, the geometry and structural details, the cracking pattern and the construction techniques, the material properties and the global behaviour [2,3]. These information can be obtained through both in situ and laboratory experimental investigations [4,5] connected with structural analyses with adequate models [2,6–

8]. Nevertheless, the difficulties on inspections and on performing extensive and destructive experimentations for historic constructions, give rise to limited information on the constructive system and material properties.

The Italian Guidelines for seismic vulnerability assessment of cultural heritage [9] have taken into account these aspects, through the concept of knowledge level for monumental buildings and by associating, to the material properties, the confidence factors obtained with in situ tests and investigations. The above issues demonstrate the particular attention which must be devoted in modelling strategies of historic masonry constructions. Indeed, each monumental building has unique characteristics related to its construction phase, restorations and modifications occurred over time. Due to these facts, the study of monumental constructions requires specific attention in the understanding of their structural behaviour since both the building history and the difficulties in the acquisition of experimental data, produce several uncertainties in the model definition. In the scientific literature, a significant number of case studies have been proposed, which analyse the seismic behaviour of a wide range of historic masonry structures.

In this instance, Lourenço [10] and Romera *et al.* [11] analyse two churches (Church of Saint Christ in Outerio, Portugal, and Basilica of Pilar in Zaragoza, Spain, respectively) underling the effective information provided by suitable numerical models of reproducing structural pathologies, for understanding the existing damages, and check the efficiency of historic restoration. With the same aim, Betti and Vignoli [12] analyse an Italian Romanesque church. Taliercio and Binda [13] take advantage from the results of in situ topographical and mechanical investigations to build a global finite element model of the Basilica of San Vitale in Ravenna (Italy) considering the diffused cracking of the church surveyed. This latter aspect is studied also in Betti *et al.* [14] with specific reference to a historic Italian palace, providing an interpretation of the manifested damage in the palace, and using the numerical output to design an extensive in situ investigation on the building. The results of experimental campaign on old masonry buildings is used also in Betti *et al.* [2], which focus the attention on some aspects of numerical modelling, thus providing a contribution in the seismic analyses of historic buildings, by using two case studies: the masonry church in Inpruneta (Tuscany, Italy) and an ordinary building in Fivizzano (Lunigiana, Italy).

Besides churches and palaces, recent years have seen increasing interest in conducting vulnerability analyses on slender masonry structures, such as civic towers, bell towers and similar structures [15–19]. As a matter of fact, these structures have revealed their great vulnerability during the last Italian seismic events, as reported in [20,21]. Due to both these facts and the widespread of these buildings on the Italian (and European) territory, their investigation and conservation has become a heightening concern, as is reflected by growing research and

experimentation on this topic. Several examples of these researches are shown in Table 2.1, where the content of the studies is classified in three levels: collection of experimental data, definition of numerical models and analyses typologies.

Specifically, the experimental campaigns, composed of both *in situ* and laboratory tests, are performed to assess the global structural behaviour and the local masonry characteristics. Due to the low invasiveness with the structures and due to the particular sensitivity of masonry towers to ambient excitations (wind, traffic, swinging of the bell, earthquakes, etc.), the dynamic identification is confirmed the most used experimental technique. Indeed, only in a few studies (indicated in Table 2.1 as "other") different types of experimental data are acquired (*e.g.* flat-jack tests, dynamic tests, sonic pulse velocity tests, thermography, etc.). In any case, the experimental data are aimed at tuning a finite element model to be used to assess the vulnerability of the tower. In this respect, the scientific literature shows a great variability of both the employed numerical model and the typologies of analyses. These assumptions may have relevant effects on the structural response, making necessary careful assessments and comparisons among the most influencing aspects. In this respect, Salvatore *et al.* [22] report a study on the collapse of a masonry tower subjected to earthquake loadings and propose a comparison between analytical and numerical model, which reveals a good agreement between the behaviour of the tower considered as a cantilever beam and the tower represented through a three-dimensional (3D) model. Casolo *et al.* [23] shows a comparative seismic vulnerability analysis on ten masonry towers in the costal Po valley. These structures have some affinities in terms of location, mechanical properties and period of construction, but different geometries (*e.g.* slenderness, thickness of the walls, height, etc.). The research underlines the effect of the geometry on the seismic behaviour of such towers, making a comparison through full nonlinear dynamic analyses on 2D discretization model. The results suggest of developing more sophisticate analyses in order to improve the seismic vulnerability assessment of the towers. Indeed, despite the results of nonlinear static analyses provide reasonable synthetic prediction of the towers vulnerability, in general they are unable to give precise information on the failure mechanisms and the areas which undergo severe damages. Concerning the analyses typologies, the assessment of the effectiveness of nonlinear static procedure for slender masonry towers is developed by Pintucchi and Zani [24]. The research compares the pushover-based methods in predicting the seismic response through the results from a large number of time-history dynamic data. The results reveal that the key issue in the accuracy of pushover methods is the nature of the lateral load applied, by demonstrating that the displacement-controlled procedure is quite suitable in the case of masonry towers.

Table 2.1 – Researches on historic masonry towers, where: LSA indicates Linear Static Analysis, LDA Linear Dynamic Analysis, NSA and NDA Static and Dynamic Nonlinear analysis.

Ref.	Year	Experimental data		Numerical model		Analysis typologies				
		Dynamic Id.	Other	Beam/2D	3D	LSA	LDA	NSA	NDA	Other
[16]	1998			●	●				●	
[25]	2000	●(*)								
[26]	2000	●		●			●			
[22]	2003			●	●	●				
[27]	2006	●		●	●		●			
[28]	2006			●	●		●			
[29]	2007	●			●		●	●		
[30]	2008			●	●		●	●	●	
[31–41]	2001-15	●			●		●			
[42]	2010	●			●		●	●		
[43]	2009	●(*)			●		●			
[44]	2010	●	●		●		●			●
[23]	2012			●					●	
[45]	2013	●			●		●	●	●	
[46]	2013	●		●			●			
[47]	2013	●	●		●		●			
[45]	2013				●		●	●	●	
[48]	2014	●		●	●		●			
[24]	2014				●			●	●	
[20]	2014				●	●	●	●	●	
[49] [50]	2015	●(*)		●			●			
[51]	2017	●(*)			●		●			
[52]	2017	●		●			●			●
[53–56]	2014-2017	●(*)					●			

(*) Structural Health Monitoring

A recent research, developed by Marra *et al.* [57], proposed a comparison between incremental dynamic and nonlinear static analyses for seismic risk assessment of masonry towers. The analyses are carried out on a numerical model composed by discrete rigid blocks interacting through nonlinear elastic damageable interfaces. The results confirm that nonlinear static analyses (NSA), with both triangular and uniform load distributions, are conservative and suitable for design scopes.

Another interesting aspect, underlined from Table 2.1, is related to the growing applications of the Structural Heath Monitoring (SHM) approaches, based on long-term continuous dynamic monitoring, for historic masonry towers. The Gabbia tower in Mantua (Italy) [58], the San Pietro bell tower in Perugia (Italy) [54], the San Giovenale bell tower in Fossano [55](Italy), and the Asinelli tower in Bologna (Italy) [56], are the most recent examples. In this respect, the idea of using modal properties (main frequencies, mode shapes, mode shapes curvatures, etc.) both as an updating of the structural model and an indicator of damage occurrences seems promising.

These two aspects represent two important challenging issues in order to ensure the conservation of these constructions over time. As far as the model updating is concerned, all the considered studies aim to obtain a more reliable numerical model by taking advantage from the experimental data. The effect is twofold, first, the improvement of the knowledge on the dynamic behaviour of masonry towers and second, the calibration of the numerical model by reducing the discrepancy between the experimental data and the model output. It is worth noting that the result is a deterministic case (or more deterministic cases) which fulfils a regression method, *e.g.*, least square method. Since the uncertainties, deriving from both the low level of knowledge of historic building (*e.g.* the nonlinear behaviour of the masonry), and the forcing actions (*e.g.* earthquake), cannot be easily eliminated; statistical approaches can be useful of estimating the effect of the most important factors which affect the structural response. However, for monumental buildings, the wide variability in terms of construction techniques, geometric characteristics and material properties, makes a parametric evaluation difficult. Indeed, the existing researches are mainly focused on the analyses of case studies, without a comprehensive assessment in terms of sensitivity analyses.

Masonry towers, while maintaining wide variability on construction techniques and material properties, are characterized by similar geometric configuration, which allows to carry out more general considerations. In this respect, Casolo [16] proposes exhaustive parametric study aimed to show the main features determining the global seismic behaviour of the tower, considering the interaction between ground motion and masonry characteristics. More recently, Salvatori *et al.* [59] proposed a procedure for the probabilistic seismic performance of masonry tower, through a generic procedure based on NSA of a simplified model, realized by a geometrically nonlinear

Timoshenko beam with no-tensile and limited-compressive strengths, in which the effect of the uncertain structural parameters on the seismic vulnerability is represented through fragility curves for different levels of damage. Similar research is developed, for ordinary masonry buildings, by Rota *et al.* [60], by defining a methodology for the seismic vulnerability of masonry structures based on stochastic nonlinear analyses performed on a prototype building representative of a common structural typology in Italy. In this probabilistic framework, the introduction of available experimental data, in order to improve the accuracy of the numerical models, can represent a promising technique, not yet sufficiently developed for historic masonry towers.

2.2. Bayesian approach

The challenging problem of updating a structural model and its associated uncertainties by using dynamic response data, was originally presented by Collins *et al.*[61] but a more rigorous and comprehensive Bayesian framework for model updating is described by Beck and Katafygiotis [62]. They define the concept of system identification and show how to treat common difficulties that usually characterize the updating problem, such as ill-conditioning and lack of identification. The development of this approach derives from the necessity of combining all the available information: the experimental data, the theoretical models and the judgment based on experience. Moreover, in the last decades, the need to handle the modelling errors associated with the definition of the behaviour of a structure gives rise to an increasing interest of these approaches. These errors, in fact, can lead to uncertain accuracy in the predicted response.

Papadimitriou *et al.* [63] integrate the Bayesian probabilistic methodology for system identification with probabilistic structural analysis tools with the aim to update the assessment of the robust reliability based on dynamic data. They use the concept of robustness in order to indicate that modelling uncertainties are explicitly taken into account. In this methodology, the definition of the likelihood function is a crucial point and provides a measure of the plausibility of each model. In this respect, Beck and Au [64] proposes an adaptive Markov chain Monte Carlo simulation in order to obtain the posterior distribution by using a sampling approach rather than closed-form expression. With the same aim, Cheung and Beck [65] investigate Hybrid Monte Carlo method and show how can be used to solve higher-dimensional Bayesian model updating problems. The effectiveness of the method is evaluated through a simulated data example involving a ten-story building with 31 modal parameters to be updated. Another recent research, developed by Cheung and Bansal [66], introduced a stochastic simulation algorithm based on Gibbs sampler for Bayesian model updating of a linear dynamic system. The focus is the identification of a robust method and the assessment of its effectiveness through the application

to two numerical examples. These researches, as well as [67–69], aim to developed general theoretical procedures with ideal application cases. However, the application of the Bayesian framework has been extended to existing buildings, to reach different purposes: (i) the combination of different types of tests, (ii) the evaluation of existing structures, and (iii) the assessment of the uncertainties in fragility and reliability analyses. In this respect, the Bayesian methodology seems to represent a useful tool to overpass the difficulties of choosing the right value for certain parameters when experimental data are carried out and qualitative information are gathered. This aim is reached by Giannini *et al.* [70] for reinforced concrete structures, through the updating of the concrete strength, and by Ramos *et al.* [71] for the Saint Torcato church case, through the updating of the elastic modulus of the masonry. Moreover, the results of the Bayesian model updating are recently used also to calibrate confidence factors both for concrete reinforced structures, as proposed in Jalayer *et al.* [72], and for ordinary masonry buildings, as illustrated in Bracchi *et al.* [73]. In both cases, the methodology allows to update the knowledge on material properties and to compare these results by using several reference structures. These structures are assumed to be perfectly known and representing the real buildings to be assessed.

Generally speaking, the Bayesian model updating does not identify a single model but allows the updating of a probability distribution over a set of structural models, which includes the different sources of uncertainties involved in the assessment. The application of this procedure has been motivated by the necessity to improve the accuracy of the system response prediction against different actions (*e.g.* earthquake and wind loadings). Indeed, the employment of the Bayesian updating approach in a comprehensive probabilistic framework seems promising in order to quantify the different sources of uncertainties involved in the response prediction of a structure. This aspect is demonstrated by recent researches [74–80].

As an example, Mishra *et al.* [74] introduce a two-stage Bayesian updating approach in order to define the predictive distribution of the capacity of a roof-to-roof connection and finding the probability of failure against wind loading. Specifically, the results of the Bayesian updating are employed in the definition of the model with the aim to integrate the analytical capacity and the experimental results in order to quantify the uncertainty in the model predictions. Other similar researches are developed for seismic prediction of reinforced concrete structures [77] [75]. This aspect is underlined in Table 2.2, which reports the state of art herein introduced and reveals an increasing interest of the scientific community to the employment of these methodology in civil engineering fields. It is worth noting that, for masonry constructions the same comprehensive uncertainty assessment in fragility and reliability analyses with the use of the results of the Bayesian approach, cannot be found.

Table 2.2 – Probabilistic approach for civil engineering applications.

Ref.	Year	Application	Bayesian Model updating	Fragility curves assessment
[62–67,81,82]	1998-2017	Theoretical statistical framework on structural models	•	
[68]	2000	Structural health monitoring	•	
[60,76,83]	2006-16	Masonry buildings		•
[75]	2007	Reinforced concrete column	•	•
[78,84]	2008-13	Reinforced concrete buildings		•
[85,86]	2008-16	Historical monuments	•	
[77]	2009	Reinforced concrete bridges	•	•
[87]	2009	Geotechnical field	•	
[72,80,88,89]	2010-16	Reinforced concrete buildings	•	
[90]	2014	Masonry church	•	
[57,91]	2015-17	Historic masonry towers		•
[79]	2016	Masonry arch bridge		•
[73,92]	2016-17	Masonry buildings	•	
[74]	2017	Wooden structures (wind loading)	•	•

Chapter 3

On the experimentation of masonry towers

For non-engineered masonry or monumental structures, the unavoidable lack of knowledge in the construction process and the uncertainties in the building parameters (material properties, geometry, boundary conditions, etc.) still makes their numerical modelling difficult.

For increasing the level of knowledge, experimental tests are usually collected but, for historical structures, the difficulties in using advanced and extensive testing make necessary the development of methodologies without direct contact with the constructions. Just with this aim, recent researches considered several historic masonry towers as case studies, in order to collect the experimental natural frequencies by means of techniques based on recording ambient structural vibrations.

Some examples of these researches are the Saint Andrea masonry bell tower in Venice (Italy) [44], the bell tower of the Monza's Cathedral (Italy) [33], the bell tower of Nuestra Sra. De la Misericordia Church of Santas Justa and Rufina in Orihuela (Alicante, Spain) [38] and the "Mangia" tower in Siena (Italy) [40]. All these studies involve both analytical and experimental analyses. The field survey of the actual configuration, the identification of the main natural frequencies and (in a few cases) the employment of slightly invasive tests (*e.g.* flat-jack tests, sonic pulse velocity tests, etc.) are aimed at tuning finite element models to be used to assess the vulnerability of the towers. In this background, the RiSEM project (Seismic Risk of Historic Buildings, 2011-2013) was developed, considering the towers of San Gimignano (Italy) as an

effective case study in order to collect experimental dynamic data on similar towers, in terms of geometric characteristics, material properties and construction techniques.

In particular, the identification of the dynamic properties of masonry towers at low vibration level plays a relevant role in the assessment of their seismic vulnerability (*e.g.*, in Milani *et al.* [93] and Bartoli *et al.* [94]). Indeed, although the structural response of a construction under seismic action depends on the evolution of its dynamic characteristics during the excitation, the knowledge of the main frequency may represent a relevant datum since the seismic response starts with these dynamic properties. Due to this fact, an accurate knowledge of the modal properties in operational conditions can be useful both for the seismic vulnerability assessment and damage detection purposes. The full-scale experimental measurements can be demanding and a growing number of works have proposed simplified empirical correlations for the estimation of their fundamental modal properties [95–98]. However, a systematic study is not comprehensive yet on the identification of the main structural features affecting the fundamental modal properties of masonry towers on the base of a wide and homogeneous database.

With this aim, the present chapter reports a large database of historic masonry towers starting from the experimental data collected during the RiSEM project. The database is then completed with the data gathered through a systematic literature review, thus obtaining the geometrical features, the construction materials and the dynamic properties of 43 towers.

The collected characteristics provide a clear example of the data usually available for historic masonry towers, giving the possibility to examine in depth an alternative use of these information, as well as to check the effectiveness of the available formulations for the main frequency estimation. Finally, novel semi empirical formulations are proposed, accounting for increasing levels of knowledge on geometric and mechanic characteristics of the towers.

3.1. Database

3.1.1. Outcomes of the RiSEM project

During the RiSEM project, the effectiveness of experimental techniques without direct contact on the structures was tested in order to define a general framework useful to promote simplified seismic risk analyses at a territorial scale. San Gimignano was identified as a significant case study due to the typological structural homogeneity of its historic masonry towers, date back to the 12th and 13th centuries. In the period of maximum splendour, the skyline of the city revealed 70 masonry towers, up to 70 meters tall. Only 13 of these are still preserved, continuing to represent a hallmark of this city (Figure 3.1), whose historic centre is included in the list of UNESCO World Heritage Sites list since 1990.

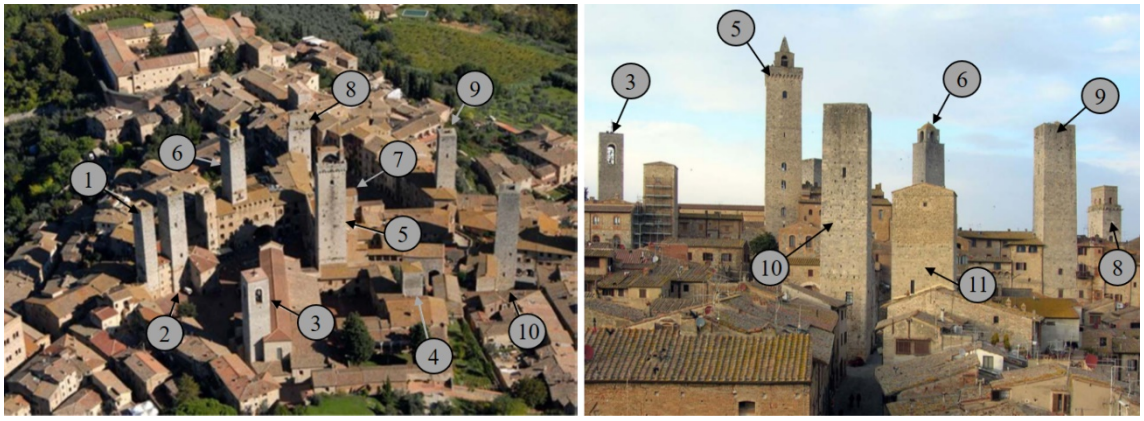

Figure 3.1 Two views of the historic towers of San Gimignano:
1) Salvucci North, 2) Salvucci South, 3) Collegiata, 4) Propositura, 5) Grossa, 6) Rognosa, 7) Ardinghelli North 8) Diavolo, 9) Becci 10) Cugnanesi and 11) Coppi-Campatelli.

The towers of San Gimignano represent a typological example of *tower house*, built to demonstrate the power of the competing families. Only two exceptions can be identified: the Grossa tower (#8) and the bell tower of Collegiata church (#3).

Within the RiSEM project, detailed surveys were carried out with laser scanner and traditional manual investigations for each tower, thus collecting several information on construction techniques, materials, cracking patterns, as well as the demolitions and reconstructions occurred over the time [99,100]. These studies have allowed to analyse a whole system of the towers, thus highlighting the common elements in order to understand the features and the changes occurred. These structures are characterized by a high quality of the masonry and a large thickness of the walls that reveal a typical construction technique for the era. This multi-leaf stone masonry is usually composed by the internal and the external faces, made by stone masonry, and the thick inner core, composed by heterogeneous stone blocks tied by a good mortar. The high quality of the central part of the walls can be investigated at the bottom level of the towers, where over the time, the construction of the neighbouring buildings made necessary realizing new openings in the masonry walls.

For the sake of example, Figure 3.2 reports three views of masonry wall of the Collegiata tower (#3), thus underlying the quality of the external and internal faces as well as that of the inner part.

(a) (b) (c)

Figure 3.2 - Three views on masonry wall of the Collegiata tower (#3): a) external and b) internal faces, c) inner part.

The knowledge process of these towers was completed with the acquisition of the experimental data. As concern the measurement natural frequencies, two techniques were employed by considering the recording ambient structural vibrations. The first one consists in the use of the interferometric radar to remotely perform dynamic measurements. The technique, referred to as *IR* in the following, is based on the detection of the displacement in the line of sight between the radar and the structure [40,101,102]. The differential displacements of the targets in the radar cone of view are detected by exploiting the phase information of the back-reflected microwave signal. This method was employed to perform measurements from different points of view on each tower, to assess the natural frequencies. The second technique consists in the measurement of the towers vibration under environmental loads (mainly wind) by single-station measurements performed employing a three component (E-W, N-S and Vertical) mini portable seismograph. The analysis of the Horizontal-to-Vertical Spectral Ratio (HVSR) curves allows the detection of seismic resonance phenomena and the natural frequency estimation by a peak-picking procedure [103]. This approach will be referred to as *SSR* in the following, since Standard Spectral Ratios (i.e. the ratios between the average spectral amplitudes of ambient vibrations obtained inside and outside the investigated buildings) were used to highlight the natural frequencies.

Both procedures allowed the estimation of the natural frequencies along the two main directions of the towers. These frequencies for the sake of brevity are denoted as N-S and E-W, even if the towers are not exactly aligned with respect to the geographical reference system. The obtained results are reported in Table 3.1. It is worth noting that the experimental datum was calculated as the average value when measurements from both methods were available.

The relevance of defining the main frequency of a structure is twofold: first, its primary role in the evaluation of the seismic demand and in addition, the prospect of tuning the numerical model employed to assess the seismic capacity.

As in common knowledge, the main frequency of a structure depends on its mass, stiffness and geometric properties. Due to this fact, the main mechanical and geometrical characteristics of the towers of San Gimignano are collected. In Table 3.2 these properties are shown, denoting with: E the elastic modulus, γ the specific weight and v_p the velocity of propagation of the elastic compression waves (P-waves), H the total height of the tower, a and b the cross-section of the tower and s the thickness of the masonry walls at the base.

The geometric characteristics of the towers were defined with specific reference to the work of Giorgi and Matracchi [99] and Tucci and Bonora [100]. For every tower, along with the total height (H) the effective one was also reported. This parameter is indicated with H_{eff} and represents the free-standing part of the tower, *i.e.* out of the restraints offered by the neighbouring buildings. In particular, when the buildings on two opposite sides have different heights, the average value was used to quantifying this parameter. For the identification of mechanical properties of the masonry, direct experimental measurements were unavailable. Due to this fact, the parameters E and γ were estimated according to the results of flat-jack tests on the Grossa tower (#5), as reported in Bartoli et al. [47], and the results of the mechanical identification of different types of Italian masonries, as reported in several scientific papers (*e.g.* [104,105]).

In order to define a relationship between E and γ, the velocity of propagation of the P-waves (v_p) can be introduced. This term, in a homogeneous isotropic medium, is given by the following relationship:

$$v_p = \sqrt{\frac{\lambda + 2\mu}{\rho}} \tag{1}$$

where λ and μ are the first and the second Lamé parameters and ρ=γ/g is the mass density of the material through which the wave propagates. The Lamé parameters can be expressed in terms of elastic modulus, E, and Poisson's coefficient, υ:

$$\lambda = \frac{\upsilon \cdot E}{(1+\upsilon)(1-2\upsilon)} \quad ; \quad 2\mu = \frac{2E}{(1+\upsilon)} \tag{2}$$

Eq. (1) becomes:

$$v_p = \sqrt{\frac{E}{\rho} \cdot \frac{(1-\upsilon)}{(1+\upsilon)\cdot(1-2\upsilon)}} \cong \sqrt{\frac{E}{\rho}} \tag{3}$$

The second term under the square root in Eq.(3), is often neglected; indeed, it assumes values around 1.0, when υ is assumed in the range from 0 to 0.25 (for masonry).

The benefit of the introduction of the P-waves propagation velocity is twofold: firstly, it allows to define a relationship between E and γ and secondly, this parameter can be obtained through sonic tests. These latter tests represent a non-destructive investigation technique widely adopted for masonry structures and it is considered a promising investigation, even if the notable heterogeneity of the historic masonry makes still complicated using of these results to gain the mechanical properties of the masonry.

Table 3.1: Experimental frequencies of the towers of San Gimignano.

#	Tower	N-S direction [Hz]			E-W direction [Hz]		
		IR	SSR	$f_{N\text{-}S}$	IR	SSR	$f_{E\text{-}W}$
1	Salvucci (North)	1.25	1.30	1.28	--	1.22	1.22
2	Salvucci (South)	1.73	1.73	1.73	--	1.58	1.58
3	Collegiata	1.71	1.69	1.70	1.84	1.88	1.86
4	Propositura	--	4.02	4.02	--	4.13	4.13
5	Grossa(*)	1.32	1.39	1.36	1.29	1.34	1.32
6	Rognosa	1.44	1.47	1.46	1.53	1.53	1.53
7	Ardinghelli	2.85	3.08	2.97	--	4.67	4.67
8	Diavolo	--	2.63	2.63	2.23	2.38	2.31
9	Becci	1.37	1.36	1.37	--	1.67	1.67
10	Cugnanesi	1.46	1.38	1.42	1.31	1.27	1.29
11	Coppi-Campatelli	--	2.97	2.97	--	3.16	3.16

(*) Data from Bartoli et al. [47]

Table 3.2: Mechanical and geometrical properties of the towers of San Gimignano.

#	Tower	E [MPa]	γ [kN/m^3]	v_p [m/s]	H [m]	H_{eff} [m]	a [m]	b [m]	s [m]
1	Salvucci (North)	2,300	18	1,120	41.5	27.5	6.0	5.2	2.0
2	Salvucci (South)	2,300	18	1,120	42.8	27.3	7.1	7.2	2.3
3	Collegiata	2,600	18	1,190	38.8	27.6	7.0	7.3	2.0
4	Propositura	1,800	22	896	21.0	14.0	6.7	6.7	2.2
5	Grossa	2,600	22	1,077	52.3	34.5	9.1	9.7	2.4
6	Rognosa	2,300	22	1,013	44.0	25.0	6.2	7.2	2.0
7	Ardinghelli	2,000	18	1,044	27.6	14.9	4.3	5.4	1.4
8	Diavolo	2,800	22	1,117	32.0	20.0	5.6	8.6	1.2
9	Becci	2,300	18	1,120	39.4	24.4	6.3	6.5	2.3
10	Cugnanesi	2,300	18	1,120	42.8	29.8	7.5	7.7	2.6
11	Coppi-Campatelli	2,600	18	1,190	31.0	16.0	6.4	8.2	1.5

3.1.2. Collected data from scientific literature

The data collected for the towers of San Gimignano (Table 3.1 and Table 3.2) were completed with 32 additional case studies, selected according to an extensive review of the scientific literature (Table 3.3). The geometrical and mechanical properties of these towers were directly derived by the corresponding papers. Only in a few cases (marked with a star in Table 3.3), the mechanical properties (E and γ) were missed in the corresponding work and plausible values were assumed according to the available information on similar structures.

Note that, some researches were excluded from the database herein reported due to the scarcity of geometric and mechanical parameters reported in the relative papers or, sometimes, for the distinctive and unusual traits of some towers; such as the tower of the Vistula Mounting Fortress in Gdansk (Poland) [106] with its circular cross section.

Table 3.3: Database by literature review (mechanical, geometrical and dynamic data).

#	Tower	E	γ	vp	H	Heff	a	b	s	f1
		[MPa]	[kN/m3]	[m/s]	[m]	[m]	[m]	[m]	[m]	[Hz]
12	Bongiovanni et al. [25]	700	16	655	18.5	11.0	3.00	3.35	0.50	2.43
13	Carone et al. [39]	1,340	20	811	20.0	13.0	3.50	3.50	1.00	2.62
14	Ramos et al. [37]	3,100	20(*)	1,233	20.4	20.0	4.50	4.70	1.00	2.56
15	Bayraktar et al. [35]	1,900	18	1,018	23.0	20.6	5.50	5.00	1.50	2.55
16	Ceriotti et al. [43]	1,100	18	774	31.0	19.6	4.50	7.80	0.80	1.25
17	Ivorra et al. [38]	1,400	18	873	35.5	21.4	7.16	7.16	1.50	2.15
18	Gentile and Saisi [46]	1,500	20(*)	858	36.7	26.8	5.80	5.70	1.30	1.21
19	Ivorra and Cervera [31]	1,100	16(*)	821	37.2	27.2	4.68	4.68	1.45	0.73
20	Casciati and Al-Saleh [36]	1,600	18	934	39.2	29.2	5.96	5.96	1.55	1.05
21	Ivorra and Pallarés [27]	2,500	18	1,167	41.0	28.0	5.60	5.60	1.20	1.29
22	Kohnan et al. [107]	1,960	19	1,006	41.4	34.4	7.60	7.60	1.10	1.37
23	Diaferio et al. [48]	2,200	20(*)	1,039	57.0	29.6	7.50	7.50	1.40	2.04
24	Russo et al. [44]	1,800	18	990	58.0	44.7	7.60	7.64	1.04	0.61
25	Ceroni et al. [108]	850	18(*)	681	68.0	40.5	11.00	11.00	2.70	0.69
26	Gentile and Saisi [33]	1,600	18	934	74.1	56.7	10.00	10.00	1.40	0.59
27	Bonato et al. [26]	970	19(*)	708	26.0	14.5	3.82	5.52	1.20	1.66
28	Zonta et al.[109]	1,700	18(*)	963	61.6	39.0	7.30	7.30	1.30	0.85
29	Cosenza and Iervolino [29]	1,800	19	964	34.0	19.5	5.42	5.42	1.35	1.95
30	Jùlio et al. [34]	3,000	19	1,245	33.5	22.0	5.60	5.70	1.30	2.13
31	Ferraioli et al. [42]	2,200	20	1,039	45.5	45.0	14.00	14.00	3.80	1.05
32	Ferraioli et al. [42]	2,800	20	1,172	41.0	41.0	11.30	11.30	2.80	1.26
33	Bassoli et al. [49]	1,500	18	904	68.0	45.0	8.00	8.00	2.30	0.55

#	Tower	E	γ	vp	H	Heff	a	b	s	f1
		[MPa]	[kN/m3]	[m/s]	[m]	[m]	[m]	[m]	[m]	[Hz]
34	Gentile et al. [46]	1,700	18	963	54.0	32.0	7.10	7.15	2.30	0.97
35	Lancellotta and Sabia [41]	1,700	18	963	88.8	50.0	11.00	11.00	2.00	0.74
36	Pieraccini et al. [40]	2,000	18	1,044	88.0	52.0	7.00	7.00	2.50	0.35
37	Casarin et al. [110]	2,300	20	1,062	53.0	37.8	6.15	6.15	0.80	0.79
38	Bennati et al. [32]	1,800	18	990	34.3	29.0	7.00	11.00	1.08	1.20
39	Colapietro et al. [45]	1,900	18	1,018	46.0	30.0	6.25	6.25	1.20	1.41
40	Castellacci et al. [111]	1,400	18	873	22.0	14.0	3.58	3.67	0.98	2.15
41	Abruzzese and Vari [112]	1,900	20	975	36.2	34.1	8.60	8.60	2.00	2.00
42	Rainieri and Fabbrocino [96]	1,230	18	819	35.0	20.0	6.47	7.15	1.34	1.96
43	Rainieri and Fabbrocino [96]	1,100	18	774	27.5	15.0	4.95	5.20	1.25	2.27

(*) Data evaluated assuming available values for similar structures

3.1.3. Analysis of the database

The extensive database collects 43 masonry towers located in the European territory, most of them in Italy. The geometric and mechanic characteristics of these structures are summarized in Table 3.2 and Table 3.3. For the sake of clarity, the case studies are numbered from 1 to 43 and this numeration will be maintained in the following comparisons. This database can be considered as uniform due to the presence of the same structural typology, which is characterized by the high slenderness. Despite this common and recursive feature, the analysis of the geometric and mechanic characteristics reveals a relevant variability due to different intended use of the tower (*e.g.* bell tower, civic tower and tower house), different techniques and period of construction.

From a geometrical point of view, the total height ranges from 18.50 m (#12, bell tower of San Giorgio church in Trignano, [25]) to 88.8 m (#35, Ghirlandina tower, [41]), while the width of the walls at the lower level varies from 0.5 m (#12, bell tower of San Giorgio church in Trignano, [25]) to 3.8 m (#31, bell tower of Aversa, [42]). The cross-section is almost square, except for few cases: Diavolo tower (#8), Aquila tower (#16, [43]), bell tower of SS. Annunziata church (#27, [26]) and bell tower of Matilde (#38, [32]) which have a unambiguously rectangular plan. The length of the outer side of the base cross-section ranges from 3 m (#12, bell tower of San Giorgio church in Trignano, [25]) to 14 m (#31, bell tower of Aversa, [42]). Moreover, considering the slenderness as the ratio between the total height *H* and the minimum length of the outer side of the base cross-section, its value ranges from 3.1 for the Propositura tower (#4) to 10.3 for the Mangia tower (#36, [40]). Note that, these two latter towers are also characterized by the minimum and maximum value of the experimental main frequency, respectively equal to 0.35 Hz and 4.2 Hz.

It is straightforward to observe, looking the collected database, that the fundamental frequencies are highly influenced by the height of the towers and their slenderness. However, despite such a general coherence, to obtain an effective and comprehensive dependence between these factors and the frequency, additional parameters should be taken into account. Due to this fact, the collected database was used to calibrate simple predictive formulations by considering, at first, only the geometrical characteristics of the towers. The main natural frequency was thus defined as function of the height and the slenderness of the towers; by comparing both the total and the effective height in order to evaluate the effect of the adjacent buildings, as shown in Table 3.4. This table reports the equations with the values of the introduced coefficients (A, α and β) and the relative prediction capability through the R-squared value. This parameter, in fact, is useful to quantify how the observed outcomes were replicated by the model. In particular, to calibrate the values of the parameters introduced in the equations of Table 3.4, a simple least squares procedure was applied to the collected database (Table 3.2 and Table 3.3), as reported in Figure 3.3. The results highlight the relevance of the effective height H_{eff} (*i.e.* the average height of the tower without the neighbouring buildings) which produces a higher value of R-squared compared to the total height *H*. Indeed, the R-squared value increases from 0.59 to 0.64.

A further improvement can be obtained if the side *L* of the tower is considered as an additional parameter in conjunction with the effective height H_{eff}. In fact, the highest R-squared value is obtained with the fourth equation reported in Table 3.4, where the frequency is evaluated as a function of the ratio between the side and the effective height of the tower.

In general, the results suggest both that the effective height play a relevant role and that other parameters should be considered to enhance the predictive performance of the formulations (Table 3.4, Figure 3.3).

Table 3.4 – R-squared values of general formulations for main frequency estimation, calibrated with the database reported in Table 3.2 and Table 3.3.

Equations	Coefficients	R-squared
$f_1 = \frac{A}{H^{\alpha}}$	A=36.42, α=0.90	0.59
$f_1 = \frac{A}{H_{eff}^{\alpha}}$	A=19.54, α=0.79	0.64
$f_1 = A\frac{L^{\beta}}{H^{\alpha}}$	A=47.29, α=1.08, β=0.22	0.60
$f_1 = A\frac{L^{\beta}}{H_{eff}^{\alpha}}$	A=33.97, α=1.42, β=0.81	0.72

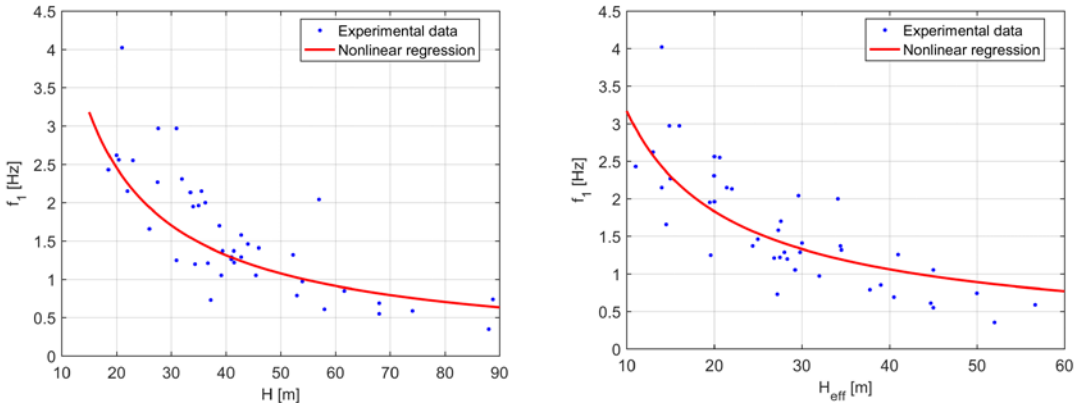

(a) (b)

Figure 3.3 - Nonlinear regression of the first experimental natural frequency as function of a) the total height and b) the effective height of the towers.

3.2. Formulations for the main frequency estimation

3.2.1. Existing formulations

Empirical formulations for the first natural frequency estimation (or, conversely, the first natural period) of slender structures are defined by different European recommendations such as the Italian NTC2008 [113] or the Spanish NCSE2002 [114] codes. In addition, in the last few years, new empirical formulations have been proposed by Rainieri and Fabbrocino [96] and Shakya et al. [97], which focused their studies on the dynamic behaviour of several slender masonry structures. Rainieri and Fabrocino [96] collect a database of masonry towers located in southern Italy. Shakya et al. [97] extend the database to different slender structures, considering both masonry towers and minarets, chimneys and Pagoda temples.

The Italian recommendation proposes two formulae to predict the fundamental period of structures. The first, reported in NTC2008 [113], is applicable for structures with a height up to 40 m and allows the evaluation of the period as a function of its height *H*:

$$T_1 = C_1 \cdot H^{3/4} \tag{4}$$

where *H* is expressed in meters and C_1 is 0.050 for all the structural typologies (other coefficients are suggested for steel and reinforced concrete structures). This formula is used especially for ordinary buildings, the application to slender structures can provoke a large scattering. In many cases, the height of the towers is greater than 40 m and Eq. (4) could not be applied.

The second correlation proposed by the Italian recommendation is included in the DPCM2011 [9]. This code rules the procedure for assessing the seismic risk of monumental buildings, within

the context of an explanatory application. The formula for the assessment of first natural period is proposed by Faccio et al. [95] and is specifically intended for masonry towers, despite no references about its calibration are provided. The main period of the tower is expressed as a linear function of the total height *H* (in meters):

$$T_1 = 0.0187 \cdot H \tag{5}$$

The Spanish Standard (NCSE2002 [114]) estimates the main frequency of masonry structures and, despite this formulation is not specifically intended for slender structures, it is interesting for the work purposes. Indeed, in addition to the total height of the tower (*H*), the plan dimension (*L*) along the direction of oscillation are taken into account:

$$f_1 = \frac{\sqrt{L}}{0.06H\sqrt{\frac{H}{2L+H}}} \tag{6}$$

The reliability of the above formulations is checked by Rainieri and Fabbrocino [96], using the results of an extensive experimental campaign based on output-only modal identification of about 30 masonry towers in southern Italy. This study shows that Eq. (4) and Eq. (5) lead to an overestimation for low values of the natural period and, vice versa, to an underestimation for higher values of the period. Analysing the collected database, [96] proposes a new empirical formulation. In order to maintain the basic structure of Eq. (4) and considering *H* expressed in meters, the coefficients were updated on the base of the acquired experimental data:

$$T_1 = 0.0113 \cdot H^{1.138} \tag{7}$$

Recently, Shakya et al.[97] collect a wider database of 58 slender structures, composed by 32 masonry towers, 16 minarets, 7 chimneys and 3 Pagoda temples. These data are employed to propose four novel correlations as function of the main characteristics for three typologies of slender structures: a) all type of slender masonry structures; b) towers such as bell towers, clock towers, civic towers and c) minarets.
The first formulation, as Eq. (5), is function only of the total height (*H*), expressed in meters:

$$f_1 = \frac{1}{\alpha \cdot H^{\beta}} \tag{8}$$

The coefficients α and β were evaluated according to a linear R-squared approach and their values, proposed for masonry towers (case b), were: $\alpha = 0.0151$ and $\beta = 1.08$.

The second formulation maintains the structure of Eq. (6) and suggests new coefficients based on the collected experimental data:

$$f_1 = \frac{L^{\varphi}}{\mathrm{C} \cdot H \left(\frac{H}{L+H}\right)^{\delta}} \tag{9}$$

for masonry towers (case b): C = 0.03, φ = 0.17 and δ = 0.50.
The third formulation is based on the classical theoretical expression valid for an elastic cantilever beam with uniform cross section. An empirical coefficient (X=1.375 for masonry towers, case b) is introduced to improve the prediction capability:

$$f_1 = \frac{1.875^2}{2\pi \cdot H^2} \sqrt{\frac{\mathrm{X} \cdot \mathrm{EJ}}{\bar{m}}} \tag{10}$$

In the previous expression, $\bar{m}$ is the mass per unit of length and J denotes the moment of inertia.
The last formula proposed by Shakya et al. expresses the main frequency as a function of the minimum slenderness, *i.e*. the ratio between the total height of the tower (*H*) and the minimum length of the outer side of the base cross-section (*B*):

$$f_1 = \mathrm{Y} \cdot \left(\frac{H}{B}\right)^{-\mathrm{Z}} \tag{11}$$

following values are suggested masonry towers (case b): Y = 3.58 and Z = 0.57.
From the above formulations, the total height of the tower is considered as the crucial parameter to define the main frequency. This consideration allows to define simple formulations but, as demonstrated by Shakya et al. [97], other parameters should be considered to improve the prediction capability.

3.2.2.Novel formulations

The structural configuration of masonry towers allows to consider their dynamic behaviour very close than a cantilever beam with a hollow square section. Consequently, the first natural frequency of these structures should be described by the following expression:

$$f_1 = \frac{1.875^2}{2\pi \cdot H^2} \sqrt{\frac{\mathrm{E} \cdot \mathrm{J}}{\rho \cdot \mathrm{A}}} \tag{12}$$

where J indicates the moment of inertia and A, the area of the transversal section. Some considerations were developed on these parameters. In order to perform approximate formulations, the following relations for a hollow squared section can be easily obtained:

$$J = \frac{a^4}{12} - \frac{(a-2s)^4}{12} = \frac{1}{12}(8a^3s - 24a^2s^2 + 32as^3 - 16s^4) \tag{13}$$

$$A = a^2 - (a-2s)^2 = 4as - 4s^2 \tag{14}$$

The thickness *s* was normalized with respect to the side length *a*, thus obtaining the follow expression of the radius of inertia of the square hollow section:

$$r = \sqrt{\frac{J}{A}} = \frac{a}{\sqrt{12}} \cdot \sqrt{\frac{2 - 6n + 8n^2 - 4n^3}{1-n}} = \frac{a}{\sqrt{12}} \cdot \chi \tag{15}$$

where the non-dimensional quantities *n* and χ were introduced:

$$n = \frac{s}{a} \qquad\qquad \chi = \sqrt{\frac{2 - 6n + 8n^2 - 4n^3}{1-n}} \tag{16}$$

The graph of χ as a function of the normalised thickness *n* is shown in Figure 3.4. The variability of the parameter *n* resulted very limited, in fact, an average value of μ_n = 0.25 with a standard deviation σ_n = 0.06 was obtained considering the collected data. Moreover, in the range $[\mu_n - \sigma_n , \mu_n + \sigma_n]$, the best linear approximation of χ (*n*) is expressed by the following expression:

$$\chi = 1.343 - 0.892 \cdot n \tag{17}$$

In order to simplify the final formulation, an approximation can be considered:

$$\chi \cong 1.5 \cdot (1-n) \tag{18}$$

In particular, Eq. (18) produces the same values of Eq. (17) near the average value μ_n.
Due to these facts, the radius of inertia of a square hollow section can be expressed by the following simplified expression:

$$r = \sqrt{\frac{J}{A}} \cong \frac{a}{\sqrt{12}} \cdot 1.5 \cdot (1-n) \tag{19}$$

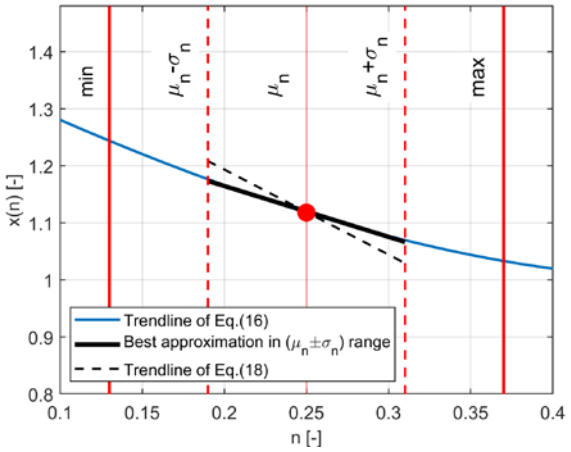

Figure 3.4 - Values of the function χ(n) and linear approximation in the selected range.

As discussed above, a first effective improvement can be introduced in Eq. (12) by assuming the parameter H_{eff} instead of the total height H. With this consideration, the first natural frequency can be expressed as follows:

$$f_1 = \frac{1.875^2}{2\pi} \cdot \frac{1}{H_{eff}^2} \sqrt{\frac{E \cdot J}{\rho \cdot A}} = \frac{1.875^2}{2\pi} \cdot X \tag{20}$$

where the X parameter was introduced:

$$X = \frac{1}{H_{eff}^2} \sqrt{\frac{E}{\rho}} \cdot \sqrt{\frac{J}{A}} \tag{21}$$

The experimental frequencies of the database were plotted as function of the X parameter in Figure 3.5. In the same figure is reported the trend line of Eq. (20), thus confirming its effective prediction capability of the experimental first natural frequency when the parameter H_{eff} is employed. Moreover, the figure reports the approximation introduced with Eq.(18) which produces negligible discrepancies respect to the exact expression (at least as far as the collected database is concerned).

The results underline that the specific formulation for a cantilever beam tends to overestimate the value of the experimental frequency, in the majority of samples. Indeed, the formulation neglects the openings along the height of the tower and the effective degree of restraint offered by neighbouring buildings. As a matter of fact, the section at which the tower is considered as restrained (*i.e.* the section where the free height of the tower is equal to H_{eff}) is restrained by adjacent building with a level of restraint lower than the clamped one considered in the theoretical

formulation. Both these aspects lead to a reduction of the natural frequency of the tower, then to an overestimation offered by Eq.(20). In order to improve the estimation of the fundamental frequency, a further coefficient can then be introduced to take into account this evidence. From the collected data, a reduction coefficient of 20% can be estimated, obtained as the best linear fit on available data (red continuous line in Figure 3.5).

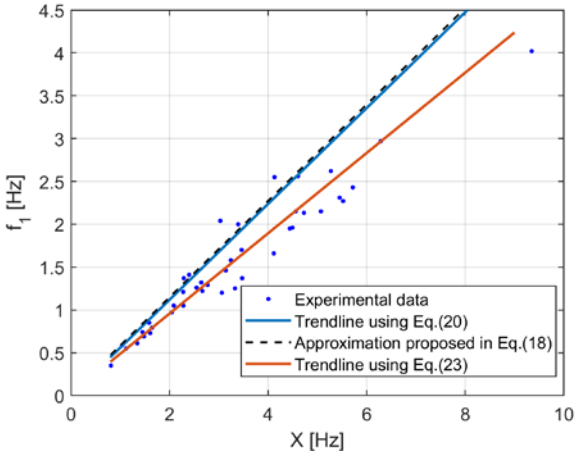

Figure 3.5 - Experimental frequency as function of the X term.

Eventually, the semi empirical formulation for the main frequency estimation can be expressed as follow:

$$f_1 \cong 0.8 \cdot \frac{1.875^2}{2\pi} \cdot \frac{1}{H_{eff}^2} \cdot \sqrt{\frac{E}{\rho}} \cdot \frac{a}{\sqrt{12}} \cdot 1.5 \cdot (1-n) \cong \frac{0.2 \cdot a}{H_{eff}^2} \cdot (1-n) \cdot \sqrt{\frac{E}{\rho}} \tag{22}$$

Moreover, taking into account that the square root of the ratio between E and ρ is the P-waves velocity v_p, the final proposed expression can be written:

$$f_1 \cong \frac{0.2 \cdot a}{H_{eff}^2} \cdot (1-n) \cdot v_p \tag{23}$$

It is worth noting that, Eq. (23) requires the knowledge of geometrical and mechanical parameters which sometimes can be unavailable. Due to this fact, two additional simplified formulations were introduced, thus considering different levels of knowledge on the towers:

$$f_1 \cong \frac{0.15 \cdot a}{H_{eff}^2} \cdot v_p \tag{24}$$

$$f_1 \cong \frac{\alpha \cdot a}{H_{eff}^2} \tag{25}$$

where $\alpha \cong 150$ m/s.

The first additional formulation, Eq. (24), removes the dependence of the masonry thickness, by calculating the *n* coefficient on the base of the geometrical characteristics of the towers collected in Table 3.2 and Table 3.3. A tentative value of $n = 0.25$ can be assumed, corresponding to the mean value μ_n from the database. This assumption is justified by the low value of the standard deviation for the *n* coefficient which ranges from 0.13 (#37 bell tower of Burano, [110]) to 0.37 (#9 Becci tower).

The last formulation, Eq. (25), provides the main frequency of the tower as a function of two geometric parameters (the effective height and the side length of the tower), by removing the dependence of the P-waves velocity v_p (mechanical parameter that synthetize the modulus of elasticity *E* and the mass density ρ). In this respect, according to the masonry characteristics collected in the database, and considering the data reported in scientific literature, Table 3.5 proposes an approximate estimation of the P-waves velocity for different typologies of masonry. Eq. (25) proposes an extremely simple formula derived by the data collected database, considering the average value for v_p of about 1000 m/s with a standard deviation of 160 m/s. Indeed this parameter ranges from about 650 m/s (#12 bell tower of San Giorgio church in Trignano, [25]) to 1200 m/s (#3 bell tower of Collegiata Church in San Gimignano).

It is worth noting that in several cases at least a rough estimation of both the elastic modulus and the specific weight is available, as these two parameters are necessary for even very simple structural assessments of every building.

Table 3.5 - Proposed values of P-waves velocity for different types of masonry.

Type of masonry	v_p [m/s]
Irregular stone masonry (pebbles, erratic and irregular stone)	650 – 750
Soft stone masonry (tuff, limestone, etc)	750 – 850
Full brick masonry with lime mortar	850 – 1000
Dressed rectangular stone masonry	>1000

3.3. Results and discussion

The formulations introduced in the previous section were applied for the towers reported in the database, herein presented. It is worth noting that these equations (summarized in Table 3.6) consider the height of the tower expressed in meters for obtaining the frequency in hertz. To evaluate the overall prevision capability of the various formulations on the collected database, the following global error is introduced:

$$e = \frac{\sum_{i=1}^{N} \frac{|f_i - \bar{f}_i|}{\bar{f}_i}}{N} \tag{26}$$

where N denotes the number of samples, f_i is the estimated frequency of the tower while $\bar{f}_i$ denotes the experimental frequency. The obtained results are summarized in Table 3.6, highlighting the improvement gained with the proposed formulations, Eq. (23), (24) and (25). As explained before, these expressions were derived starting by the general theoretical formulation for a cantilever elastic beam with some modifications that accounting for the typological specificity of masonry towers. In addition, after having performed a linear fitting on experimental results, further coefficients were introduced to account for the differences between the theoretical model and experimental data.

The analysis of the results reveals a considerable improvement in the main frequency estimation when the effective height of the tower is considered, thus confirming the remarkable role of the restraint conditions provided by the adjacent buildings on the dynamic behaviour of masonry towers. Moreover, also the introduction of the mechanical properties of the masonry seems to reduce the discrepancy between the experimental value of the natural frequency and the estimated one. In this respect, in addition to the use of the P-wave velocity v_p, also the shear deformability may be relevant in masonry structures and a specific evaluation of the shear modulus G, could be of interest since its effective value may be lower than the one obtained through the classical elastic theory.

Table 3.6 - Errors in the estimation of the first natural frequency of masonry towers, based on the collected database (Table 3.2, Table 3.3).

Eqn. #			Error e [%]
Eq. (4)	NTC2008 [113]	$f_1 = \frac{1}{0.050 \cdot H^{3/4}}$	31 %
Eq. (5)	Faccio et al. [95]	$f_1 = \frac{1}{0.0187 \cdot H}$	32 %

Eqn. #			Error e [%]
Eq. (6)	NCSE2002 [114]	$f_1 = \frac{\sqrt{L}}{0.06H\sqrt{\frac{H}{2L+H}}}$	30 %
Eq. (7)	Rainieri and Fabbrocino [96]	$f_1 = \frac{1}{0.0113 \cdot H^{1.138}}$	30 %
Eq. (8)	Shakya et al. [97]	$f_1 = \frac{1}{0.0151 \cdot H^{1.08}}$	27 %
Eq. (9)	Shakya et al. [97]	$f_1 = \frac{L^{0.17}}{0.03 \cdot H\left(\frac{H}{L+H}\right)^{0.5}}$	29 %
Eq. (10)	Shakya et al. [97]	$f_1 = \frac{1.875^2}{2\pi \cdot H^2}\sqrt{\frac{1.375 \cdot \mathrm{EJ}}{\overline{m}}}$	42 %
Eq. (11)	Shakya et al. [97]	$f_1 = 3.58 \cdot \left(\frac{H}{B}\right)^{-0.57}$	33 %
Eq. (20)		$f_1 = \frac{1.875^2}{2\pi} \cdot \frac{1}{H_{eff}^2}\sqrt{\frac{\mathrm{E} \cdot \mathrm{J}}{\rho \cdot \mathrm{A}}}$	21 %
Eq. (23)		$f_1 = \frac{0.2 \cdot \mathrm{a}}{H_{eff}^2} \cdot (1-n) \cdot \mathrm{v}_p$	9 %
Eq. (24)		$f_1 = \frac{0.15 \cdot \mathrm{a}}{H_{eff}^2} \cdot \mathrm{v}_p$	11 %
Eq. (25)		$\mathrm{f}_1 = \frac{150 \cdot \mathrm{a}}{H_{eff}^2}$	20 %

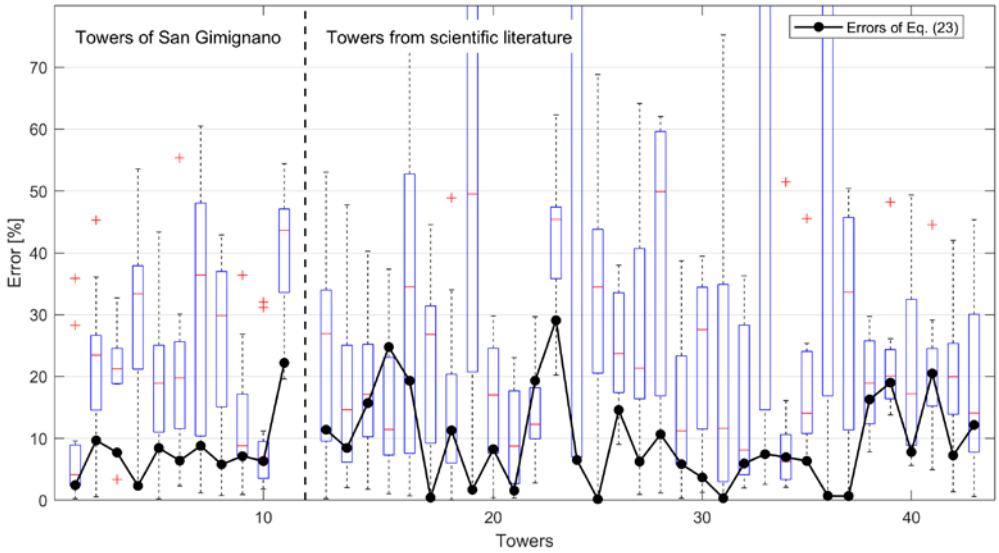

Figure 3.6 - Box plot reporting the scattering of the errors in the formulations for the main frequency estimation, based on the collected database. The continuous black line refers to the results obtained by using Eq. (23).

The predictive capabilities of the considered formulations are graphically reported in Figure 3.6, using boxplot method for each tower included in the collected database. Moreover, the predictive errors of the proposed semi empirical formulation, Eq. (23), are reported in the same graph. This latter formulation provides a good estimation of the main natural frequency of the selected towers, especially compared to the other ones.

3.4. Conclusions

In this chapter, an extensive literature review has been carried out in order to identify the main experimental data collected for historic masonry towers. These results, and those derived by the RiSEM project related to the towers of San Gimignano (Siena, Italy), have confirmed the difficulties in using destructive and extensive testing. This aspect makes necessary the employment of experimental campaigns with a limited contact with the constructions. This latter aim has been usually achieved through dynamic identification of these structures, thus obtaining their natural frequencies, and sometimes the modal shapes. These data provide information on the global behaviour of the tower and are usually employed to improve the knowledge on some uncertain parameters of the model. Specifically, the experimental measurements of the natural frequencies are the most common available data for historic masonry towers.

In this respect, the analyses of the collected database have allowed to identify the more relevant structural parameters, which influence this datum. These results have been considered in the following, in order to reach one of the aim of the present dissertation: the updating of the model by using experimental dynamic data.

As additional result, the analysis of the collected database has been used to develop a novel semi empirical formulation for the estimation of the fundamental frequency of slender masonry towers, with the aim to improve the prediction capabilities of the existing simplified formulations. In particular, some improvements could be achieved when:

- the effective height of the tower H_{eff} (*i.e.* the length of the portion of the tower which is free from the restraint offered by adjacent buildings) is used rather than the total height H
- other geometrical (side and thickness of the tower) and mechanical (elastic modulus and mass density of the masonry) characteristics are introduced as additional parameters influencing the first natural frequency value

The proposed formulation was derived by manipulating the theoretical expression for a simple cantilever beam with a hollow square section; only small approximations were introduced, and a correction coefficient was adopted to take into account the discrepancies from the theoretical expression and the current configuration. Moreover, the formulation retains only those quantities

with a clear physical soundness, such as the velocity of propagation of the elastic compression P-waves (v_p) which plays a significant role in first natural frequency estimation.

The proposed formulation leads to considerable improvements. If it is compared with the prediction capability of existent formulations, the average error level can be decreased from about 30% to a value as low as 9%. Note that, these values are based on the available experimental results, collected in the database herein introduced. However, compared to the other formulations, the knowledge (or the estimation) of more parameters, both geometric and mechanic, is needed. In order to allow the application of the proposed formulation also when the level of knowledge is considerably low, additional simplified formulations are proposed on the base of the characteristics of the towers inserted in the database.

As concluding remark, this chapter has demonstrated the wide employment of experimental measurements of the natural frequency for masonry towers, in order to improve the level of knowledge on the structure. These data are mainly affected by both of the velocity of propagation of elastic compression P-waves and the height of the restraint conditions offered by adjacent buildings. Starting from these considerations, the next chapter has been developed.

Chapter 4

Bayesian FE-Model updating

An effective seismic risk assessment of existing structures requires numerical models which take into account the many sources of uncertainty involved. Indeed, the knowledge on the seismic response of existing buildings is usually lacking and a probabilistic approach seems necessary to assess the combined effects of the parameters affecting the structural behaviour.

The largest uncertainties regard the earthquake ground motion: both in terms of intensity, usually identified by the hazard curves, and in terms of frequency content as well as other characteristics of the ground motion records, as witnessed by the so-called record-to-record variability. Moreover, additional uncertainties are associated with the numerical model used to represent the structure which can lead errors in the prediction of its response. Due to these facts, the definition of a framework which both handles and combines different sources of uncertainties, by reducing the lack of knowledge on the model parameters with the use of experimental data, becomes relevant especially for historic constructions. Indeed, for these structures the achieved level of knowledge (*e.g.*, on material properties and boundary conditions) is very low.

In the last decades, the issue of the structural model updating based on experimental tests, acquired a growing relevance in the scientific community. In particular, several researches have proposed the use of dynamic test data (*i.e.*, natural frequencies and modal shapes) to update the numerical model thus providing a more accurate structural behaviour under dynamic loads [62,65,115]. In this respect, the Bayesian methodology is considered a promising tool in order to describe the probability distribution related to uncertain events and considering all the available information.

Slender structures (*i.e.*, civic towers, bell towers, tower houses) have a considerable sensitivity to dynamic actions; this aspect together with the difficulties in performing destructive and extensive testing on historic buildings, makes the dynamic identification widely used.
Indeed, several researches propose this technique in order to improve the knowledge on the dynamic behaviour of masonry towers and to calibrate the numerical model by reducing the discrepancy between the experimental data and the model output [27,39,42,53,54,116].
This chapter proposes an alternative use of the experimental data based on the Bayesian FE-model updating, which represents the first step of the methodology proposed in this dissertation (Figure 1.3) aimed of quantifying the role of the uncertainties in the seismic risk chain of historic masonry towers. This first step allows of including the different sources of uncertainties (*i.e.* measurement errors and modelling uncertainties) as well as all the available information (*e.g.*, experimental data and expert judgments), in order to improve the prediction of the uncertain parameters. The procedure and the results are herein presented through the application on a case study: The Becci tower in San Gimignano. In particular, the experimental measurements of the natural frequencies, achieved during the RiSEM project, are considered to update the FE-model. Nevertheless, it is worth noting that the proposed procedure is general and can be applied to other structures.
In the following sections, the methodology is presented. First, the probabilistic framework as well as the adopted assumptions are described and then, the modal data and the structural model are defined. Eventually, the results are presented by considering their sensitivity on the assumptions and the uncertainties introduced in the process.

4.1. Bayesian approach

The Bayesian model updating provides an effective method of using different types of information to update an initial description of the structural model, based on expert judgement. In this respect, the posterior distribution become a measure of the uncertainty on an event, which can be modified when additional data become available, as resumed in Figure 4.1.

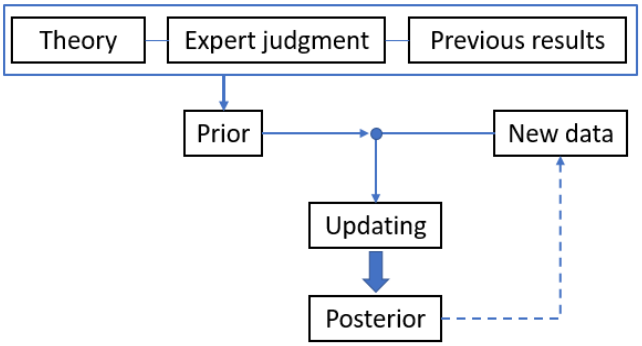

Figure 4.1 – Scheme of the Bayesian process.

The plausibility of the model is quantified by the probability distribution of the uncertain model parameters and the Bayes' theorem is herein used to convert this initial distribution of the $\boldsymbol{\theta}$-parameters into the posterior distribution, $p(\boldsymbol{\theta}|\overline{D})$, by using experimental data, $\overline{D}$:

$$p_{\overline{D}}(\boldsymbol{\theta}) = p(\boldsymbol{\theta}|\overline{D}) = \frac{p(\overline{D}|\boldsymbol{\theta})p_0(\boldsymbol{\theta})}{\int p(\overline{D}|\boldsymbol{\theta})p_0(\boldsymbol{\theta})\mathrm{d}\boldsymbol{\theta}} \tag{27}$$

where $p_0(\boldsymbol{\theta})$ is the *prior* probability distribution based on the expert judgment, which reflects the initial knowledge on the uncertain parameters, before utilizing the data $\overline{D}$; $p(\overline{D}|\boldsymbol{\theta})$ is the *likelihood* function and represents the probability of obtaining the data $\overline{D}$ from the model-output based on the plausible values of the model parameters, $\boldsymbol{\theta}$. Lastly, the denominator is the *evidence* and represents the normalizing constant. In this respect, Eq. (27) gives a better description of response predictions of the model using the data $\overline{D}$ and considering, through the likelihood function, different uncertainties.

A first source of uncertainty is inherent in the numerical model usually employed to represent the real system, this model maintains a discrepancy between its output, y($\boldsymbol{\theta}$), and the real system behaviour, D. Moreover, as modelling errors can be considered the uncertainties in the material properties identification and the lack of knowledge on the construction process as well as on the boundary restraint conditions. Therefore, modelling uncertainties can be expressed as:

$$D - y(\boldsymbol{\theta}) = \varepsilon \tag{28}$$

Another source of uncertainty regards the experimental data, collected to improve the knowledge on the real system behaviour. Also between these measurements and the real system behaviour remains a discrepancy due to several aspects: the instrument accuracy and the signal processing are just two examples. This error can be represented as follows:

$$D - \overline{D} = \bar{\varepsilon} \tag{29}$$

Both the errors expressed in Eq. (28) and Eq. (29), influence the response prediction and their quantifications play a relevant role in the reliability of the model. Indeed, the major purpose of model updating is to modify the model parameters ($\boldsymbol{\theta}$) to obtain a better agreement between model results and test data. The likelihood function considers these two aspects by taking into account the uncertainties in the acquisition of the experimental data and the differences between the output of the numerical model and the real system.

The two sources of uncertainties are considered as statistically independent and, using the axiom of probability, the likelihood function can be obtained by:

$$p(\overline{D}|\boldsymbol{\theta}) = \int p(\overline{D}|D, \boldsymbol{\theta}) p(D|\boldsymbol{\theta}) dD \tag{30}$$

where D represents the real behaviour of the structure and $p(\overline{D}|D, \boldsymbol{\theta})$ and $p(D|\boldsymbol{\theta})$ account for, respectively, the measurement and the modelling uncertainties. These two uncertainties have been modelled through the Gaussian probability density functions with zero mean and centred, respectively, on the experimental data value and on the model output value. In both cases, also the standard deviation can be treated as uncertain parameter. However, in this work these values are considered as known but their effect on the posterior distributions of the **θ**-parameters, is evaluated, as highlighted in the next sections.

The experimental data $\overline{D}$ from historic structures usually consists into N set of modal data, composed of modal frequencies and modal shape vectors. In this work, the measurements of modal frequencies are used to update a FE-model. The identification of the random variables (**θ**-parameters), which can be updated with the Bayesian approach, may not be a simple matter and requires the knowledge of the parameters affecting the experimental data.

As shown in the previous chapter, the natural period of slender structures (or conversely natural frequency) is strongly dependent on the elastic modulus of the material and on the boundary conditions (*i.e.* lateral restraints imposed by adjacent buildings on the tower). Thus, these characteristics are selected to represent the relevant parameters of the linear model. Moreover, on the base of the same case study, different FE-model updating will be performed by considering different choices of: **θ**-parameters, modelling and measurement uncertainties.

4.2. Applications

4.2.1. Case study: Becci tower of San Gimignano

The Becci tower, one of the biggest towers in the centre of San Gimignano, was selected as reference case, representing a typological example of *tower house* and showing a regular geometry (Figure 4.2). Moreover, the availability of experimental data, *i.e.* geometric survey and measurements of natural frequencies, make this structure particularly useful to test the proposed methodology.

The tower is characterized by a height of about 38 m and a cross-section length of 6.8 m and width of 6.9 m (Table 4.1). The thickness of the walls ranges from 1.1 m to 1.9 m and these are constituted by a multi-leaf stone masonry with the internal and external faces made with the same typology of material: a soft stone masonry. The internal core is unknown but, likely, is composed of heterogeneous stone blocks tied by a good mortar. The section size, as well as the thickness of

the walls, are almost constant along the height of the tower except for the lower level where larger size openings were created to allow the connection of the tower with the adjacent buildings. The tower, except for the South side (Figure 4.2), is incorporated into an architectural complex built in a later period. These structures, as highlighted in the previous chapter, influence the dynamic behaviour of the tower, playing a fundamental role in its numerical modelling together with the mechanical properties of the masonry.

Figure 4.2 - Three views of the Becci tower.

Numerical model

A three-dimensional numerical model is employed to reproduce the geometry of the tower and to represent its linear dynamic behaviour by using the commercial code ANSYS. Maximum dimension of the mesh is about 50 cm, realized with SOLID285, a three-dimensional tetrahedral structural solid. The element has a linear behaviour and is defined by four nodes having four degrees of freedom at each node: three translations in the nodal *x*, *y* and *z* directions, and one hydrostatic pressure.

In order to perform linear modal analyses, the numerical model requires the identification of both material properties (*i.e.* elastic modulus and mass density) and boundary conditions. As underlined in the previous sections, invasive experimental in situ tests to identify the mechanical properties of the masonry, are usually infeasible for monumental buildings. Due to this fact, the information related to the mechanical properties of the masonry are acquired through detailed visual examinations and on the base of expert judgment. The Italian recommendations [117] provide a classification of the main typologies of existent masonry, including the variability range for their mechanical characteristics, as reported in Table 4.2.

As far as the boundary conditions are concerned, the base of the model is supposed to be fixed and the effect of the adjacent structures is reproduced as horizontal constraints. The assumption of neglecting the soil-structure interaction is based on a research of Madiai *et al.* [118] which studies this aspect on the San Gimignano towers. This research demonstrates small differences

(approximately 2%) in the fundamental natural frequency by means a comparison with a fixed-based model of the tower.

Commonly, the geometry and the boundary conditions of the structures are considered as perfectly known and the experimental data are used to choose the proper values of the mechanical properties in order to reduce the discrepancy between the model output and the experimental evidence. In this work, the geometry of the tower is considered as known but the boundary conditions (*i.e.*, the effect of the lateral buildings) and the mechanical properties of the masonry are considered as uncertain.

Table 4.1 - Becci tower sections (*H* total height, *S* base section dimensions and $\lambda_{x,y}$ slenderness) and FE-model.

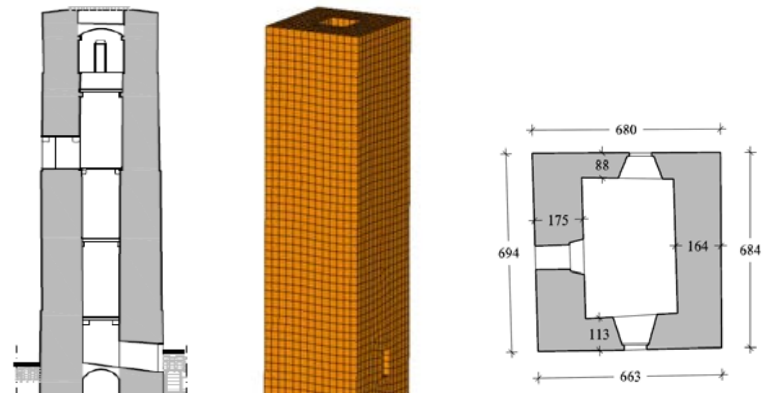

H [m]	38.4
S [m]	~ 6.8x6.9
λ_x [-]	5.7
λ_y [-]	5.6

Table 4.2 – Mechanical properties of masonry typologies (data from CNR-DT 212/2013).

Masonry typology		f_c [MPa]	E [MPa]	G [MPa]	w [kN/m^3]
Irregular stone masonry (pebbles, erratic and irregular stone)	μ	1.40	870	290	19
	σ_{ln}	0.29	0.21	0.21	
Uncut stone masonry with facing walls of limited thickness and infill core	μ	2.50	1230	410	20
	σ_{ln}	0.20	0.17	0.17	
Regular stone masonry with good texture	μ	3.20	1740	580	21
	σ_{ln}	0.19	0.14	0.14	

Masonry typology		f_c [MPa]	E [MPa]	G [MPa]	w [kN/m^3]
Soft stone masonry (tuff, limestone, etc.)	μ	1.90	1080	360	16
	σ_{ln}	0.27	0.17	0.17	
Dressed rectangular stone masonry	μ	7.00	2800	860	22
	σ_{ln}	0.14	0.14	0.09	

Note: f_c = compressive strength, E = elastic modulus, G = shear modulus, w = specific weight. These properties, except for the specific weight, are expressed with the mean of the associated Gaussian distribution and the standard deviation of the corresponding lognormal distribution.

Experimental data

As mentioned before, the interferometric radar was used for measuring the natural frequencies of the towers of San Gimignano. This expeditious and no-contact technique has some limitations when used in field. Vegetation, scaffoldings, lightning rods, and narrow streets are all possible hindrances that can prevent a correct measurement of the displacement in time, as reported in [102]. The aim of the measurement is to observe the movement of the structure at several heights. Each measurement position provides information about a projection of the real movement along the direction of view, and by combining all information an estimate of the mode shape and the direction of the movement at each resonance frequency can be obtained. As measurements from different points of view were carried out at different times, possible changes on the environmental conditions (noise sources, weather conditions, etc.) could occur. This aspect affect the amplitude and phase of detected modes, but not their shape and frequency that are rather insensitive to the environmental conditions. In addition, other measurements investigation were carried out by using a three component portable seismograph and estimating the resonance frequency of the towers [103]. According to these experimental campaigns, the first two natural periods along the two main directions of the Becci tower were collected and shown in Table 4.3. The uncertainties related to these measurements, without more detailed analyses and information, are assumed independent to the $\boldsymbol{\theta}$-parameters value and can be represented through zero-mean Gaussian distributions, centred on the experimental values. The standard deviation is assumed the same for each measurement but two levels of accuracy are hypothesized by considering the values of 0.01 and 0.02 Hz, as reported in Figure 4.8. These two values allow to take into account the effect of non-accurate measurements; indeed, 0.02 Hz is considered the maximum achieved level of uncertainty for the experimental measurements.

Table 4.3 - Experimental measurements of the Becci tower.

Tower	Direction	Natural period, T [s]
Becci	N-S	0.73
	E-W	0.60

4.2.2.FE-Model updating

The aim of the FE-model updating is twofold: firstly, to reduce the uncertainties on the material parameters estimation and secondly, to provide an alternative use of the dynamic experimental data usually available for historic masonry towers, in order to update and improve the knowledge on the FE-model. Two cases are herein considered in detailed. The first, reported as *Case 1*, considers as unique random variable the elastic modulus of the masonry and the height of the lateral restraints is considered as modelling uncertainty. The second, reported as *Case 2*, considers as random variables both the elastic modulus of the masonry and the effective height (*i.e.* the height of the tower out of the restraints offered by the adjacent buildings at the lower levels). Indeed, the sensitivity analysis on the natural periods of slender masonry structures, presented in Chapter 3, has revealed a great relevance of these two parameters.

4.2.2.1. ***Case 1**: Elastic modulus updating*

The knowledge on the elastic modulus of the masonry, *E*, is updated with the Bayesian approach, by using the measurements of the first two natural periods, $\bar{T} = \{\bar{T}_1, \bar{T}_2\}$. As result, but without loss of generality, Eq. (27) becomes:

$$p_{\bar{T}}(\mathrm{E}) = p(\mathrm{E}|\bar{T}) = \frac{p(\bar{T}|\mathrm{E})p_0(\mathrm{E})}{\int p(\bar{T}|\mathrm{E})p_0(\mathrm{E})\mathrm{dE}} \tag{31}$$

In which, the prior distribution, $p_0(\mathrm{E})$, takes into account a population of possible values, including all plausible ones. Different prior distributions, represented by probability density functions, are chosen in order to reflect a range of situations from good prior knowledge (low value of standard deviation) to limited knowledge (large value of standard deviation) or event no knowledge. This means that the Bayesian approach uses these PDFs as initial measure of the uncertainty. Note that, direct data are unavailable on the mechanical characteristics of the masonry used to construct the Becci towers, thus a plausible range of values of elastic modulus can be firstly established on the base of visual investigation. In this process, literature values for the elastic modulus are used as a first input according to Table 4.2, that reports the masonry typologies supplied in Italian building code. Two distributions, characterized by the same median value, are considered: the first is a lognormal PDF with associated Gaussian distribution mean equal to 1,600 MPa and standard deviation equal to 0.17 MPa, the second is a uniform PDF ranging from 1,052 MPa to 2,084 MPa (Figure 4.3).

As far as the specific weight is concerned, two possible values are selected: 16 kN/m^3 and 19 kN/m^3 (Table 4.2), which represent two limit values for the considered typology of masonry. The

correlation of this parameter with the elastic modulus (as underlined also in the previous chapter) could be considered as random variable. However, due to the low variability of the specific weight, its effect on the results is considered by analysing the two selected values in terms of the elastic modulus updating.

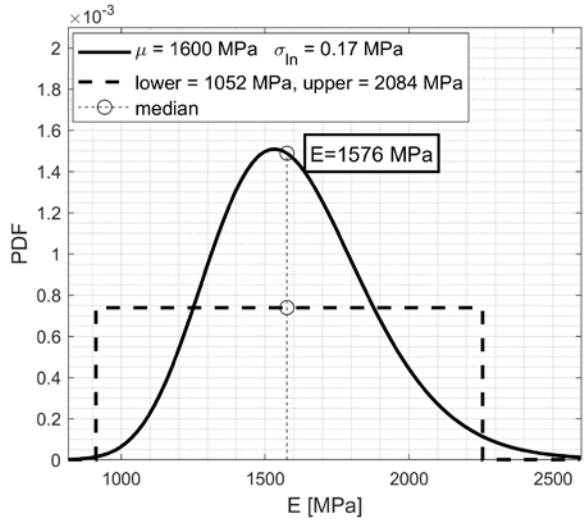

Figure 4.3 – Two possible prior distributions of the elastic modulus: lognormal and uniform.

The likelihood function can be expressed as follows:

$$p(\bar{T}|E) = \int p(\bar{T}|T,E)p(T|E)dT \tag{32}$$

$p(\bar{T}|T,E)$ represents the measurement error, as defined in Figure 4.8, while $p(T|E)$ denotes the PDF used to characterized the modelling uncertainties, which accounts for the variability of the boundary conditions. As shown in Figure 4.2, the Becci tower is incorporated into the neighbouring buildings, which clearly interact with the tower, influencing its dynamic behaviour and making a difficult task the definition of the restraint conditions to be assumed in the FE-model. This source of uncertainty is treated by modelling the tower as a rigidly laterally-restrained structure with a fixed base. The height of the free-standing part of the tower (or conversely the height of the lateral restraints) is different along the four sides as shown in Figure 4.4 for the North-South direction (N-S) corresponding to the first natural period, and in Figure 4.5 for the East-West (E-W) direction corresponding to the second natural period. In order to represent these levels of restraint, two types of lognormal distributions for the two main directions of the tower are considered to investigate their effect on the results. In particular, A1 and A2 distributions are characterized by a standard deviation of 0.04 m and a mean value equal to 25 m and 23 m, respectively for N-S and E-W directions. In addition, two other lognormal distributions, denoted

as B1 and B2, are built with standard deviation equal to 1.2 m and a mean value of 4 m shifted of 23 m and 21 m, respectively for N-S and E-W directions. These two groups of distributions, indicated in the following as A and B, are characterized by the same median value for each side of the tower, and represent the uncertainty related to the effectiveness of the lateral buildings in terms of restraint conditions.

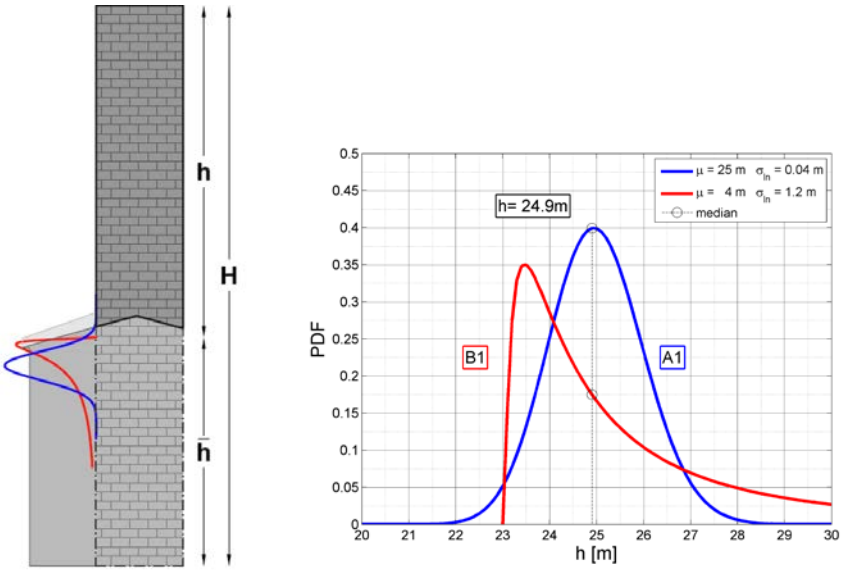

Figure 4.4 - PDFs of the height of the unrestrained part of the tower, N-S direction.

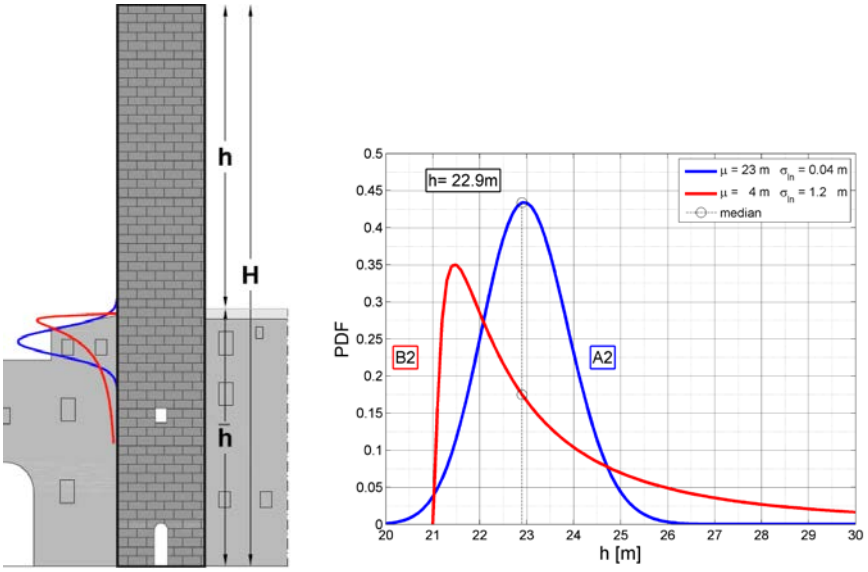

Figure 4.5 - PDFs of the height of the unrestrained part of the tower, E-W direction.

In order to generate representative draws from probability distributions, the classical sampling techniques are employed. One of the most widely used methods is Monte Carlo (MC) technique

but, requiring a great number of samples, it is usually replaced with alternative sampling methods which provide smaller but representative values from the probability distributions. In this work, Latin Hypercube (LH) sampling is employed to represent the PDFs of the unrestrained height of the tower *h*.

The effectiveness of this method is tested through a comparison with traditional MC simulation. For the sake of example, A1 distribution is sampled with both MC and LH method, obtaining respectively, 10^4 and 200 values of *h*. These values are used to obtain the variability of the first natural period provided by modal analyses on FE-model, by using the sampled restraint conditions *h* and a single value of *E*. Figure 4.6 shows these results, by comparing MC and LH methods in terms of Exceedance Density Function (EDF) of the first period. This figure highlights a good agreement between the two compared methods, allowing the use of LH method to reduce the computational effort of the analyses. In this respect, 200 values of *h* are sampled in order to represent the distributions shown in Figure 4.4 and Figure 4.5 (A1, A2 and B1, B2).

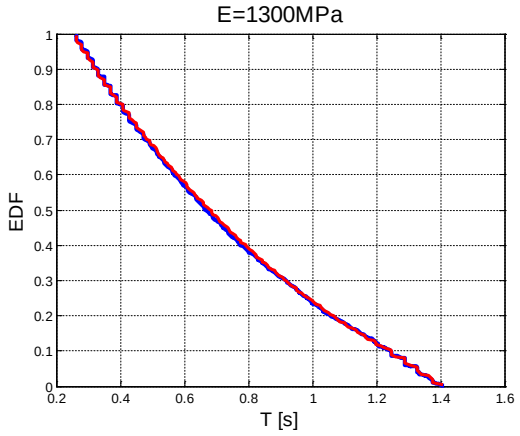

Figure 4.6 – Results of the modal analyses in terms of Exceedance Density Function (EDF) of the natural period. The blue line represents MC method and the red line the LH method.

The variability of the lateral restraints is combined with the uncertain mechanical characteristics of the linear model. The elastic modulus *E*, considered in this case as unique random variable, ranges from 800 MPa to 2,600 MPa; in this interval 200 values are selected. Moreover, as far as the specific weight is concerned, two representative values (16 kN/m^3 and 19 kN/m^3) are taken into account. 40,000 modal analyses are then carried out in both directions and for the two types of restraint conditions selected: A1, B1 for N-S direction and A2, B2 for E-W direction.

200 values of elastic modulus (from 800 MPa to 2,600 MPa), considered as random variable are selected, obtaining for each value of specific weight, 40,000 modal analyses. These modal analyses are carried out for the two types of restraint conditions selected (A and B), which

consider the different height of lateral buildings (A1, A2 and B1, B2) for the two main directions of the tower. It is worth noting that, the first two frequencies are considered dependent on only the lateral restraint along the corresponding direction. Indeed, the first natural period, corresponding to the N-S direction, is only influenced by the restrained conditions provided by the adjacent buildings located in this direction (A1 and B1 distributions).

For the sake of example, Figure 4.7 represents the results in terms of EDF of the modal analyses carried out considering A1 distribution and w (specific weight) equal to 16 kN/m^3. The Figure highlights the variability of the first natural period for each value of elastic modulus; this is due on the modelling uncertainties, *i.e.* the height of lateral restraints.

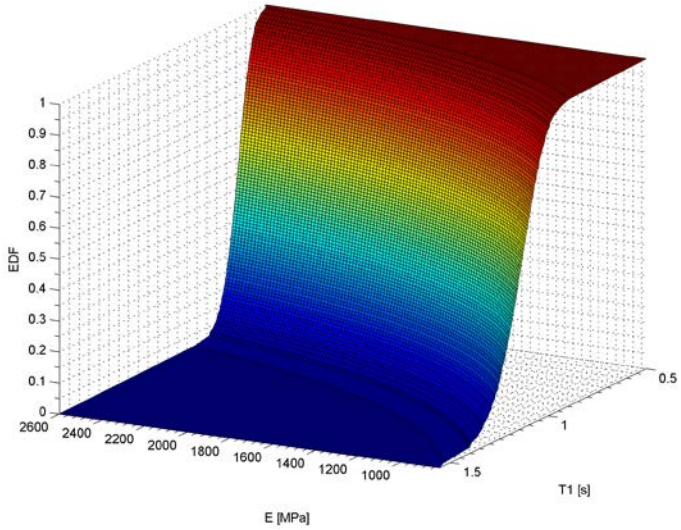

Figure 4.7 – EDF of the first natural period.

Lastly, for each value of elastic modulus, the modelling uncertainties $p(T|E)$ are multiplied for the measurement errors ($p(\bar{T}|T,E)$, Figure 4.8), which are independent on the value of E.

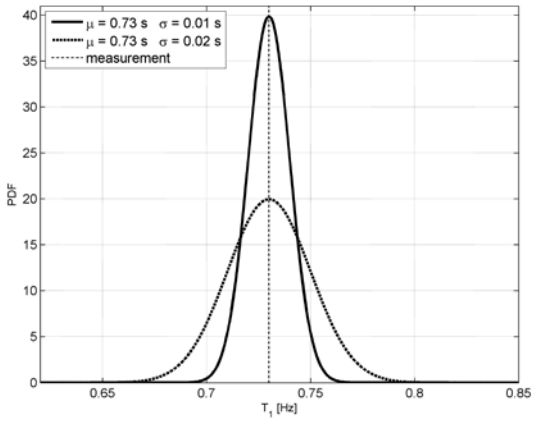

Figure 4.8 - PDFs of two measurement errors for the first natural period of the Becci tower.

Since two experimental data are available for the Becci tower, the posterior distribution $p(\mathrm{E}|\bar{T})$ is herein presented as the result of two successive updates. The sensitivity of the posterior distribution is evaluated for different assumptions of prior distributions, material density, modelling and measurement error. The introduction of the second natural period produces, in each case, a relevant reduction of the uncertainty (in terms of standard deviation) and a minimum variation in terms of the mean value.

A first comparison, the posterior distributions of *E* related to different modelling uncertainties are proposed. The effect of the two selected types of restraint conditions, previously introduced as A and B, are shown in Figure 4.8, highlighting the significant variations both in terms of the mean value and standard deviation. The median value of the posterior distribution ranges from 1989 MPa for the modelling uncertainties A, to 1662 MPa for the modelling uncertainties B; thus causing an increment of 20% and 5% on the prior distribution median value, respectively.

Moreover, Table 4.4 shows the comparison in terms of percentiles underling a considerable reduction of the variability, especially for the case B.

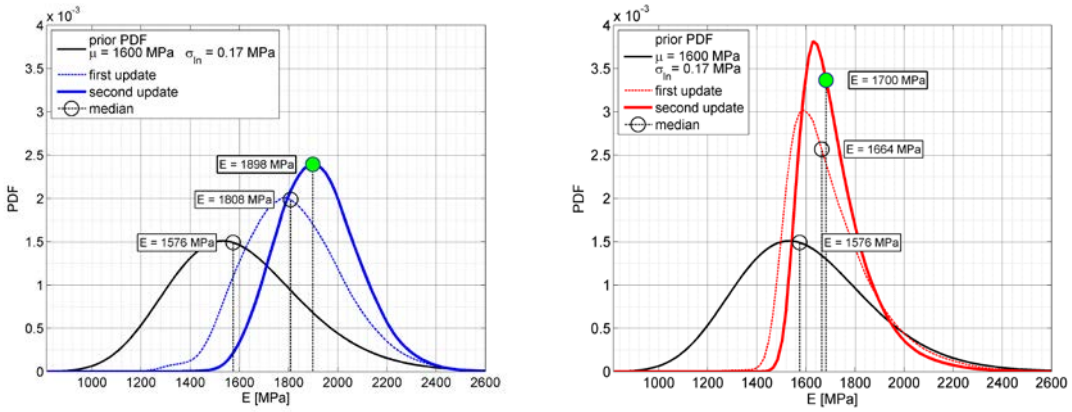

(a) (b)

Figure 4.9 – Posterior distributions of *E* for modelling uncertainties: (a) A and (b) B.

Table 4.4 – Percentiles of the posterior distributions (MPa) related to the considered modelling uncertainties (A and B).

Percentiles	25th	50th	75th
Prior PDF	1396	1576	1756
A	1790	1898	2024
B	1610	1700	1772

Another comparison is proposed in Figure 4.10 and Figure 4.11, changing the specific weight from 16 kN/m^3 for the cases indicated with (a) to 19 kN/m^3 for the cases indicated with (b). This

variation causes a shift of the posterior curves, as shown in Figure 4.10 and Figure 4.11 for the model uncertainty A and B, respectively. These results seem to confirm a correlation between the elastic modulus and the mass density.

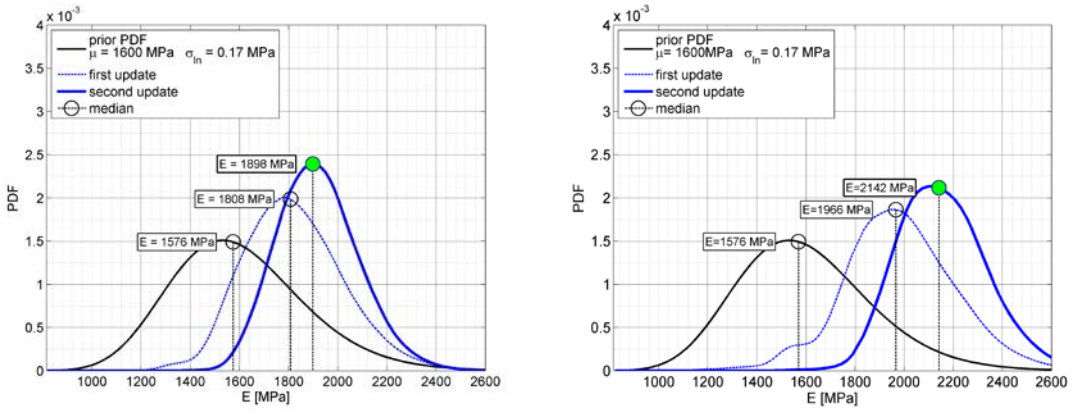

(a) (b)

Figure 4.10 – Posterior distributions of *E* for modelling uncertainty A, considering w equal to (a) 16 kN/m^3 and (b) 19 kN/m^3.

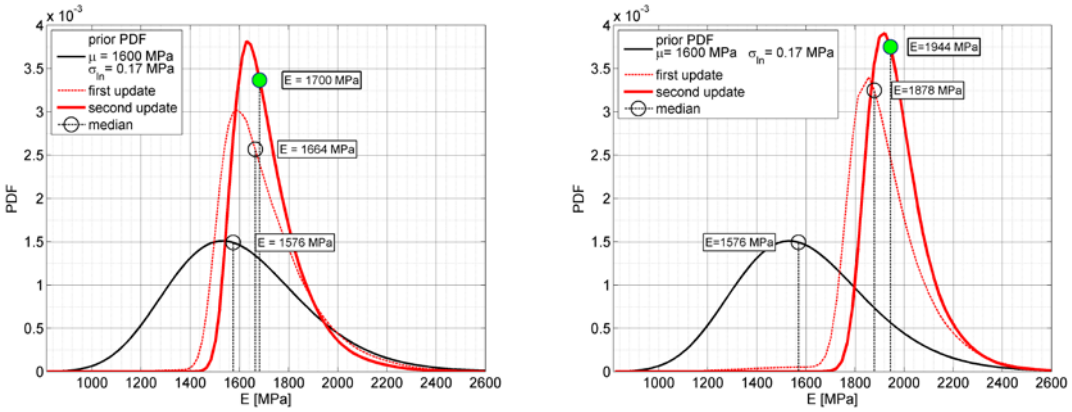

(a) (b)

Figure 4.11 – Posterior distributions of *E* for modelling uncertainty B, considering w equal to (a) 16 kN/m^3 and (b) 19 kN/m^3.

Table 4.5 - Percentiles of *E* distributions (MPa) related to both the modelling uncertainties (A and B) and two values of w. In addition, the value of the velocity of propagation of the P-waves (m/s) related to the 50th of *E* is reported.

	w = 16 kN/m^3				w = 19 kN/m^3			
Percentiles	25th	50th	75th	$v_p = \sqrt{E/\rho}$	25th	50th	75th	$v_p = \sqrt{E/\rho}$
Prior PDF	1396	1576	1756	992	1396	1576	1756	992
A	1790	1898	2024	1,088	2010	2142	2274	1,062
B	1610	1700	1772	1,019	1878	1944	2032	1,011

Different measurement errors are considered according to the PDFs reported in Figure 4.8; but this effect seems to have a less relevance compared to the other assumptions. Especially in terms of median value, no substantial differences are observed.

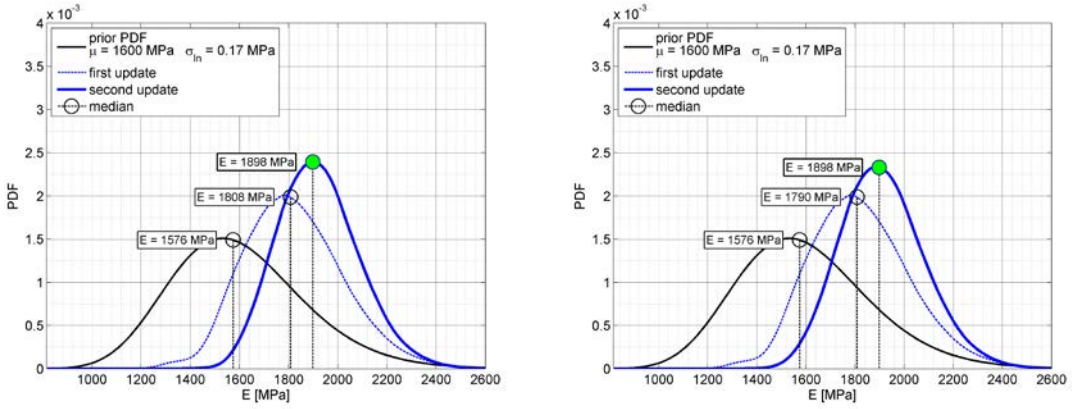

(a) (b)

Figure 4.12 – Posterior distributions obtained by considering modelling uncertainty A and measurement errors characterized by a standard deviation equal to (a) 0.01 Hz and (b) 0.02 Hz.

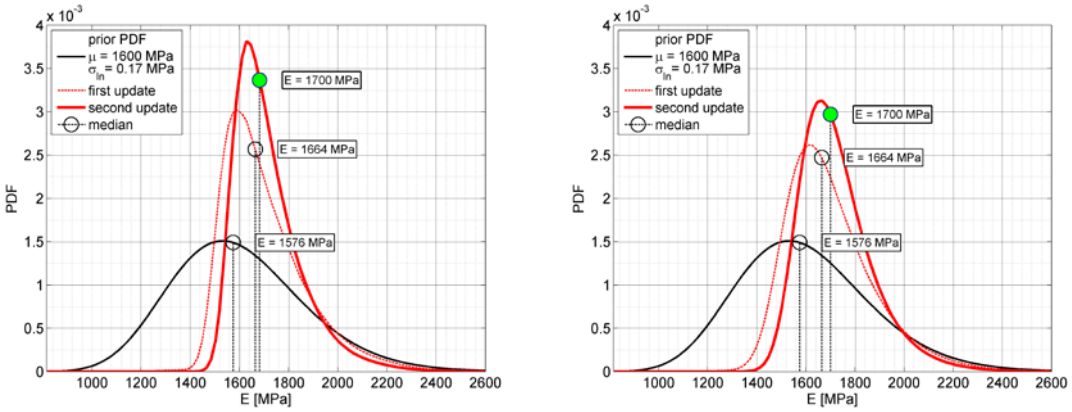

(a) (b)

Figure 4.13 – Posterior distributions obtained by considering modelling uncertainty B and measurement errors characterized by a standard deviation equal to (a) 0.01 Hz and (b) 0.02 Hz.

Table 4.6 - Percentiles of the posterior distributions (MPa) related to both the modelling uncertainties (A and B) and different measurement errors.

$p(\bar{T}\|T,E)$	$\mu = \bar{T}\ ;\ \sigma = 0.01$ Hz			$\mu = \bar{T}\ ;\ \sigma = 0.02$ Hz		
Percentiles	25th	50th	75th	25th	50th	75th
Prior PDF	1396	1576	1756	1396	1576	1756
A	1790	1898	2024	1772	1898	2006
B	1610	1700	1772	1610	1700	1790

The last comparison regards the effect of three different choice of prior PDFs for the two typologies of modelling uncertainties considered.

Specifically, the rows of Figure 4.14 introduce the posterior PDFs of *E* for two lognormal and one uniform prior PDFs; in addition, the columns of the same figure show the comparison between A and B modelling uncertainties.

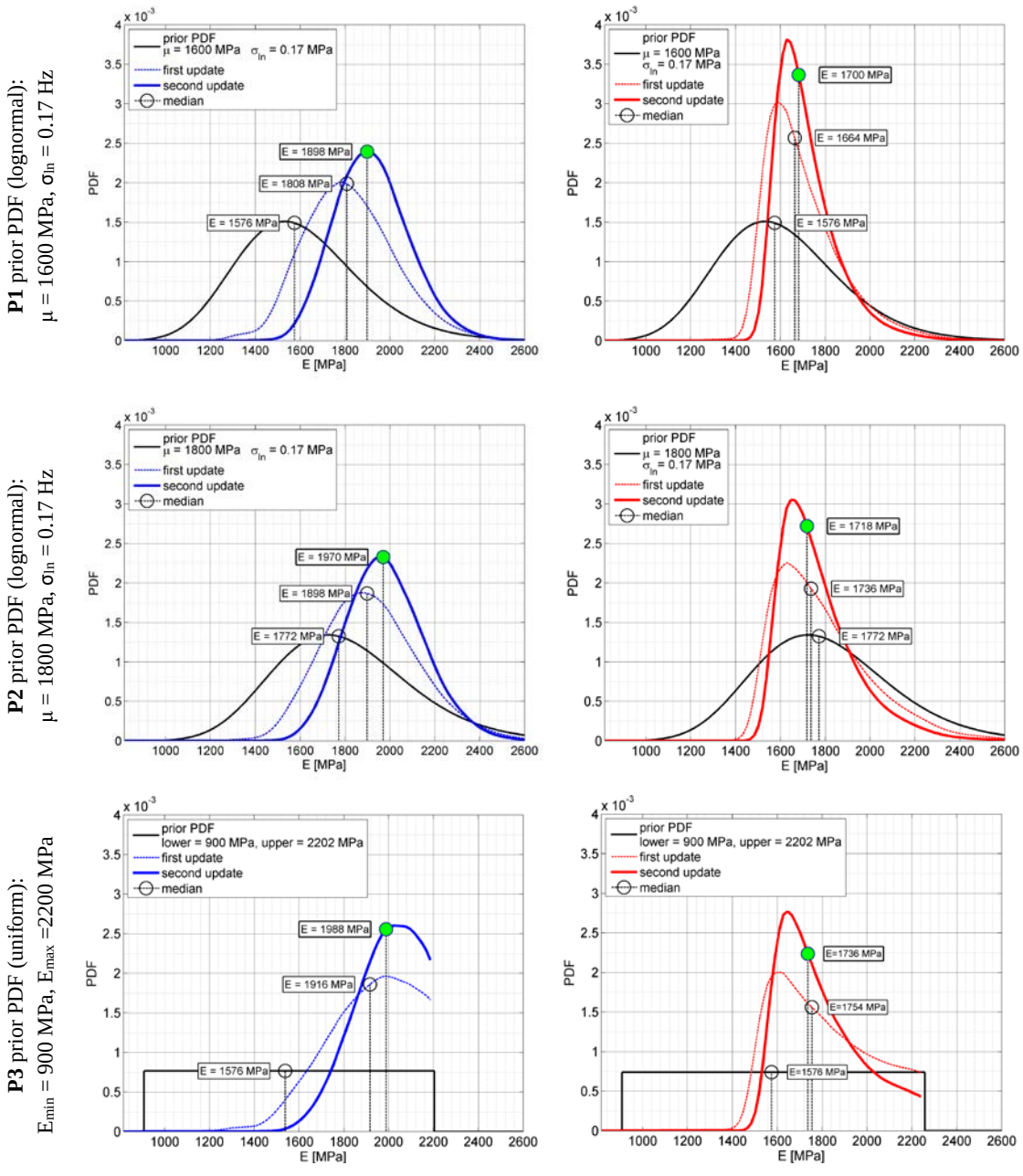

Figure 4.14 – Posterior distributions of *E* for different prior PDFs and considering modelling uncertainty: (a) A and (b) B.

Table 4.7 - Percentiles of the posterior distributions (MPa) related to both the modelling uncertainties (A and B) and different prior distributions (P1, P2 and P3).

Percentiles	25th	50th	75th	25th	50th	75th	25th	50th	75th
		P1			**P2**			**P3**	
Prior PDF	1396	1576	1756	1576	1772	1976	1225	1576	1875
A	1790	1898	2024	1844	1970	2078	1880	1988	2078
B	1610	1662	1772	1628	1718	1844	1646	1736	1880

The three prior distributions of *E* are chosen in order to assess their effect on the posterior ones, both in terms of different median value (P1 and P2 in Figure 4.14) and in terms of different typology of distribution (P1 and P3 in Figure 4.14).

Specifically, the comparison between the first two rows of Figure 4.14 allows to assess the effect of a considerable variation of the prior median value on the posterior PDFs of *E*. These lognormal prior distributions, characterized by the same standard deviation, have different mean values equal to 1,600 MPa (P1) and 1,800 MPa (P2).

In addition, the comparison between the first and the third row of Figure 4.14 allows to consider the effect of a different typology of distribution (lognormal P1, and uniform P3) maintaining the same median value equal to 1576 MPa.

Analysing these results emerge that the posterior PDFs of *E* are almost insensitive to variation of priori PDFs both in terms of mean value and in terms of distribution typology. Furthermore, this consideration is valid for both the considered modelling uncertainties, confirming the good selection of the random variable and its relevant effect on the experimental data used in the Bayesian updating.

As conclusive remarks for the *Case 1*, the following considerations can be drawn:

- the choice of the modelling uncertainty distribution plays a relevant role on the posterior PDFs of *E* both in terms of median value and standard deviation.
- ρ influences considerably the median value of the posterior PDFs of *E*, confirming that the natural period depends on a functional relationship between these two material properties. This aspect is underlined also from the values of v_p related to the 50^{th} percentile of the *E* distributions, shown in Table 4.5.
- the effect of measurement uncertainty is neglected compared to the other assumptions.
- the posterior PDFs of *E* are insensitive to variations of prior PDFs.

4.2.2.2. ***Case 2**: Elastic modulus and lateral restraints height updating*

The results presented in the previous section have confirmed the no negligible effect of the lateral restraint of the numerical model on its Bayesian updating. Due to this consideration, a second case is analysed taking into account the vector $\theta = \{E, h\}^T$, that collects two random variables: the elastic modulus, E, and the height of lateral restraints, h. This vector is updated through the Bayesian approach by using as new information the measurement of the first natural period of the tower. In this case, the procedure is applied by employing only one measurement of the natural period; indeed, considering as effective only the restraint conditions in the direction of the considered period, the use of the second period needs the introduction of an additional random variable: the restraint conditions in the relative direction. This aspect, for the sake of simplicity, is neglected.

The posterior joint-probability density function, $p(\boldsymbol{\theta}|\bar{T})$, is updated starting from a prior joint-probability density function defined as the product of the two marginal distributions (Figure 4.15 and Figure 4.16), indeed the two random variables are considered as independent:

$$p_0(\boldsymbol{\theta}) = p_0(E, h) = p_0(E)p_0(h) \tag{33}$$

$$p_{\bar{T}}(\boldsymbol{\theta}) = p(\boldsymbol{\theta}|\bar{T}) = \frac{p(\bar{T}|\boldsymbol{\theta})p_0(\boldsymbol{\theta})}{\int p(\bar{T}|\boldsymbol{\theta})p_0(\boldsymbol{\theta})\mathrm{d}\boldsymbol{\theta}} \tag{34}$$

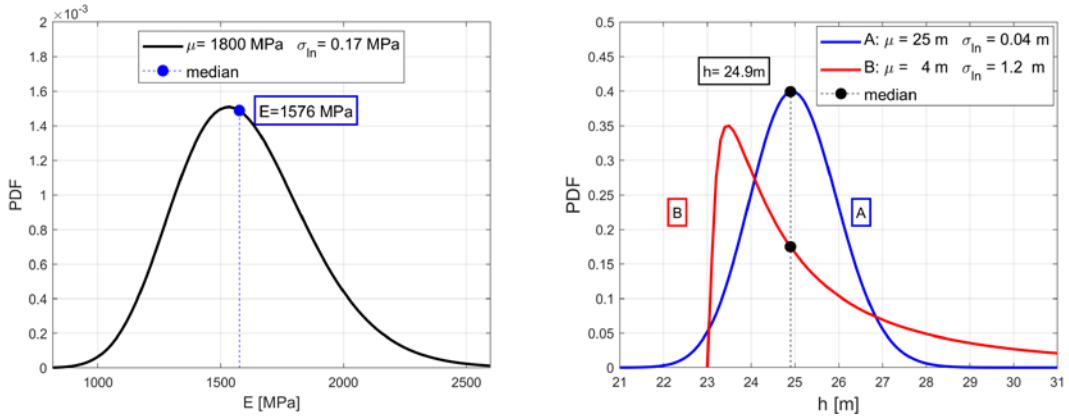

(a) (b)

Figure 4.15 - Prior distributions of (a) the elastic modulus and (b) the effective height of the tower.

Note that in the following the results are referred to the A distribution, shown in Figure 4.15b.

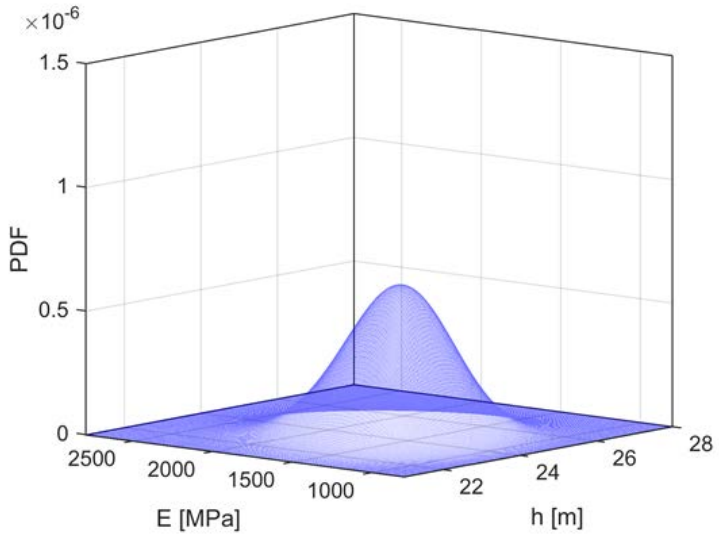

(a)

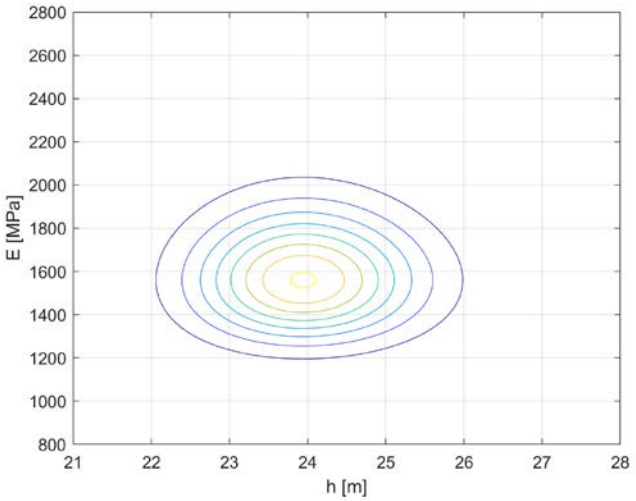

(b)

Figure 4.16 – Two views of prior joint-probability distribution of elastic modulus, *E*, and the effective height of the tower, *h* (distribution A).

Also in this case, the likelihood function accounts for both the modelling and measurements uncertainties:

$$p(\bar{T}|\boldsymbol{\theta}) = \int p(\bar{T}|T, \boldsymbol{\theta}) p_0(T|\boldsymbol{\theta}) \mathrm{d}\boldsymbol{\theta} \tag{35}$$

In this case, both these uncertainties are represented by zero-mean Gaussian distributions. Specifically, the former term is the modelling uncertainties, selected according to the results of

the previous case, which have underlined a negligible effect of different dispersion of this parameter. Thus, only one value of the standard deviation is considered (equal to 0.01 s, Figure 4.17) and the distribution is considered centred at the experimental measurement $\bar{T}$.

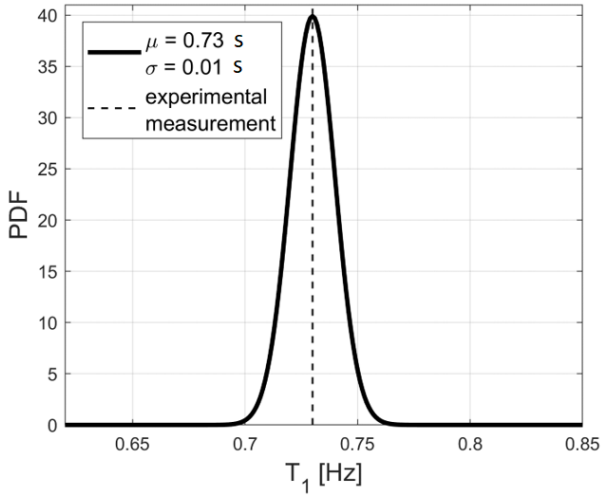

Figure 4.17 - PDFs of the measurement error.

In this second case, also the modelling errors, represented as the latter term in Eq. (35), is modelled with an analogous Gaussian distribution centred at the prediction of FE-model of the tower, in terms of natural period T. Without additional and reliable information on this uncertainty, a standard deviation is assumed equal to 0.04.

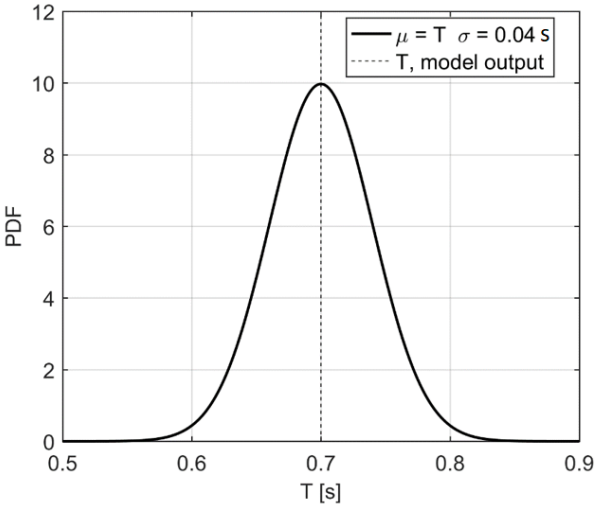

Figure 4.18 - PDFs of the modelling error.

The result of Eq. (34) is shown in Figure 4.19 and Figure 4.20 through the comparison between prior and posterior joint-probability density function of the vector **θ**.

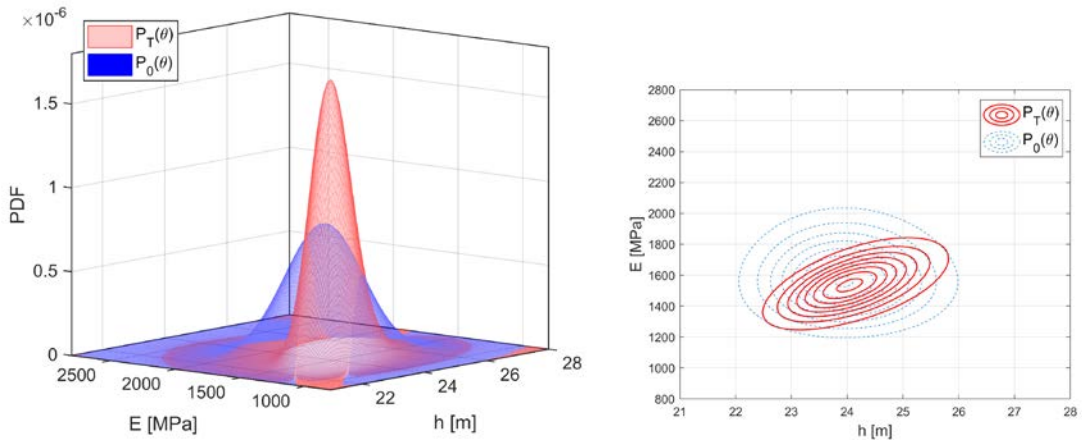

Figure 4.19 – Two views of prior (blue surface) and posterior (red surface) joint-probability distributions of the elastic modulus, *E*, and the unrestrained height of the Becci tower, *h*.

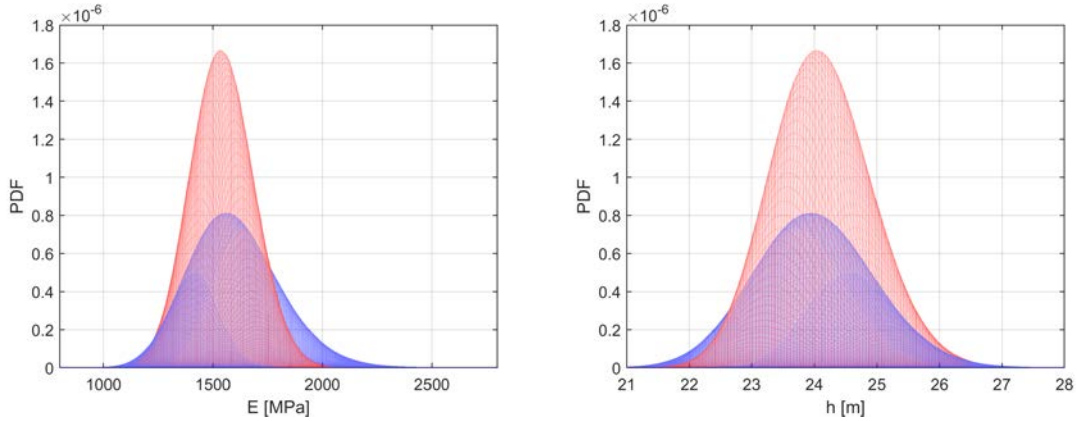

(a) (b)

Figure 4.20 – Two views of prior (blue surface) and posterior (red surface) joint-probability distributions of (a) the elastic modulus, *E*, and (b) the unrestrained height of the Becci tower, *h*.

As previously proposed, also in this case a comparison between posterior distributions in terms of different prior assumptions, can be useful to test the sensitivity of the results. For this purpose, Figure 4.21 reports the selected prior distributions. Specifically, a different lognormal prior distribution of the elastic modulus is considered, with mean and standard deviation equal to, respectively, 1800 MPa and 0.17 MPa (Figure 4.21a).

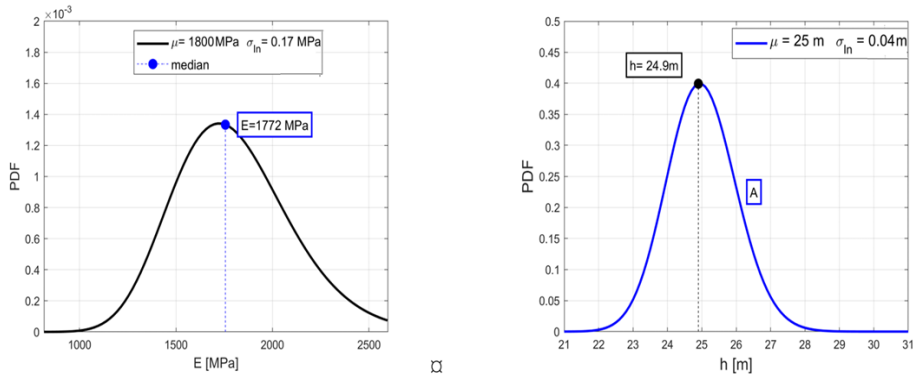

(a) (b)

Figure 4.21 - Prior distributions of (a) elastic modulus and (b) restrained conditions of the tower.

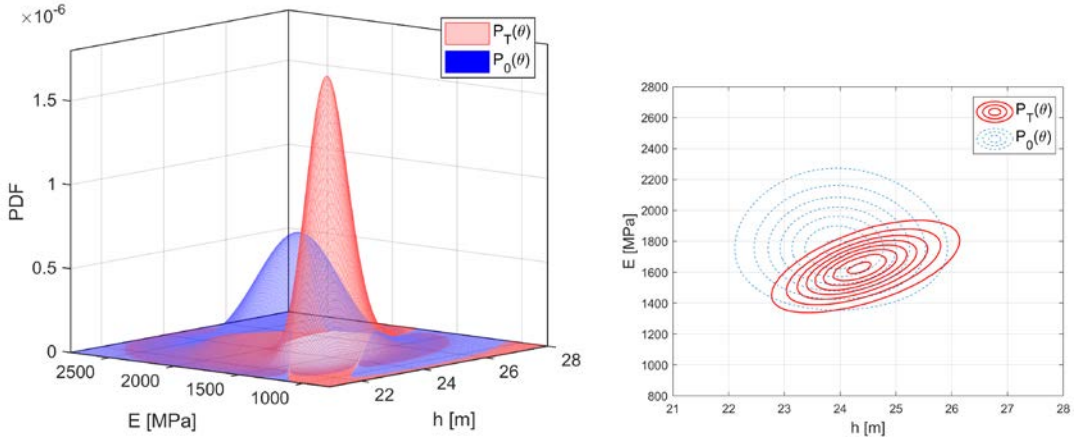

Figure 4.22 – Two views of prior (blue surface) and posterior (red surface) joint-probability distributions of the elastic modulus, *E*, and the unrestrained height of the Becci tower, *h*.

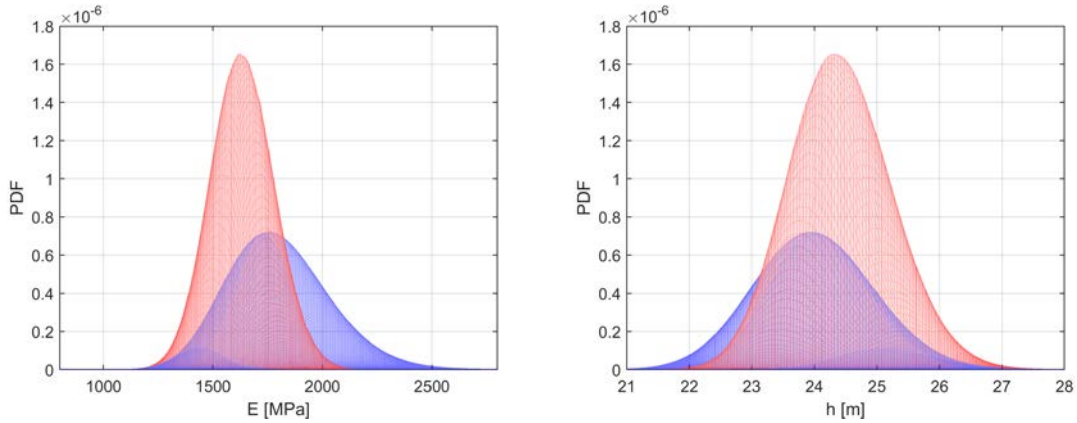

(a) (b)

Figure 4.23 – Two views of prior (blue surface) and posterior (red surface) joint-probability distributions of (a) the elastic modulus, *E*, and (b) the unrestrained height of the Becci tower, *h*.

4.3. Conclusions

In this chapter, the Bayesian FE-model updating has been introduced in the analysis of historic masonry towers, by using the measurement of natural periods. The experimental data was herein employed to identify a variation range of the structural parameters, which are usually strongly dependent on the expert judgment. The procedure has been presented according to a specific reference case (the Becci tower of San Gimignano) but preserves general features, which makes this framework easily applicable to other case studies.

The results have been evaluated considering different assumptions in terms of prior distributions, modelling and measurement errors, in order to both evaluate their sensitivity and explicitly consider different sources of uncertainties. Two cases have been considered in detail: the first has taken into account the elastic modulus of the masonry as unique random variable, including as modelling uncertainty the level of lateral restraints; the second has proposed the updating of both the elastic modulus of the masonry and the level of lateral restraints. In both cases the Bayesian procedure was applied using the experimental measurement of natural periods as new information, providing the opportunity to take advantage of these dynamic data by increasing the accuracy of the model by reducing the statistical uncertainty. Note that, the use of only few experimental data gains much relevance for historical masonry constructions, indeed, for these structures extensive and invasive experimental campaigns are usually infeasible.

The obtained posterior PDFs have shown a significant improvement of the predictive capability of the selected random variables, showing a small variation of the mean values both of E and h with a considerable reduction of the uncertainty. These results have allowed to obtain a more reliable numerical model which will be used for the successive seismic analyses, providing more accurate information about the expected performance of the structure.

Chapter 5

Robust seismic fragility curves

The challenging issues of giving more accurate estimates of the seismic vulnerability of masonry towers, and of providing a quantitative assessment of this accuracy, can be considered two important steps in the seismic risk chain. These goals are addressed in this dissertation integrating the Bayesian probabilistic methodology for system identification, introduced in the previous chapter, with probabilistic structural analyses. The result, which composes the second step of the framework proposed at the initial chapter in Figure 1.3, provides the definition of seismic fragility curves based on a robust reliability model, updated with dynamic test data. The concept of robust reliability is introduced considering the uncertainties from structural modelling in addition to the uncertain actions on the structure during its lifetime [63,64]. The updated reliability curves may be used to identify potentially unsafe scenario and to promote control strategies when the structure appears vulnerable to possible future severe loads.

In the scientific community, the issue of the quantification of the role of different sources of uncertainties on the global structural behaviour, has been gaining an increasing attention as confirmed by the several applications in different engineering fields, *e.g.* [74–78]. However, only few cases are related to masonry constructions *e.g.* Tecchio et al. [79], which reports seismic fragility curves of as-built single-span masonry arch bridges, assessing the variability of both model parameters and seismic action and Rota et al. [60], which proposes a methodology for deriving fragility curves for ordinary masonry buildings based on stochastic nonlinear analysis. For masonry constructions, in fact, the inherent complexity and the computational effort of nonlinear seismic analyses still make the comprehensive probabilistic assessment difficult, thus the use of approximate structural models and simplified methods become necessary. In this

respect, masonry towers can represent an interesting application to test a more general procedure, due to their structural simplicity.
In this chapter, robust reliability of seismic fragility curves of masonry towers is defined taking into account different sources of uncertainties and considering both measured data and prior engineering information.

5.1. Methodology

In a probabilistic framework for seismic risk assessment, structural response predictions and performance reliability are updated using experimental test data, $\overline{D}$, by considering the predictions of a whole set of possible structural models that are weighted by their updated probability. This involves to integrate the model prediction of a response quantity of interest, and the updated probability density function for the structural parameters, which provides a measure of how plausible each model is, given the data.
The failure event *F* is defined by using the PGA as intensity measure of the ground-motion and by evaluating the condition $PGA_c \leq PGA_d$ (*c* stands for capacity and *d* for demand).
$P_{\overline{D}}(F) = P(F|\overline{D})$ represents the *robust* failure probability which incorporates the knowledge from the system, and the updated information from $\overline{D}$ [63,64]:

$$P_{\overline{D},j}(F) = \int P_j(F|\boldsymbol{\theta})\, p_{\overline{D}}(\boldsymbol{\theta})\, d\boldsymbol{\theta} \qquad j = 1, \dots, N \tag{36}$$

In Eq. (36) the theorem of total probability is used, *j* represents each PGA value considered for the definition of the probability of collapse and $\boldsymbol{\theta}$ is the vector that collects the random variables; $P_j(F|\boldsymbol{\theta})$ is the probability of failure for the *j-th* PGA given the parameters $\boldsymbol{\theta}$ and $p_{\overline{D}}(\boldsymbol{\theta})$ represents the joint-probability distribution of the model parameters $\boldsymbol{\theta}$. This latter term is herein considered as the result of the Bayesian updating introduced in the previous chapter through Eq. (27). Indeed, the elastic modulus of the masonry and the effective height of the tower (*i.e.* the unrestrained part of the tower) are considered as random variables and collected in the vector $\boldsymbol{\theta} = \{E, h\}^T$.
The first part of the integral of Eq. (36) represents the probability of failure conditioned to the values of the parameters *E* and *h* for each PGA of demand. This term is evaluated through nonlinear static analyses, taking into account the variability of the inelastic behaviour of the masonry. The second term of the integral of Eq. (36) represents the joint-probability distribution of the model parameters $\boldsymbol{\theta}$. In this dissertation, this term represents the posterior joint-probability distribution of *E* and *h*, obtained through the Bayesian updating proposed in §4.2.2 by using, as experimental data, the measurement of the first natural period on the tower.

5.2. Conditional probability of failure surface

In the previous chapter, the behaviour of the Becci tower, still considered as reference case, has been described using linear elastic models. Nevertheless, to predict the nonlinear behaviour of the tower against seismic action, nonlinear models must considered, requiring the modelling of the masonry constitutive behaviour over the elastic range, whose characteristics should include heterogeneity and differing responses under tension and compression of the material [1].
The conditional probability of failure of the tower is obtained through a significant number of nonlinear analyses, including the variability of the uncertain model parameters. The procedure is herein presented through the description of the following steps:

- *Numerical model*
- *Numerical analyses typology*
- *Seismic analyses*
- *Sensitivity analyses*
- *Failure surfaces*

5.2.1. Numerical model

A numerical model is used to replicate the nonlinear behaviour of the structure, namely the Becci tower, under seismic action. Its definition, despite preserves general features, is herein introduced with specific reference to the commercial FE code ANSYS.
In order to draw some general conclusions, a simplified geometry is introduced, able to represent the main features of the seismic response of masonry towers. In particular, plan and vertical irregularities, large openings, variation of the cross-section and masses, etc., are neglected. Moreover, as far as the boundary conditions are concerned, the identification of the soil-structure interaction is a difficult task and requires a deep knowledge of the soil characteristics and the definition of adequate numerical models. In this respect, Casolo *et al.* [119] Madiai *et al.* [118] and Ivorra *et al.* [38] report recent studies by focusing the attention on the impact of the dynamic interaction between a masonry tower and the soil. In general, the presence of a stiff soil has often little influence on the first natural frequency, and on the corresponding modal shape. Nevertheless, the higher modes, can be quite modified both in terms of frequency value and in shape. In this dissertation, being aware that is not possible to present an exhaustive study that covers all the possible configurations of the towers, the soil-structure interaction is neglected and

the base of the model is supposed to be fixed. Another critical point is the computational representation of the masonry, because of it is an anisotropic non-homogenous and nonlinear material composed by units (bricks and stones) and mortar joint [120,121]. In this work, these elements are represented by single continuous elements (macro-modelling approach), whose mechanical properties depend on the single components and are evaluated according to both the classification proposed in the Italian recommendation and expert judgment. To model this masonry assemblage, 8-nodes isoparametric finite element with three degrees of freedom at each node (*Solid65*) is employed, with a maximum dimension of the mesh of about 50 cm.

According to the results presented in Betti *et al.*, [2], the masonry is herein assumed as homogenous and isotropic material characterized by elastic-perfectly plastic numerical model with crisis surface completed by cut-off conditions. Detailed descriptions are introduced in the following sections.

5.2.1.1. *Elastoplastic model*

The constitutive low of elastoplastic model is ruled by:

$$\dot{\boldsymbol{\varepsilon}} = \dot{\boldsymbol{\varepsilon}}^{el} + \dot{\boldsymbol{\varepsilon}}^{pl} \quad ; \quad \dot{\boldsymbol{\sigma}} = \mathbf{E}\,\dot{\boldsymbol{\varepsilon}}^{el} = \mathbf{E}\,(\dot{\boldsymbol{\varepsilon}} - \dot{\boldsymbol{\varepsilon}}^{pl}) \tag{37}$$

σ and **ε** denote the stress and the total strain tensor, indicating with the dots the incremental formulation of the law.

The masonry is herein considered as a linearly elastic, homogeneous and isotropic material, the properties are the same at each point and in all directions. The constitutive laws for this material involve three parameters: Young's modulus, *E*, Poisson's ratio, υ, and shear modulus, *G* and is given by the following equation:

$$c_{ijkl} = \lambda\delta_{ij}\delta_{kl} + \mu(\delta_{ik}\delta_{jl} + \delta_{il}\delta_{jk}) \tag{38}$$

where δ_{ij} is the Kronecker-delta-operator, and λ and μ are the Lamé constants. Note that Eq. (38) is defined through two parameters, indeed, the three coefficients *E*, υ and *G* are dependent to each other. The relationship between these coefficients and the Lamé constants is given by:

$$G = \mu; \qquad E = \frac{\mu(3\lambda + 2\mu)}{\lambda + \mu}; \qquad \upsilon = \frac{\lambda}{2(\lambda + \mu)}; \qquad \lambda = \frac{\upsilon E}{(1 + \upsilon)(1 - 2\upsilon)} \tag{39}$$

which allow to find Eq. (40):

$$G = \frac{E}{2(1 + \upsilon)} \tag{40}$$

Moreover, introducing the bulk modulus, *K*, that describes the response of the material to a uniform pressure, the coefficients *E*, *υ*, *G* and *K* are related through the following expressions:

$$K = \frac{E}{3(1-2\upsilon)}; \qquad E = 2G(1+\upsilon) = 3K(1-2\upsilon) \tag{41}$$

The plastic law, which characterizes the material behaviour over the elastic range, requires the definition of three conditions:

- *yield function* that bounds the elastic domain (the beginning of plastic flow)
- *rule of plastic flow*, correlating the plastic deformation, $\dot{\boldsymbol{\varepsilon}}^{pl}$, to the current state of stress
- *hardening rule* which modifies the yield function during the plastic flow

Considering the available laws include in the ANSYS code, Drucker-Prager (DP) plasticity material model is assumed [122,123]. This criterion is a modification of the Von Mises yield criterion and is typically employed for soils, rocks and concretes, gaining an increased number of application for historic masonry constructions [2,17,124,125], due to its simplicity, its smoothness and, with exception of some of the modified criteria, its symmetric failure surface in the stress-space, which facilitates the implementation into numerical code [126].

The yield surface of the DP plasticity criterion depends on the first and the second invariant of the stress tension and remains fixed in the stress-space. Usually, the invariants considered are the mean hydrostatic stress, σ_m, and the effective shear stress, $\bar{\sigma}$:

$$\sigma_m = \frac{\sigma_{ii}}{3}; \qquad \bar{\sigma}^2 = \frac{1}{2} s_{ij} s_{ij} \tag{42}$$

where s_{ij} are the deviatoric components of the stress tensor. The DP yield criterion is defined by

$$F = 3\alpha\sigma_m + \bar{\sigma} - k = 0 \tag{43}$$

The parameters α and k can be expressed in terms of internal friction angle, φ , and cohesion, *c*, of the material, according to the following equations:

$$\alpha = \frac{2\sin\varphi}{\sqrt{3}(3-\sin\varphi)}; \qquad k = \frac{6c\cos\varphi}{\sqrt{3}(3-\sin\varphi)} \tag{44}$$

With the parameters α and k, the yield stresses in uniaxial tension $f_{t,DP}$, and compression $f_{c,DP}$, is evaluated by:

$$f_{t,DP} = \frac{k}{\frac{1}{\sqrt{3}} + \alpha}; \qquad f_{c,DP} = \frac{k}{\frac{1}{\sqrt{3}} - \alpha} \tag{45}$$

Note that, in case of elastic-perfectly plastic behaviour, the friction angle and the cohesion of the material are constant and independent from the plastic deformation.

The DP yield surface can be considered as a smooth version of the Mohr-Coulomb yield surface; indeed, the DP failure cone is circumscribed to the Mohr-Coulomb hexagonal pyramid with apex at $\rho = k/\sqrt{3}\alpha$ (Figure 5.1a). As far as the plane stress concerned, the yield function is parabolic as shown in Figure 5.1b. Indeed, for masonry the ratio between the uniaxial compressive and tensile strengths is usually greater than 3, thus obtaining α^2>1/12.

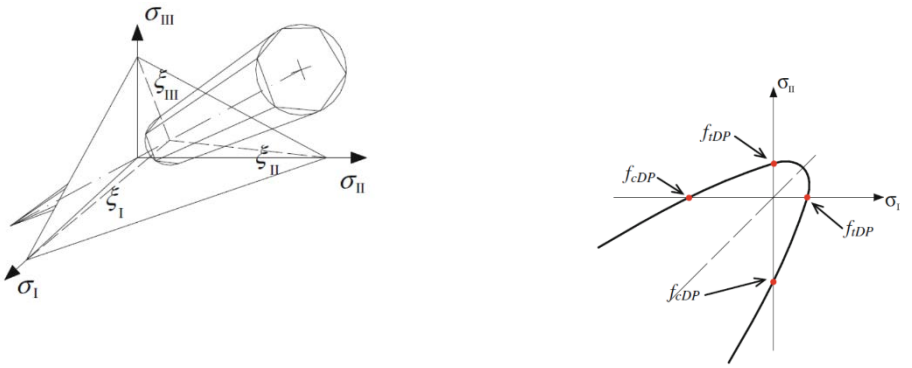

(a) (b)

Figure 5.1 – DP (a) yield surface in the Haigh-Westergaard stress-space and (b) cross-section cone for α^2>1/12.

5.2.1.2. *Smeared crack model*

A smeared crack model is introduced through the definition of a crushing and cracking rule, employing a failure surface available in ANSYS for concrete and proposed by William and Warnke (WW) [127]. The element is capable of cracking in tension and crushing in compression. The failure surface shows an elliptic trace on the deviatoric sections in each sextant, and a parabolic trace in the median sections (Figure 5.2).

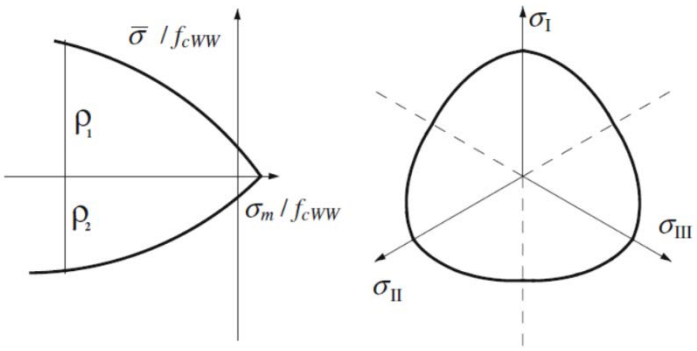

Figure 5.2 – Hydrostatic section of the yield surface and section across the deviatoric plane.

Five parameters are necessary to define the WW surface: the uniaxial compressive and tensile strength, $f_{c,WW}$ and $f_{t,WW}$, the biaxial compressive strength, f_{cb}, and two additional parameters, ρ_1 and ρ_2, necessary to define the curvature of the parabolic traces in the meridian sections.
The criterion accounts for both cracking and crushing failure modes through a smeared model and the crisis surface is completed by cut-off conditions.
Despite the definition of five constants, in most practical cases, the failure surface can be specified by means of only two parameters: $f_{c,WW}$ and $f_{t,WW}$. The other three constants can be assumed as reported in ANSYS manual [122] for this criterion:

$$f_{cb} = 1.2\, f_{c,WW}; \qquad \rho_1 = 1.45 f_{c,WW}; \qquad \rho_2 = 1.725 f_{c,WW} \tag{46}$$

Two additional coefficients can be considered, β_t and β_c, accounting for a shear reduction of the stress producing sliding across the crack face for open β_t or reclosed β_c cracks.

5.2.1.3. *Combination of DP and WW criterion*

The combination between DP plasticity criterion and WW failure criterion, provides an isotropic material with plastic deformation, cracking and crushing capabilities.
This model requires the knowledge of:

- *elastic parameters*: *E*, ρ and υ
- *plastic parameters* (DP criterion): *c*, φ and δ
- *cracking and crushing parameters* (WW criterion): $f_{c,WW}$, $f_{t,WW}$, β_c and β_t

An accurate combination of these parameters allows an elastic-brittle behaviour in case of biaxial stresses or biaxial tensile-compressive stresses with low compressions level. On the contrary, the material is elastoplastic in case of biaxial compressive strength or biaxial tensile-compressive stresses with high compression level. According to experimental evidence, to ensure the correct plastic behaviour of the masonry, the choice of the model combination, must consider:

- tensile strength smaller than the tensile strength of plasticity model

$$f_{t,WW} < f_{t,DP}$$

- compressive strength greater than the compressive strength of plasticity model

$$f_{c,WW} > f_{c,DP}$$

As far as, the calibration of the model is concerned, Betti *et al.*, [2], has proposed the results of past experimental researches [128] in order to assess both strength and deformability of masonry walls of historic masonry buildings with the aim to calibrate the combination between the smeared crack model with the plasticity model, reproducing the experimental test with a good accuracy. The results of this research are herein used to define the intersection between DP and WW criterion, as shown in Figure 5.3. In order to obtain the particular combination of DP and WW criterion, highlighted in Figure 5.3b, a relation between $f_{t,WW}$ and $f_{c,DP}$ is introduced.

$$f_{t,WW} \cong 0.22 f_{c,DP} \tag{47}$$

These choices allow the correct simulation of the masonry behaviour in the mixed zone tension-compression, obtaining a good reproduction of the experimental results in terms of shear-displacement curves.

The employment of DP and WW criterion is motivated by its extensive employment in the scientific literature to represent the inelastic behaviour of masonry constructions. DP model has been used, *e.g.* by Zucchini and Lourenço [125] for the simulation of the plastic deformation on masonry cells, and by Cerioni *et al.*, [17], to assess the seismic behaviour of the Parma Cathedral bell tower. Instead, the application of DP and WW combination criterion has been developed *e.g.* by Chiostrini *et al.*, [128], and Betti and Vignoli [12].

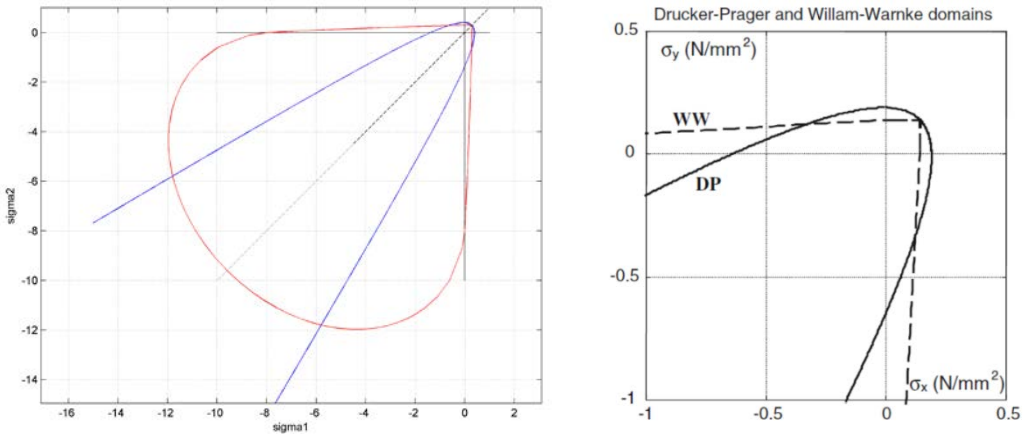

Figure 5.3 – Intersection between the plasticity (DP) and the failure (WW) domains.

5.2.2. Numerical analyses typology

A reliable estimate of the seismic risk needs to perform nonlinear dynamic analyses, which require both the knowledge of several parameters, usually unknown, and a great computational effort. Due to these facts, nonlinear static procedures based on pushover analyses are frequently employed as effective technique in seismic design and assessment. Indeed, despite nonlinear dynamic analyses represent the most sophisticate tool for assessing the seismic vulnerability of a structure, the possibility to maintain the nonlinear structural behaviour combining the simplicity of the static analysis, makes the pushover analyses widely applied also for historic masonry constructions [24,93,129], as expected also from seismic code and Italian recommendations [9,117,113]. Moreover, Marra *et al*., [57] demonstrate the safety preserving of nonlinear static analyses through a comparison with incremental dynamic analyses on a masonry tower, approximated by a Timoshenko beam with cantilever static scheme.

According to the pushover approach, different lateral force configurations can be selected (*e.g.* uniform distribution, inverted triangular distribution and distribution proportional to the first mode shape). The analyses herein proposed, monotonically increase a uniform profile of horizontal loads, under constant gravity loads. Noteworthy is the conventionality of the pushover approach assumed in this research: the load profile does not change with the progressive degradation that occurs during loading. Due to this fact, the analyses neglect the progressive changes in modal frequencies caused by yielding and cracking on the structure.

This is a critical point for the application of conventional pushover to the analysis of historic masonry buildings, because it is predictable that the progressive damage of the building may also lead to period elongation, and therefore to different spectral amplifications and load distributions along the height. However, also in its conventional form, the pushover approach can provide an efficient alternative to more expensive computational inelastic time-history analyses and can offer useful and effective information on the damage that the building can develop under dynamic seismic loads. The analyses are performed assuming a rigid ground foundation (fixed base model); more realistic description of soil-structure interaction could be incorporated, but considering its less relevance underlined in [38,130], this effect is herein neglected.

The behaviour of the tower is investigated along the direction corresponding to the first natural period that, for the reference case (the Becci tower), corresponds to N-S direction.

The results of the pushover analyses are evaluated in terms of capacity curves which show force vs displacement relationships. Capacity curves are built by assuming the base shear and the displacement of the centre of mass of the upper section of each tower as control point.

5.2.3. Seismic analyses

In order to obtain analytical fragility curves, the definition of limit states is necessary. Usually, for ordinary masonry buildings, three limit states are defined: the first, corresponding to the exceedance of the elastic limit with the changing of the initial stiffness, the second, obtained with the maximum resistance attained, and the third, considered as ultimate collapse state, identified with the resistance loss, e.g. corresponding to 20%.

However, in this work, the definition of an alternative criterion for damage quantification is necessary; indeed, the numerical model selected to represent the masonry behaviour is elastic perfectly plastic without damage, due to this assumption the analysis output cannot identify the collapse of the structure with a resistance loss in terms of base shear reduction.

Thus, considering a generic pushover curve (Figure 5.9 top), the ratio between the tangent stiffness at each point of this curve and the elastic stiffness (k/k_{el}) is defined and its behaviour is shown at the bottom part of Figure 5.9. This parameter is considered as damage criterion and its value is compared with the cracking pattern of the tower for several steps of the pushover analysis. The aim is twofold: firstly, to provide a quantitative evaluation of this ratio, and secondly, to obtain unambiguous identification of the damage levels.

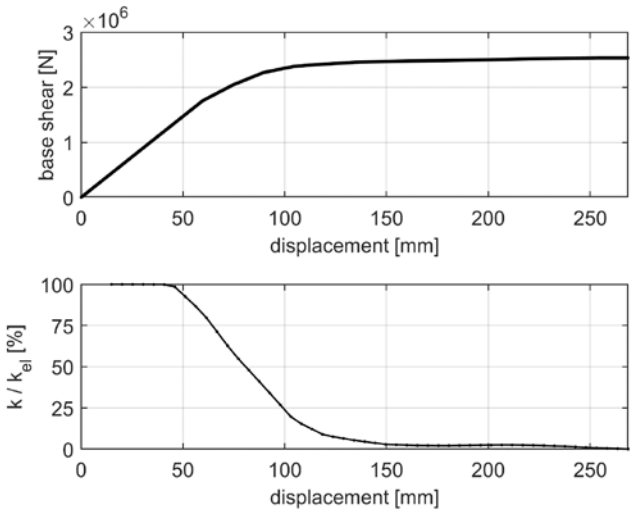

Figure 5.4 - Pushover curve and stiffness ratio vs displacement.

The cracking pattern of the tower is evaluated in several steps of the analysis through the *crack* plot option in ANSYS. This option displays circles at locations of cracking or crushing in *Solid65* elements. Cracking is shown with a circle outline in the plane of the crack, and crushing is shown with an octahedron outline. The analysis of the cracking pattern has allowed to define three damage levels by considering the widespread of the cracks in the cross section as a portion of the

tower side, as represented in Figure 5.5a, and the corresponding displacement on the pushover curve, Figure 5.5b.

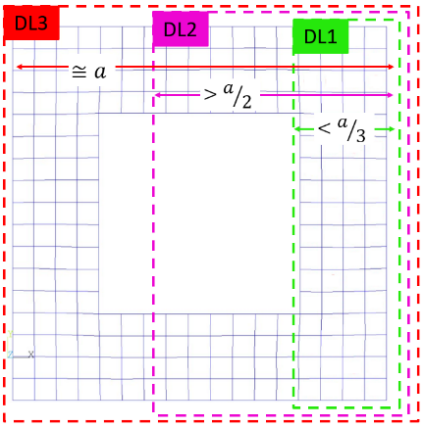

(a)

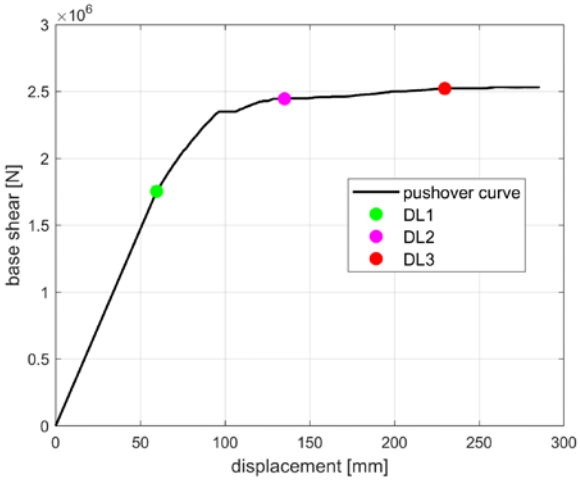

(b)

Figure 5.5 – Identification of the damage levels on pushover curve.

The first damage level DL1 is reached when the displacement exceeds the elastic limit (green dot in Figure 5.5a) and the first significant crack forms at the base of the tower appear (Figure 5.6) involving the first portion of the cross section, and changing the initial stiffness.

The second damage level DL2 identifies a widespread cracking pattern that involves more than the half cross-section but no element is crushed in compression.

The third damage level DL3 corresponds to a cracking pattern that involves almost all the cross-section and several elements crushed in compression.

Both these two last levels reach a considerable stiffness loss and the maximum level of base shear.

the

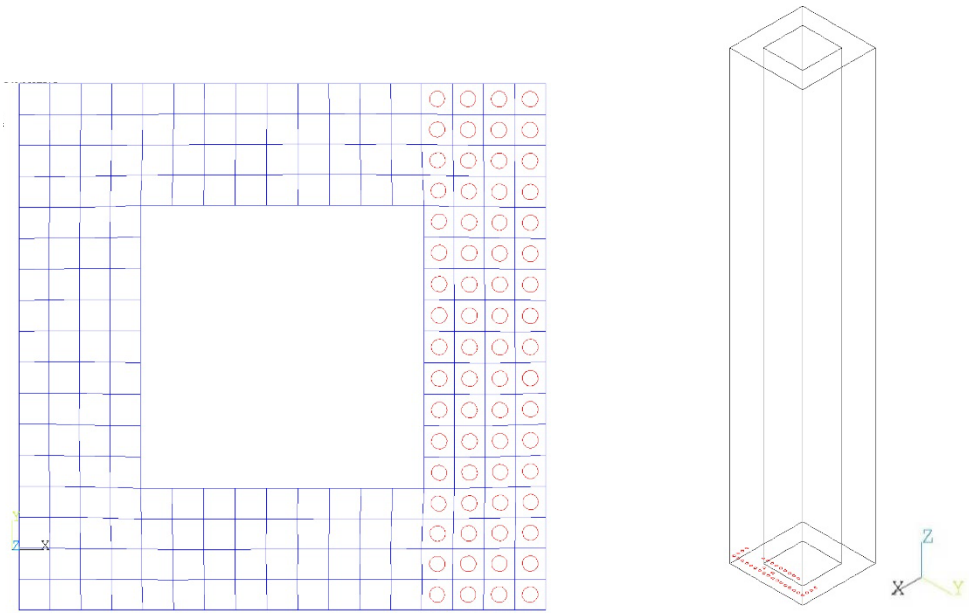

Figure 5.6 - Cracking pattern of the tower corresponding to DL1.

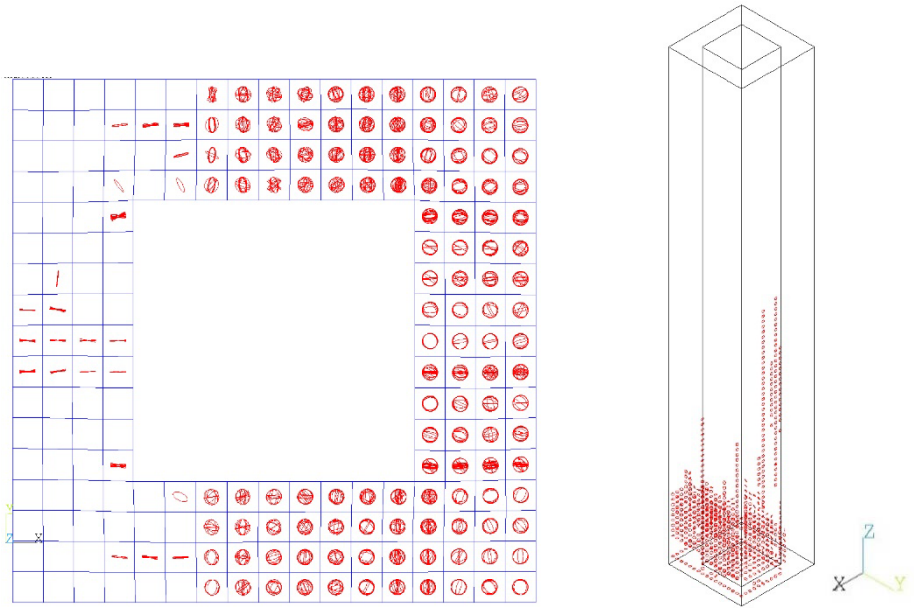

Figure 5.7 - Cracking pattern of the tower corresponding to DL2.

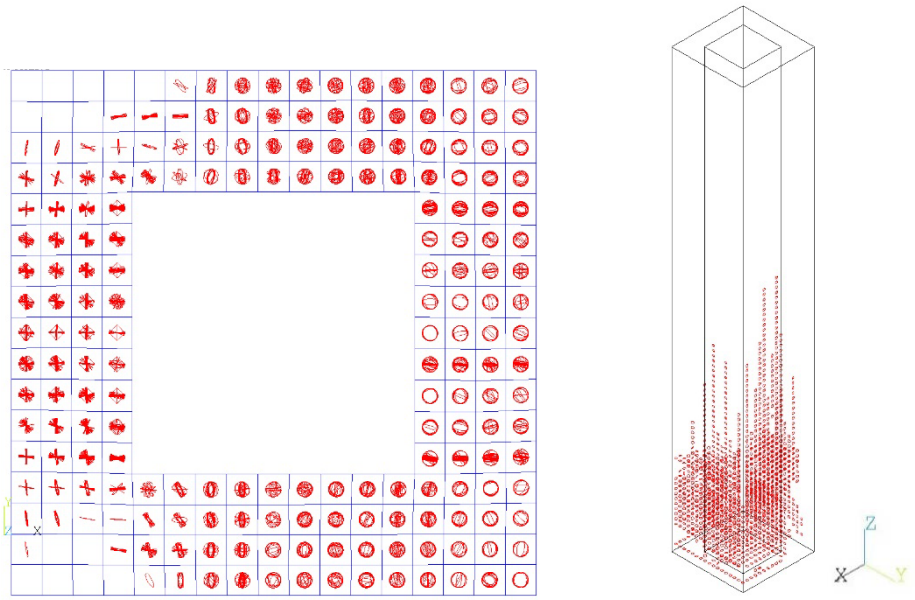

Figure 5.8 - Cracking pattern of the tower corresponding to DL3.

The unambiguous identification of DL2 and DL3 damage conditions is provided by the value of the ratio between the tangent and the elastic stiffness (k/k_{el}).

The comparison between the cracking pattern and the pushover curve has allowed to identify the following two levels of the ratio: 5% for DL2 and 2% for DL3, as shown in Figure 5.9.

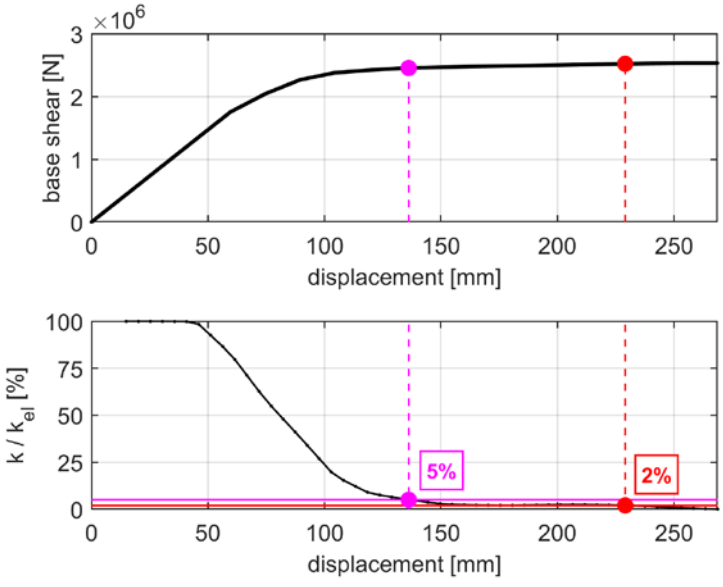

Figure 5.9 - Identification of damage states on a single capacity curve: (top) capacity curve and (bottom) stiffness ratio vs displacement.

For each damage level, the value of PGA is obtained through Capacity Spectrum Method (CSM) according to the displacement-based seismic analyses techniques, originally developed by Freeman *et al.*, [131] and Freeman [132]. In this respect, the following steps are identified:

a) calculate the pushover curve which rates the relationship between base shear and control point displacement
b) convert the pushover curve, related to the multi-degree-of-freedom (MDOF) system, in that of a single-degree-of-freedom (SDOF) system using the modal participation factor, Γ, which measures the quantity of activated masses with the considered eigenvector, φ:

$$\Gamma = \frac{\varphi^t M \tau}{\varphi^t M \varphi} \tag{48}$$

where M is the matrix of masses of the structure and τ the drag vector, which indicates the masses involved in the analysed direction. The conversion from MDOF to SDOF curve is performed simply dividing both x and y curve values with Γ.

c) describe the capacity curve in terms of spectral acceleration (y-axis) and spectral displacement (x-axis) in the Acceleration-Displacement Response Spectra (ADRS) format.
d) define the equivalent bilinear SDOF curve. This curve is identified by the stiffness of the initial phase, the maximum resistance shear (where the elastic phase ends) and the maximum displacement according to the selected damage level.

The stiffness of the bi-linear system is calculated imposing the passage of the elastic part at the 70% of the maximum base shear:

$$\mathrm{k}^* = \frac{F^*_{70\%}}{d^*_{70\%}} \tag{49}$$

The maximum value of the shear is calculated with an energetic balance, assuming that the area below the SDOF and the bilinear curve are the same. This assumption allows to obtain:

$$F^*_y = \left(d^*_u - \sqrt{{d^*_u}^2 - \frac{2A^*}{k^*}} \right) k^* \tag{50}$$

where A^* represents the area below the curves.

The period and the displacement corresponding to the yielding point of the SDOF system are calculated with the following equations:

$$T^* = 2\pi\sqrt{m^*/k^*} \tag{51}$$

$$d_y^* = F_y^*/k^* \tag{52}$$

The verification through a pushover analysis, requires the calculation of the *displacement demand* using the period of the SDOF system and the displacement spectrum of the considered site of construction, Figure 5.10. In order to calculate the acceleration which produces a certain displacement of the capacity curve (*e.g.* related to damage levels), it is necessary to refer the analytical procedure to an elastic system that is equivalent to the bi-linear one: in this way, it is possible to use the elastic spectrum in terms of displacement and acceleration. The equivalence among an elastic system and a bi-linear one needs an observation of the stiffness: flexible structures usually show deformations equal to elastic systems with the same stiffness, while rigid structures can experience more deformations than the equivalent elastic systems. In the Italian code [113], a structure is flexible if its period is greater than the period T_C, corresponding to the end of the plateau in the acceleration spectrum. This relation is fulfilled for the masonry towers considered in this work, allowing to use an equivalent elastic system which shows the same maximum displacement ($d_{u,e}^*$) of the real SDOF system (d_u^*), thus obtaining the following relations:

$$d_u^* = d_{u,e}^*$$

$$d_{u,e}^* = S_{De}(T^*) \tag{53}$$

$$S_e(T^*) = S_{De}(T^*) \cdot \omega^2 = S_{De}(T^*) \cdot (2\pi/T^*)^2$$

In this way, the displacement capacity of the tower is related to the spectral acceleration; however, these accelerations are associated to different dynamic system (in terms of mass and stiffness). In order to compare these results, the Peak Ground Acceleration is calculated. Specifically, a spectrum which gives the same spectral acceleration calculated in the capacity analyses, is defined, Figure 5.10. Note that, an acceleration spectrum is defined when the seismic hazard is identified through three parameters, as reported in [113]:

- a_g maximum expected horizontal acceleration on A type soil (rock)
- F_0 maximum value of the amplification factor of the horizontal acceleration spectrum
- T_C^* upper limit of the period of the constant spectral acceleration branch

These parameters are defined in the Italian code [113] and differ according to the return periods. In this dissertation, the spectrum is assumed with a fixed shape thus considering the value of F_0

and T_C^* as fixed, and varying a_g. This assumption can be justified considering the small variation of these parameters; indeed, some recommendations neglect this variability.
Thus, the spectrum is calculated only varying the value of the a_g into the constitutive equations shown in the following:

$$S_e(T) = a_g \cdot S \cdot \eta \cdot F_0 \cdot \left[\frac{T}{T_B} + \frac{1}{\eta \cdot F_0}\left(1 - \frac{T}{T_B}\right)\right] \qquad 0 \le T < T_B \tag{54}$$

$$S_e(T) = a_g \cdot S \cdot \eta \cdot F_0 \qquad T_B \le T < T_C \tag{55}$$

$$S_e(T) = a_g \cdot S \cdot \eta \cdot F_0 \cdot \left(\frac{T_C}{T}\right) \qquad T_C \le T < T_D \tag{56}$$

$$S_e(T) = a_g \cdot S \cdot \eta \cdot F_0 \cdot \left(\frac{T_C \cdot T_D}{T^2}\right) \qquad T_D \le T \tag{57}$$

where $S = S_S \cdot S_T$ is the coefficient that keeps into account the soil category (S_S) and the topographical conditions (S_T), η represents the coefficient that modifies the elastic spectrum in case of conventional viscous damping ζ assumed as different from the usual value of 5%. In order to avoid introducing additional variables, the viscous damping, the geotechnical and topographical conditions are assumed as constant. Indeed, in this context, the analyses are focused on the structural aspects of the masonry towers, considering all of them placed in the same type of soil. In particular, $\zeta = 5\%$ obtaining $\eta = 1$, the B category of soil is assumed, with a topographical condition T_2, achieving $S = 1.44$. Notice that, the product between a_g and S is the PGA, which becomes the only variable which describes the maximum acceleration that the structure can suffer (PGA $= a_g \cdot S = 1.44 a_g$), avoiding the problems related to the different characteristics of the dynamic systems: in fact, the definition of the maximum acceleration now is independent from the period of the considered structure.
Since only the PGA changes in this process, a common reference starting spectrum has been chosen for all the structures; considering that the analysed towers are located in San Gimignano, the following parameters have been assumed, according to [113]:

- Nominal life — V_N = 50 years
- Utilization coefficient — c_u = 1.0
- Reference life — $V_R = V_N \cdot c_u$ = 50 years
- Probability of exceedance in the reference life — P_{vr} =10 %
- Return period — $T_R = - V_R / \ln (1- P_{vr})$ = 475 years
- Type of soil — Cat. B
- Topographical conditions — Cat. T2

The seismic hazard is then defined:

$$a_g = 0.141 \qquad F_0 = 2.479 \qquad T_C^* = 0.276$$

Starting from these assumptions, the procedure can be applied by increasing the level of PGA up to the same spectral displacement is gained, as shown in Figure 5.10.

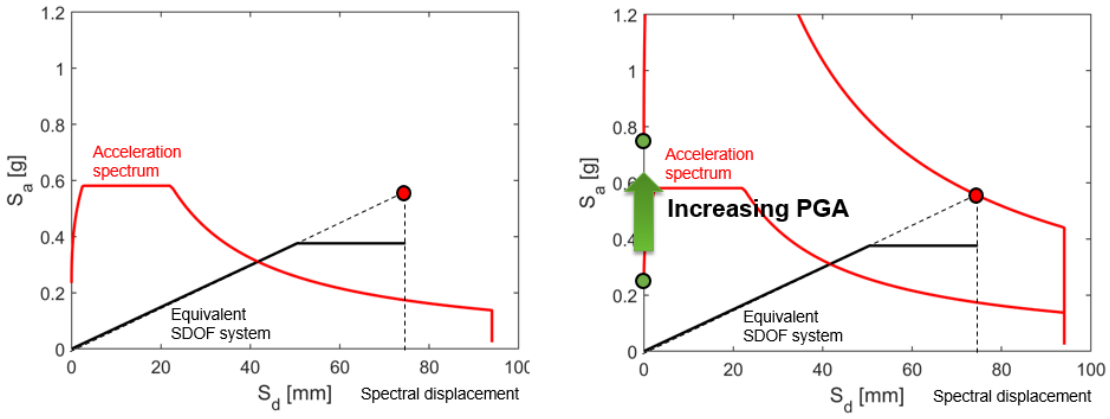

Figure 5.10 – Assessment of the PGA of the performance point.

5.2.4. Sensitivity analyses

Sensitivity analyses provide an effective method for assessing the effects of the uncertainties of the input parameters of the model, on the response quantities of interest. With this aim, a complete three-dimensional model using FE technique and the macro-modelling strategy (introduced in §5.2.1) is employed to perform nonlinear static analyses. The effect of each input parameter, both in terms of displacement and base shear, is evaluated varying the input one at time. When a parameter varies, the others are kept constant at their mean values.

The effect of each uncertain parameter is evaluated with respect the damage levels introduced in the previous section. In particular, some reference cases are taken into account considering the range of variability of the structural characteristics of the towers presented in the scientific literature and summarized in Table 3.2 and Table 3.3. A very simplified geometry is chosen: vertical cantilever beam with constant thick-walled and hollow square-cross section, neglecting openings and slabs. In this respect, Table 5.1 shows some characteristics considered as typical for the towers collected in the database and the reference values selected for the sensitivity analyses. As far as the mechanical properties are concerned, the combination of DP and WW criterion is employed to model the masonry behaviour, as reported in §5.2.1.3, and their parameters values are shown in Table 5.2.

Table 5.1 – Typical characteristics of historic masonry towers and reference cases selected.

	Range of variability	Reference towers
External side, a [m]	4.5 – 8.9	6.5
Thickness, s [m]	0.9 – 2.4	1.0, 1.5, 2.0
Total height, H [m]	30 – 80	30, 40, 50
Specific weight, w [kN/m^3]	16 – 22	16
Elastic modulus, E [MPa]	900 – 3000	1260, 1800, 2340

Table 5.2 – Reference values for DP and WW combination (cohesion c, friction angle φ, compressive and tensile strength of DP criterion $f_{c,DP}$ and $f_{t,DP}$, compressive and tensile strength of WW criterion $f_{c,WW}$ and $f_{t,WW}$, coefficient for opening β_t and reclosing cracks β_c)

c [MPa]	φ	$f_{c,DP}$ [MPa]	$f_{t,DP}$ [MPa]	$f_{c,WW}$ [MPa]	$f_{t,WW}$ [MPa]	β_c [-]	β_t [-]
0.22	40	0.94	0.28	8.0	0.204	0.75	0.25
0.32	40	1.37	0.40	8.0	0.298	0.75	0.25
0.42	40	1.80	0.53	8.0	0.387	0.75	0.25

The variations of thickness (s), total height (H), elastic modulus (E), and DP compressive strength ($f_{c,DP}$) are evaluated on the overall response of nonlinear structural behaviour. Instead, the external side and the specific weight are considered as deterministic. The variability of the results in terms of pushover curves, is shown in Figure 5.11.

Specifically, the effect of the thickness is shown in Figure 5.11a, which underline a slight variation of the initial stiffness and a considerable increase of the maximum base shear corresponding to the growth of the thickness. Figure 5.11b reports the pushover curves for different values of tower height, the variation of this parameter gives rise to considerable gain of both initial stiffness and maximum base shear; thus confirming its relevance on the seismic response. The role of the elastic modulus is evaluated in Figure 5.11c, which reveals the achievement of the same maximum base shear with different initial stiffness. In particular, the growth of the initial stiffness corresponds to the growth of elastic modulus. Conversely, Figure 5.11d shows different maximum base shear gained with the same initial stiffness. This behaviour is provided by different values of compressive strength, which have effect only when the displacement exceeds the elastic limit. Finally, Figure 5.11e proposes the effect of a correlation between elastic modulus and compressive strength, which causes a considerable variation of the response in terms of both initial stiffness and maximum base shear. Note that, the discussion of the sensitivity results thus far has focused on the variation of initial stiffness and maximum base shear, the same considerations must to be carried out in terms of maximum displacement. However, for this latter comparison, the identification of the same damage level is necessary, which usually do not correspond to the end of the pushover curve.

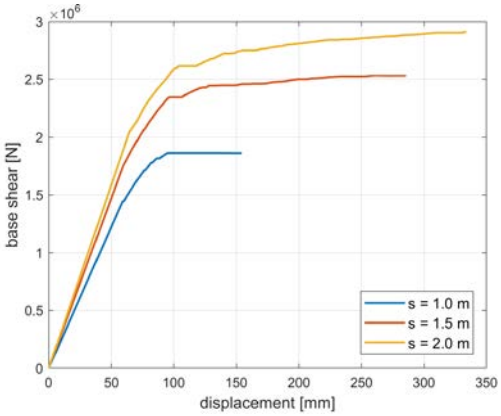

H = 40 m, E = 1800 MPa,
$f_{c,DP}$ = 1.37 MPa, $f_{t,WW}$ = 0.298 MPa

(a)

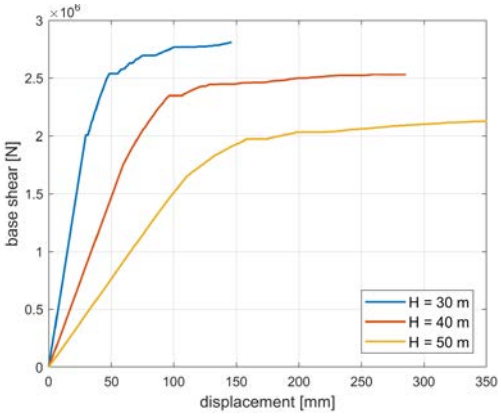

s = 1.5 m, E = 1800 MPa,
$f_{c,DP}$ = 1.37 MPa, $f_{t,WW}$ = 0.298 MPa

(b)

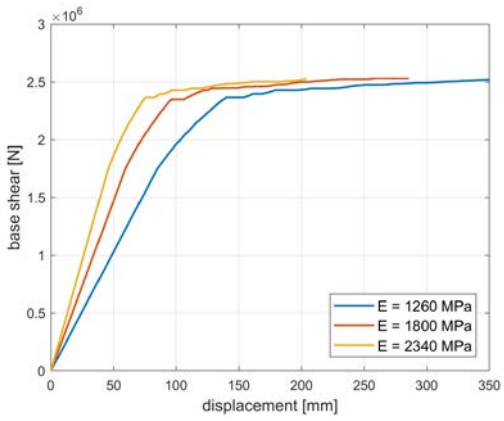

s = 1.5 m, H = 40 m, $f_{c,DP}$ = 1.37 MPa, $f_{t,WW}$ = 0.298 MPa

(c)

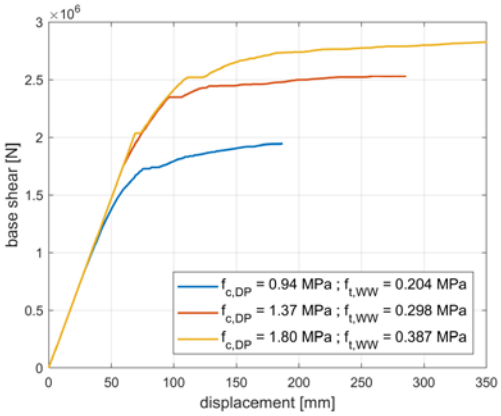

s = 1.5 m, H = 40 m, E = 1800 MPa

(d)

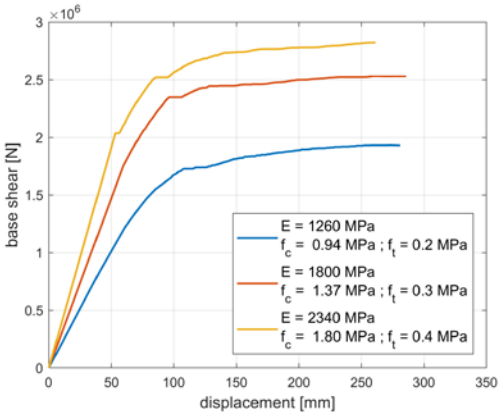

s = 1.5 m, H = 40 m

(e)

Figure 5.11 – Pushover curves obtained by considering the variability of the (a) thickness, (b) total height, (c) elastic modulus, (d) compressive strength of DP and (e) compressive strength of DP correlated to the elastic modulus.

In order to evaluate the effect of the input parameters in terms of both displacement and base shear, the three damage levels introduced in §5.2.3 are taken into account, as suggest in [91]. For the sake of clarity, Figure 5.12 reports the identification of the damage levels for the pushover curves representing the variability of H. The green dots correspond at DL1 (δ_e, T_e), the purple ones at DL2 (δ_d, T_d) and the red ones to DL3 (δ_u, T_u).

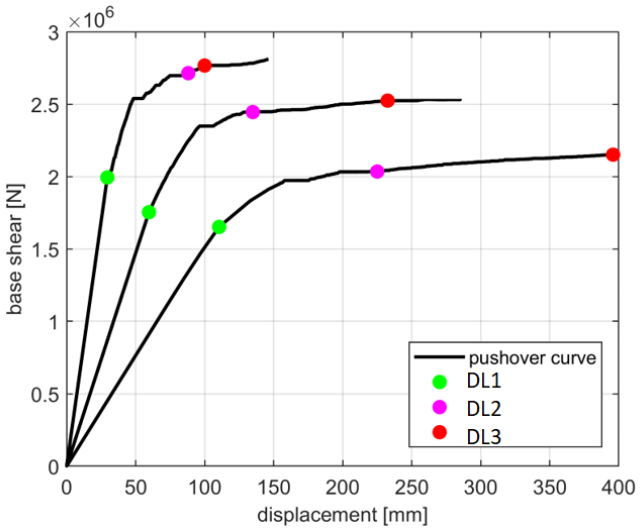

Figure 5.12 – First (DL1), second (DL2) and third (DL3) damage level for the pushover curves of Figure 5.11b.

The resulting displacements δ_e, δ_d and δ_u, are plotted in Figure 5.13 as a function of the varying input parameters (s, H, E, f_c, indicated in abscissa). An additional case is reported as function of f^*_c in the last column of the figure. These results denote the case corresponding to a correlation between elastic modulus and compressive strength. At each point, as reported in Figure 5.11e, corresponds different pairs of values which fulfil the relation: $E \cong 1300 f_{c,DP}$. Indeed, despite in the scientific literature such correlation is missing for masonry material, seems plausible suppose these two parameters as dependent each other. However, no more reliable information on that are available; the assumption of this correlation is introduced only to propose the results in the following graphs. The other results proposed in this dissertation assume the elastic modulus and the compressive strength of the masonry as independent parameters.

A quantitative assessment of the results of the sensitivity analysis, is proposed in terms of displacement and base shear of the damage levels considered, respectively in Table 5.3 and Table 5.4. The tables report, in the first row, the relative variations of the input parameters, considering $\Delta p_i = p_{i,max} - p_{i,min}$ the amplitude of the variation interval and $\bar{p}_i = (p_{i,max} - p_{i,min})/2$ the mean value of the generic parameter p_i. From the second to the fourth row, the results of relative variations of the displacements with respect to their reference values are proposed, and finally,

from the fifth to the last row, the ratios between relative variation of the selected quantities and the relative variation of the input parameters are reported.

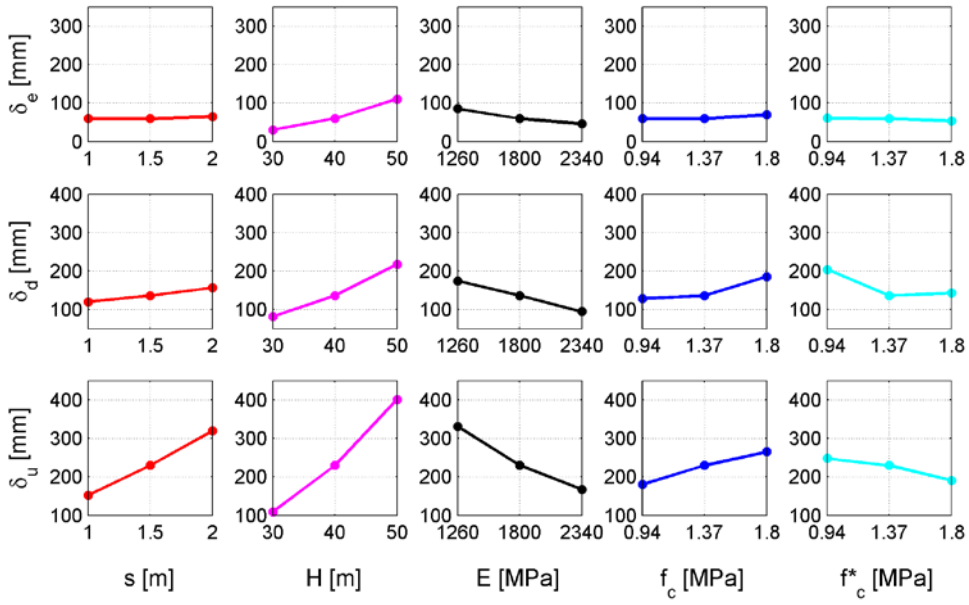

Figure 5.13 – Elastic (δ_e), damage (δ_d), and ultimate (δ_u) displacements as a function of the variation of the input parameters.

Table 5.3 – Results of sensitivity analyses in terms of displacement.

	p_i			
	s	**H**	**E**	**f_c**
$\Delta p_i / p_{i,m}$	0.67	0.50	0.60	0.63
$\Delta\delta_e / \delta_{e,m}$	0.09	1.36	-0.66	0.11
$\Delta\delta_d / \delta_{d,m}$	0.27	1.00	-0.59	0.42
$\Delta\delta_u / \delta_{u,m}$	0.73	1.27	-0.71	0.37
$[\Delta\delta_e / \delta_{e,m}] / (\Delta p_i / p_{i,m})$	0.13	2.71	-1.10	0.26
$[\Delta\delta_d / \delta_{d,m}] / (\Delta p_i / p_{i,m})$	0.40	2.00	-0.98	0.67
$[\Delta\delta_u / \delta_{u,m}] / (\Delta p_i / p_{i,m})$	1.09	2.54	-1.19	0.59

The results confirm that variations of the compressive strength have not effects on the elastic limit δ_e, which depends on the total height and on the elastic modulus. In particular, to an increase of the total height corresponds an increase of δ_e, vice versa, to an increase of the elastic modulus corresponds a decrease of δ_e. Instead, in terms of δ_d, and δ_u, all the input parameters have a considerable effect, but the height seems to have the most prominent effect. These considerations,

despite being obvious, are useful to confirm the coherence of the analyses results. In this respect, additional comparison can be introduced by normalizing the limit displacement respect to the total height of the towers. Figure 5.14 shows the results, highlighting more uniform effects of the input parameters on the normalized displacements.

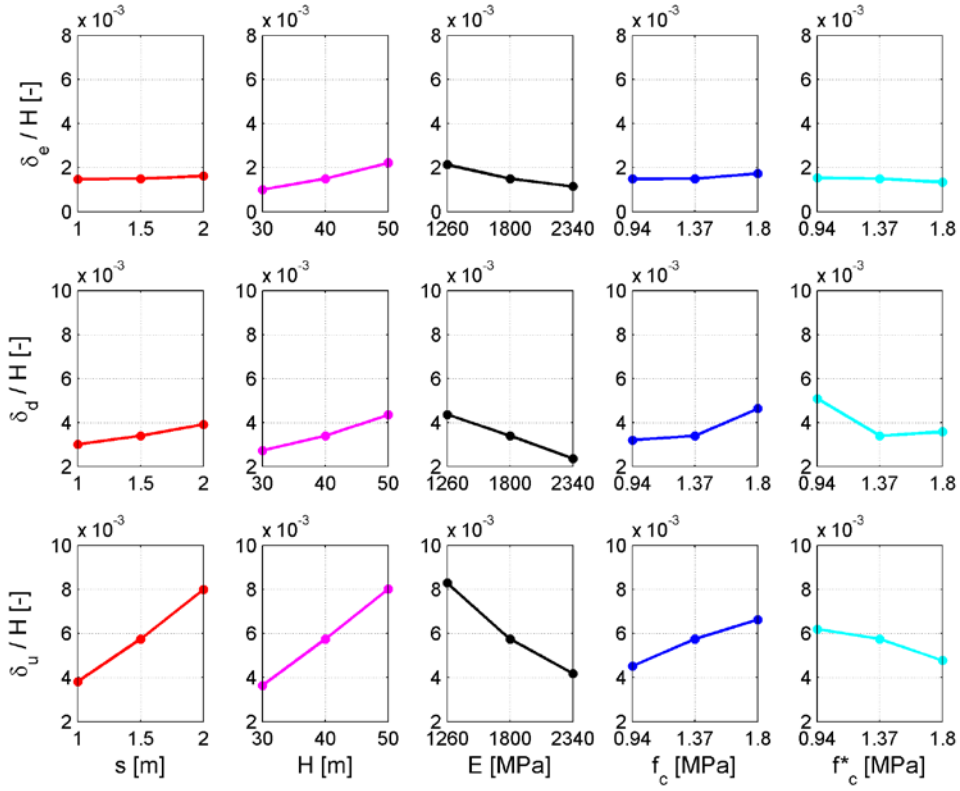

Figure 5.14 – Elastic (δ_e), damage (δ_d), and ultimate (δ_u) displacements, normalized with respect to the total height (H), as function of the input parameters variation.

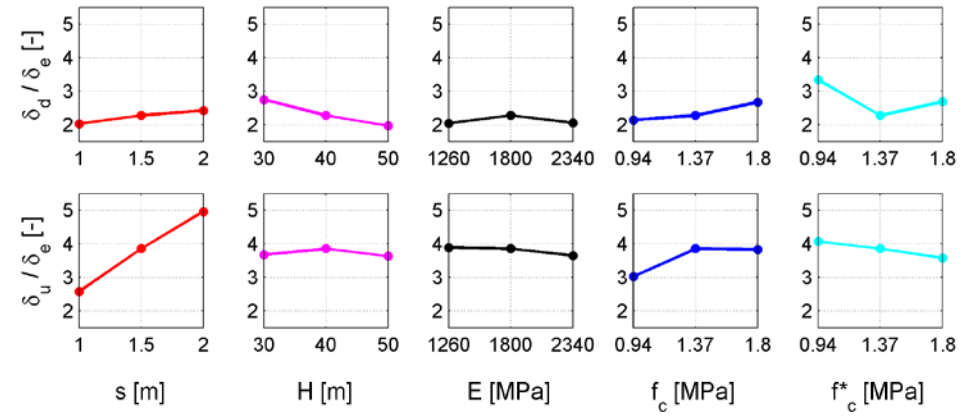

Figure 5.15 – Ductility for the second and third damage levels.

The results in terms of base shear confirm that variations of the elastic modulus have not effects on this quantity which depends especially on the total height and the compressive strength. Moreover, the base shear at DL2 is very close than the DL3 one. This latter consideration is evident also observing the pushover curves in Figure 5.12.

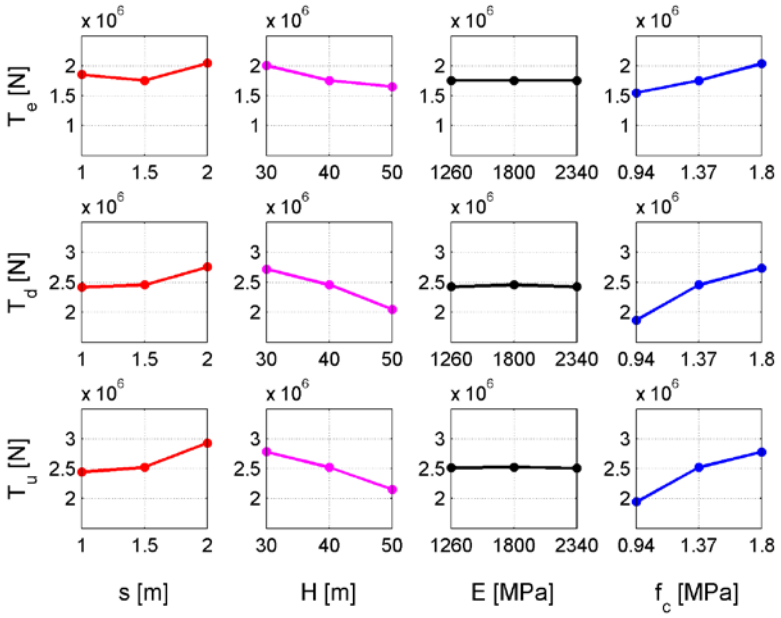

Figure 5.16 – Elastic (T_e), damage (T_d), and ultimate (T_u) base shear as function of the input parameters variation.

Table 5.4 - Results of sensitivity analyses in terms of base shear.

	p_i			
	s	**H**	**E**	**f_c**
$\Delta p_i / p_{i,m}$	0.67	0.50	0.60	0.63
$\Delta T_e / T_{e,m}$	0.11	0.20	0.00	0.28
$\Delta T_d / T_{d,m}$	0.14	0.27	0.00	0.35
$\Delta T_u / T_{u,m}$	0.19	0.25	0.00	0.33
$[\Delta T_e / T_{e,m}] / (\Delta p_i / p_{i,m})$	0.16	0.40	0.00	0.44
$[\Delta T_d / T_{d,m}] / (\Delta p_i / p_{i,m})$	0.21	0.55	0.00	0.56
$[\Delta T_u / T_{u,m}] / (\Delta p_i / p_{i,m})$	0.29	0.50	0.00	0.53

For each damage level and for each pushover curve, a value of PGA is associated through CSM method, as previously illustrated in §5.2.3. The results, shown in Figure 5.17, reveal a considerable variation of the PGA value for the selected range of the input parameters.

Note that, the input parameters thus far has been considered with a quite similar coefficient of variation, as shown in Table 5.3 and Table 5.4. This consideration seems necessary because, in practice these parameters may have level of uncertainties considerably different. Indeed, characterizing the uncertainties related to the input parameters with probability distributions, the standard deviation of the wall thickness (for the sake of example) will be considerably lower compared to the ones related to the compressive strength of the masonry.

In this respect, the results of Figure 5.17 are herein used to develop a response surface for each input parameter and for each damage level, in order to allow the assessment of the PGA for additional values of the parameters.

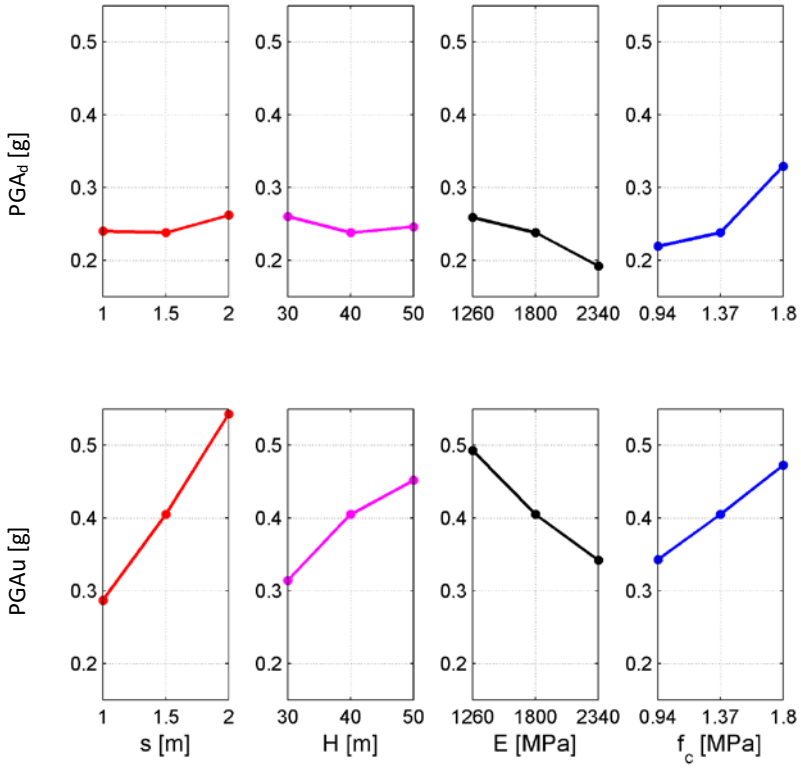

Figure 5.17 – PGA corresponding to DL2 and DL3 as a function of the input parameters.

Whit this aim, Table 5.5 reports two groups of Gaussian probability distributions (A and B), centred on the mean value of each input parameter. The effect of the variability of PGA is thus evaluated using Tornado diagrams, as reported in Figure 5.18

Table 5.5 – Two groups of Gaussian PDFs of the input parameters.

	Thickness [m]		Total height [m]		Elastic modulus [MPa]		Compressive strength [MPa]	
	μ_s	σ_s	μ_H	σ_H	μ_E	σ_E	μ_f	σ_f
A	1.5	0.02	40	0.03	1800	0.04	1.37	0.04
B		0.01		0.03		0.05		0.08

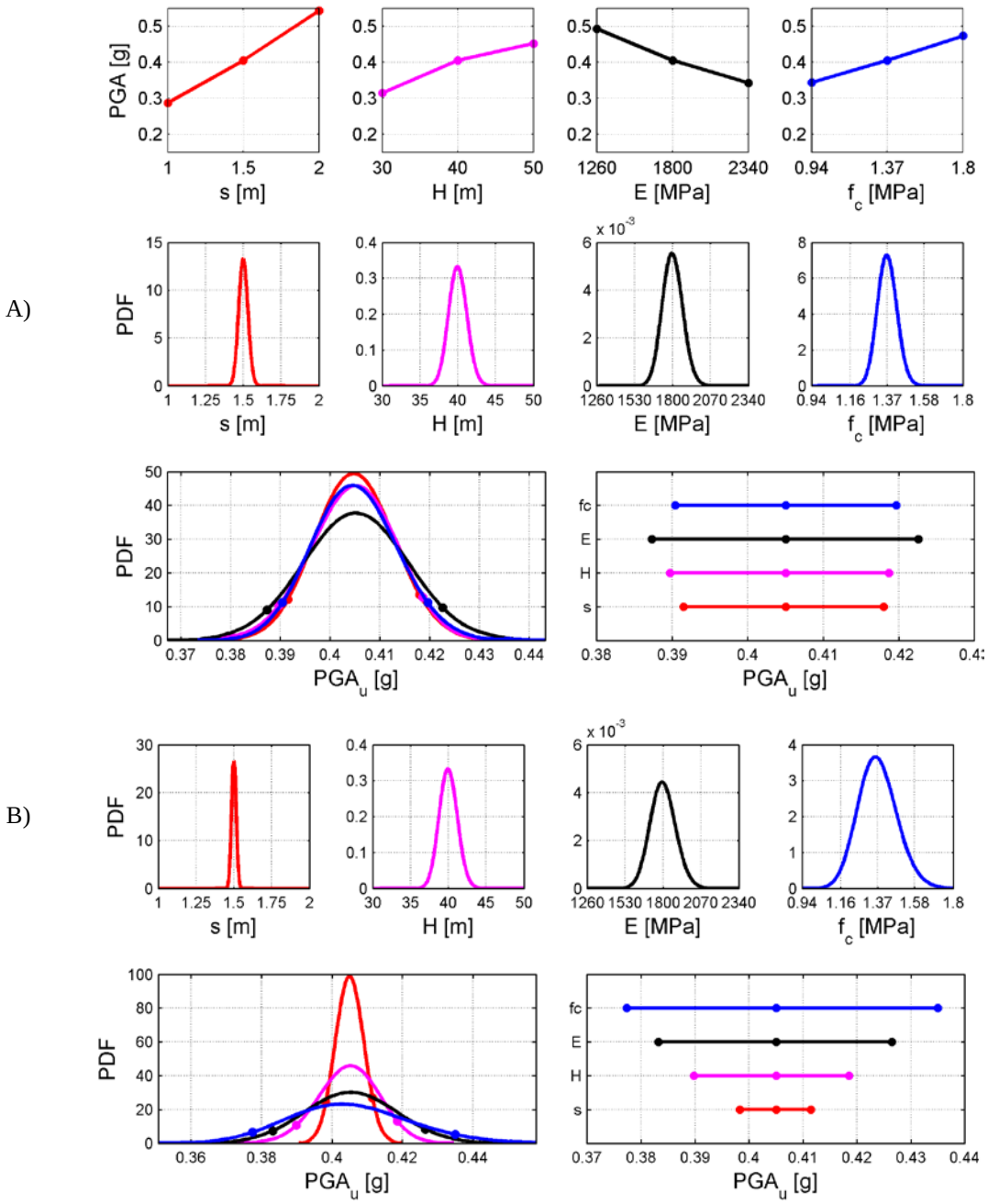

Figure 5.18 – Tornado diagram from sensitivity analysis results.

According to the results of the Tornado diagram, the thickness of the tower is considered as deterministic, due to its secondary role compared to the other parameters, especially considering the limited uncertainties involved in its definition. Moreover, a relevant effect is played by the elastic modulus and the total height of the tower; in this respect, the updating of the joint-probability distribution of these two parameters, proposed in Chapter 3, seems to be promising in order to improve the seismic assessment of these structures.

As far as the mechanical parameters of the nonlinear model are concerned, the compressive strength plays a relevant role. This parameter is the most uncertain; indeed, its assessment requires destructive tests, usually infeasible in historic masonry buildings. Actually, the definition of this parameter would be important but, since no experimental data are available, a Bayesian updating is infeasible. Thus, its variability could be considered as the modelling uncertainties related to the result of the pushover curves.

As already mentioned, no reliable information are available on the correlation between the compressive strength and the elastic modulus of the masonry even if such correlation exists; in the following these parameters are considered as independent variables.

Concluding, sensitivity analyses have been used to select the input parameters that have the most significant impact on the response. In this respect, the elastic modulus of the masonry and the height of the tower are assumed as random variables and the compressive strength of the masonry is taken into account as modelling uncertainty. As already reported, noteworthy that the record-to-record variability, despite its considerable effect on the seismic behaviour of the towers, is neglected. Indeed, the assessment of this uncertainty is outside of the scope of the present work that is concentrated primarily on the definition of the role of uncertain structural parameters. However, the proposed procedure allows the incorporation of more realistic description of the record-to-record variability.

5.2.5. Failure surfaces

Comprehensive uncertainty analyses of complex models of masonry towers often not feasible due to the computational effort they require. Classical methods, such as standard Monte Carlo and Latin Hypercube Sampling, for propagating uncertainty and developing probability density functions of model output, may in fact require performing a considerable number of simulations. These methods can become computationally prohibited if the time necessary to evaluate the limit state for each set of realizations of model random variable is non-negligible.

Indeed, an accurate estimate of the probability of failure $P_j(F|\boldsymbol{\theta})$ involve a large number of deterministic nonlinear structural analysis for different samples of the input parameters, whose computational effort is expensive. This aspect makes both Monte Carlo and Latin Hypercube Sampling difficult to apply. In such situations, the response surface method provides a powerful tool for estimating the structure failure probability and several applications can be found in the scientific literature [84,133–137]. In this way, the computational effort associated with a Monte Carlo methods can be reduced with the combination of the response surface analysis.

A response surface is a simplified relationship between the input random variables and the limit state criterion, *e.g.* collapse of the structure. The negative side of this efficiency is a loss of accuracy in the estimation of the limit state, which depends on the degree of the selected surface and the variability of the nonlinear results.

In this respect, $\boldsymbol{\theta} = \{E, h\}^T$ is the two components vector of the random variables and $f(\boldsymbol{\theta})$ the performance function. The response surface in a two-dimensional random variable space, is assumed as a function of $\boldsymbol{\theta}$ where the constants are determined by evaluating $f(\boldsymbol{\theta})$ at specified sampling points. These sampling points are selected to be located in correspondence of relevant percentiles of the joint-probability density function of the random variables, $\boldsymbol{\theta}$. Figure 5.19 reports the joint-posterior PDF of E and h obtained in §4.2.2 through the Bayesian updating and the identification of the points in which the greatest probability is concentrated. Moreover, for each of these points the uncertainty related to the compressive strength of the masonry is considered thus selecting some representative samples, reported in Table 5.6.

A global response surface is fitted on the selected points and Monte Carlo sampling is carried out on the fitted response surface to obtain failure probability estimates.

The application of this simplified method is widespread in many research fields and the scientific literature confirms its use to reduce the computational effort obtaining satisfactory results [84,133–137]. Moreover, as far as the specific case is concerned, the regularity of the pushover curves highlighted in the sensitivity analysis, allows to justify the employment of response surfaces.

As mentioned before, the main results proposed in this dissertation are referred to the case study of the Becci tower. This structure is considered as representative of a consistent number of historic masonry towers, showing geometric and mechanical characteristics close to the mean values resulting from the analyses of the collected database. Nonlinear static analyses are thus carried out considering the numerical model described in §5.2.1. Some parameters are assumed as deterministic: the square cross section (side, a = 6.5 m. and thickness s = 1.5 m), the total height (H = 38.9 m) and the specific weight (w = 16 kN/m^3).

Other parameters are considered as uncertain: the elastic modulus, the height of the lateral restraints (or vice versa the height of the free-standing part of the tower) and the compressive strength. In particular, for each combination of $\boldsymbol{\theta} = \{E, h\}^T$ (Figure 5.19), five different values of compressive strength are taken into account (Table 5.6), obtaining 245 combinations.

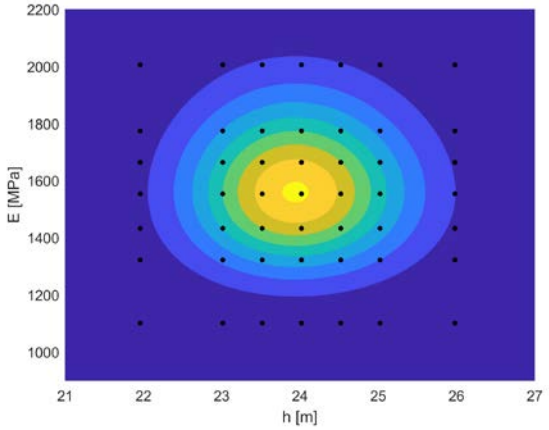

E [MPa]	h [m]
1100	22.0
1325	23.0
1437	23.5
1550	24.0
1662	24.5
1775	25.0
2000	26.0

Figure 5.19 – Joint-posterior PDF of *E* and *h* reported in §4.2.2 (Bayesian updating) and the identification of the samples to represent it.

Table 5.6 – Assumed values for the compressive ($f_{c,DP}$) and tensile ($f_{t,WW}$) strength(*).

#	c [MPa]	φ	$f_{c,DP}$ [MPa]	$f_{t,DP}$ [MPa]	$f_{c,WW}$ [MPa]	$f_{t,WW}$ [MPa]	β_c [-]	β_t [-]
a)	0.22		0.94	0.28		0.204		
b)	0.27		1.16	0.34		0.251		
c)	0.32	40	1.37	0.40	8.0	0.298	0.75	0.25
d)	0.37		1.59	0.47		0.343		
e)	0.42		1.80	0.53		0.387		

(*) Note that, the compressive ($f_{c,DP}$) and tensile ($f_{t,WW}$) strength are related according to Eq. (47).

The results of 245 pushover analyses, in terms of pushover curves, are shown in Figure 5.20. The huge computational effort of these analyses, has limited the number of simulations, making necessary the employment of response surfaces in order to define distributions of values for the damage levels considered. Indeed, for each curve, according to the procedure proposed in §5.2.3. two damage levels are identified: the first, DL2, related to damage condition, and the second, DL3, related to the collapse condition.

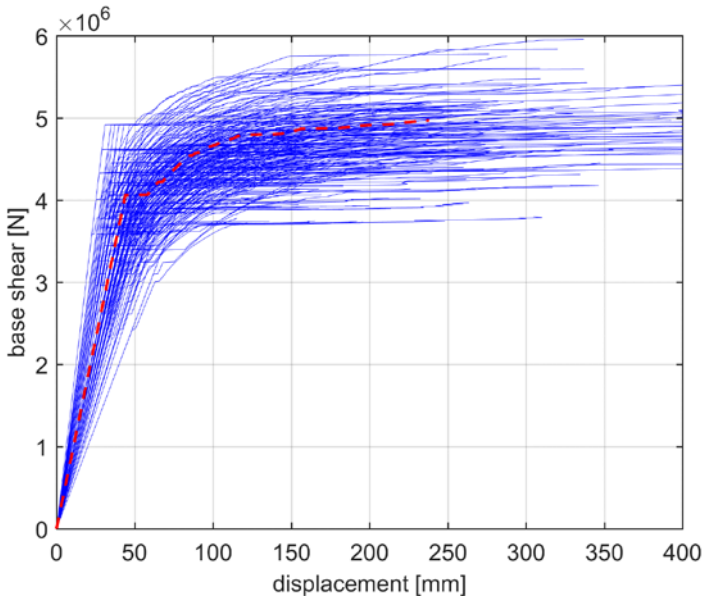

Figure 5.20 – Capacity curves with their mean value (red dotted line).

Both for the sake of clarity and to underline the effect of different values of compressive strength, Figure 5.21a reports the identification of DL2 and DL3 for $\boldsymbol{\theta} = \{E = 1662 \text{ MPa}, h = 24.0 \text{ m}\}^T$. As already demonstrated from the sensitivity analyses (§5.2.4), an increase of compressive strength gives rise to an increase of both displacement and base shear. Moreover, the discrepancy between the DL2 and DL3 displacements steady rise, maintaining a regular behaviour of the displacements (related to damage levels) as function of the compressive strength, Figure 5.21a.

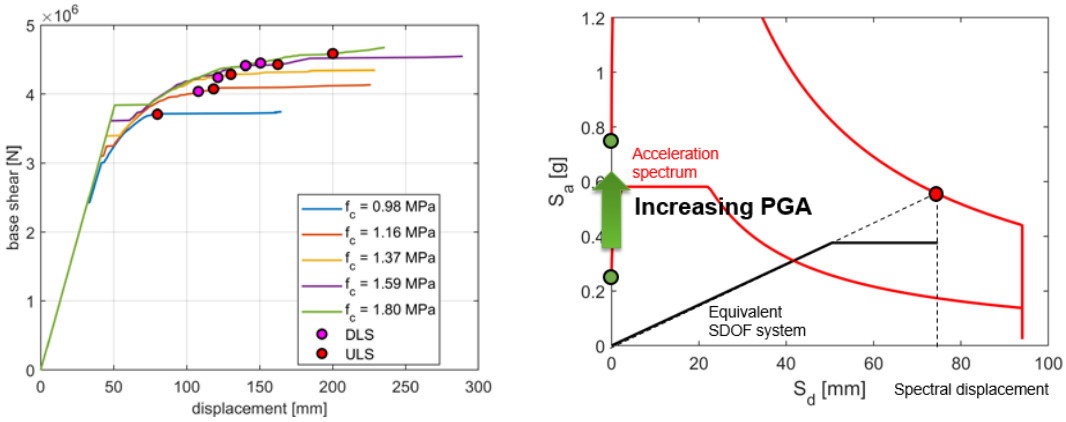

(a) (b)

Figure 5.21 – (a) Identification of the damage levels (DL2 and DL3) on the capacity curves characterized by $\boldsymbol{\theta} = \{E = 1662 \text{ MPa}, h = 24.0 \text{ m}\}^T$ and b) procedure for the definition of the relative value of PGA for each damage level.

A PGA value is then associated to each identified damage level, according to capacity spectrum method (Figure 5.21b). Its variability, related to DL3 for $\boldsymbol{\theta} = \{E = 1662 \text{ MPa}, h = 24.0 \text{ m}\}^T$, is shown in Figure 5.22a. The gradual rise of the PGA as function of f_c, allows to associate at this behaviour a linear approximation (dotted line in Figure 5.22a) in order to evaluate the PGA for values of compressive strength not directly analysed. As previously highlighted, the compressive strength of the masonry is the most uncertain parameter, therefore its variability should be expressed through a probability distribution. According to CNR [117], a lognormal distribution is initially selected (Figure 5.22b) considering mean and standard deviation respectively equal to 1.5 MPa and 0.20 MPa. This distribution can be considered as modelling uncertainty related to the output of the nonlinear analyses for each $\boldsymbol{\theta_i} = \{E_i, h_i\}^T$ vector. Indeed, through Monte Carlo simulation of the lognormal distribution considered, a significant number of compressive strength values is sampled. These samples are projected on the linear approximation, defined in Figure 5.22a, thus obtaining for each $\boldsymbol{\theta_i} = \{E_i, h_i\}^T$ vector, the PDF of PGA that takes into account the uncertainty on the compressive strength. A graphical representation is provided in Figure 5.23a.

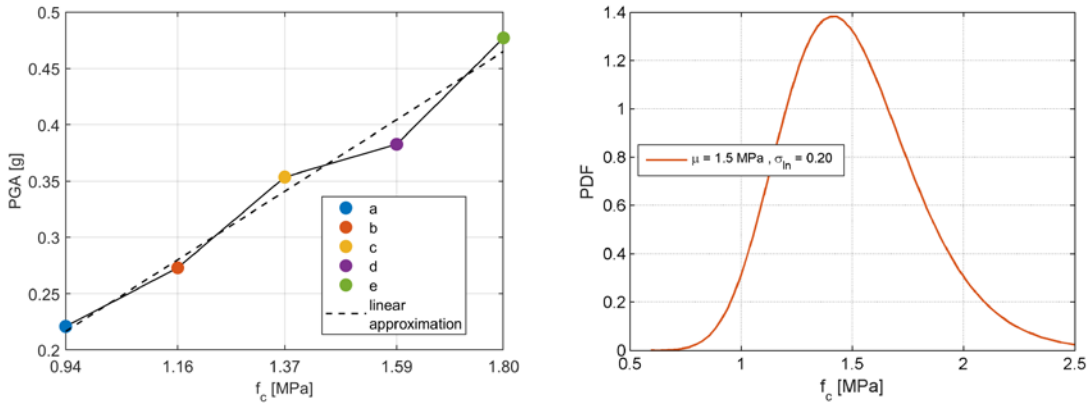

(a) (b)

Figure 5.22 – (a) Variability, in terms of compressive strength, of the PGA related to DL3 for $\boldsymbol{\theta} = \{E = 1662 \text{ MPa}, h = 24.0 \text{ m}\}^T$ (solid line) and corresponding linear approximation (dotted line), and (b) assumption on the PDF for the compressive strength.

The probability of failure is calculated for different level of PGA. For the sake of clarity, it is represented in Figure 5.23a as the area under the curve (blue surface) delimitated by a generic PGA level (horizontal red plane); its value is shown in Figure 5.23b.

The result is a surface on the two-dimensional random variable space that represents the probability of failure, conditioned to the $\boldsymbol{\theta}$ parameters and related to a specific limit state, for each level of demand in terms of PGA.

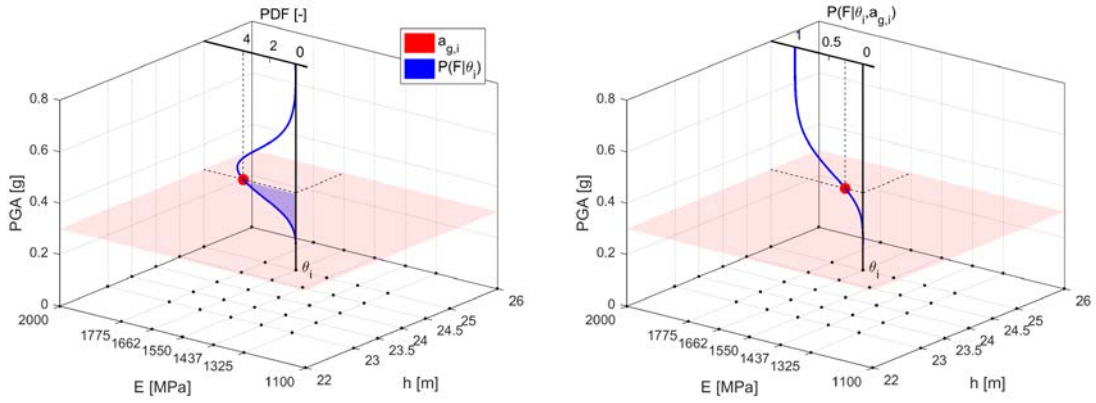

(a) (b)

Figure 5.23 – Graphical representation of the probability of failure for a given level of PGA (red horizontal plane) and for selected parameters $\boldsymbol{\theta_i}$.

5.3. Comparisons between robust seismic fragility curves

The fragility curve is derived from Eq. (36), where the first term, $P_j(F|\boldsymbol{\theta})$, has been defined in the previous section and represents the probability of failure conditioned to the $\boldsymbol{\theta}$ parameters, for the *j-th* level of demand PGA. The second term, $p_{\overline{D}}(\boldsymbol{\theta})$, has been defined in §4.2.2 and represents the posterior joint-probability distribution of the $\boldsymbol{\theta} = \{E, h\}^T$ random variables vector. Noteworthy, this latter distribution is independent to the level of PGA selected.

The fragility curve is determined point by point, which represent the probability of exceedance according to the damage level considered, for each level of PGA. The result is proposed in Figure 5.24 related to the modelling uncertainty shown in Figure 5.22b.

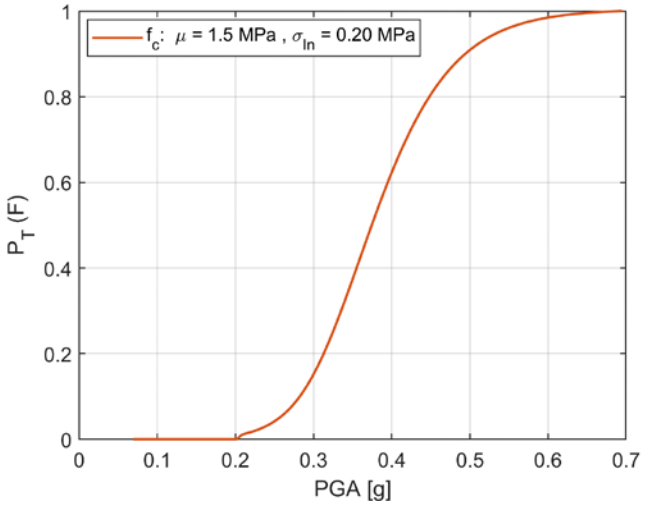

Figure 5.24 – Robust seismic fragility curve.

The resulting fragility curve describes the vulnerability of an historic masonry tower to seismic loadings in terms of the conditional exceedance probability of a seismic intensity measure: the PGA of demand.

The proposed methodology allows to take into account:

- the Bayesian FE-model updating on the $\boldsymbol{\theta} = \{E, h\}^T$ random variables vector, by using experimental dynamic data (the measurement of natural period),
- the variability of the compressive strength of the masonry, considered as modelling uncertainty on the result of each nonlinear seismic analysis,
- the specific damage level.

However, the main purpose of this dissertation was the quantification of the role of different sources of uncertainty in each step of the seismic vulnerability chain for historic masonry towers. In order to evaluate the achievement of this objective, some comparisons can be discussed.

- *Introduction of the Bayesian FE-model updating*

The proposed procedure has been started with the use of experimental measurements of natural periods as new information in a Bayesian framework for the updating of the numerical model.

As mentioned before, usually this information is used in order to reduce the discrepancy between the experimental value and the numerical model, changing the structural parameters and defining different deterministic linear model that fulfil this objective. This latter approach proposes unique values of the geometry and the elastic parameters of the material (elastic modulus and mass density). Moreover, some correlations between elastic and inelastic parameters (*e.g.* correlation between elastic modulus and compressive strength), can be introduced in order to identify a deterministic nonlinear model. These assumptions correspond to a fragility curve without uncertainties (Heaviside function). For the sake of clarity, an example is proposed in Figure 5.25, related to the last damage level, DL3. The yellow line is the deterministic case, defined in the third column of Table 5.7 and denominated as *Case 1*. If no reliable information are available on the inelastic parameters of the masonry, a more realistic case (*Case* 2) could be introduced, taking into account a PDF of the compressive strength (or cohesion), in order to represent its variability. In this respect, a lognormal distribution is selected for the compressive strength with the same median value of the *Case 1*. The corresponding fragility curve is represented in purple in Figure 5.25. The comparison between these two first cases, allows to evaluate the effect of the uncertainty on the nonlinear model of the masonry. In particular, the dispersion of the fragility curve is increased maintaining the same median collapse capacity. This latter aspect is due to the PDF of f_c selected for the *Case 2*, which maintains the same median value.

The third case, indicated as *Case* 3, represents the result of the methodology proposed in this dissertation, in which the experimental measurement of the natural period is included in a Bayesian framework, in order to define a posterior joint-PDF of some parameters of the linear model (in particular the elastic modulus and the free-standing part of the tower); maintaining the same uncertainties of the nonlinear model, introduced in the *Case 2*. This last case is represented with the green curve in Figure 5.25 and shows the effect of the uncertainties both in the linear and nonlinear model. Also in this case the median of the fragility curve is maintained and the dispersion is increased respect both the previous cases.

Table 5.7 – Characteristics of the reference cases used to evaluate the effect of different sources of uncertainty.

		Case 1	*Case 2*	*Case 3*
Geometry	External side, a [m]	6.5	6.5	6.5
	Thickness, s [m]	1.5	1.5	1.5
	Total height, H [m]	38.4	38.4	38.4
	Effective height, h [m]	24.9	24.9	$\mu = 24.3\ \sigma_{ln} = 0.1$
Elastic parameters	Specific weight, w [kN/m^3]	16	16	16
	Elastic modulus, E [MPa]	1660	1660	$\mu = 1550\ \sigma_{ln} = 0.1$
Plastic parameters	Cohesion, c [MPa]	0.34	$\mu = 0.35\ \sigma_{ln} = 0.2$	$\mu = 0.35\ \sigma_{ln} = 0.2$
	Friction angle, φ [°]	40	40	40
	Compressive strength$^{(*)}$,	1.47	$\mu = 1.5\ \sigma_{ln} = 0.2$	$\mu = 1.5\ \sigma_{ln} = 0.2$

$^{(*)}$ Dependent variable defined through Eqq. (44) and (45)(5), §5.2.1.1 $^{(**)}$ Posterior joint-PDF of E and h, §4.2.2.

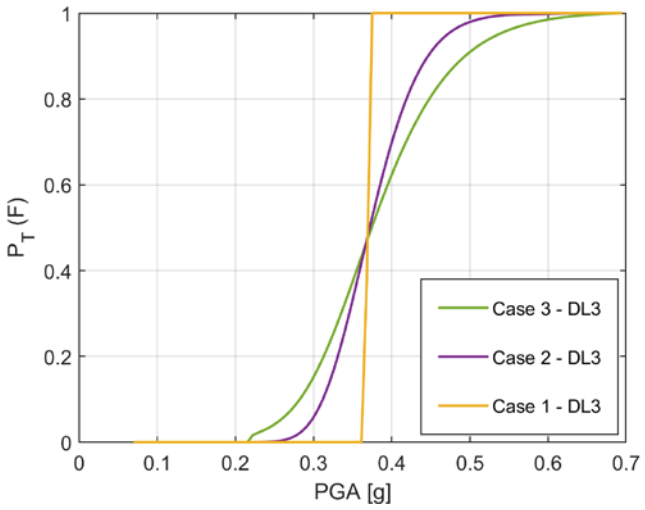

Figure 5.25 – Representation of the effect of different sources of uncertainties in terms of fragility curves.

Figure 5.25 reveals that the effect of the uncertainty nonlinear model parameters seems to have a greater effect compared to the uncertainty related to the linear model of the tower. This

consideration is confirmed also to the values of PGA which predict a probability of failure of 5%, in the three considered cases. For the *Case 1* this level is gained for PGA equal to 0.36 g, 0.24 g for the *Case 2* and 0.22 g for the *Case 3*.

- *Different modelling uncertainties, i.e. different PDFs of the compressive strength*

From the previous comparisons, the role of the modelling uncertainties of the nonlinear model appears important. Due to this fact, different PDFs of the compressive strength of the masonry are considered; their characteristics are shown in Table 5.8.

Table 5.8 - Characteristics of the lognormal distribution of f_c.

Lognormal distribution of f_c	μ [MPa]	σ_{ln} [MPa]
A	1.48	0.10
B	1.50	0.20
C	1.55	0.30

These distributions are characterized by the same median value, as demonstrate in Figure 5.26a. The results (Figure 5.26b) confirm an increment of the fragility curve dispersion, due to an increase value of the standard deviation of the masonry compressive strength. In particular, observing the values proposed in Table 5.9, the variation of the PGA (corresponding to the failure probability of 5%) steady increase from 0.21 g for the A-distribution to 0.31 g for the C-distribution, revealing the coherence of the results.

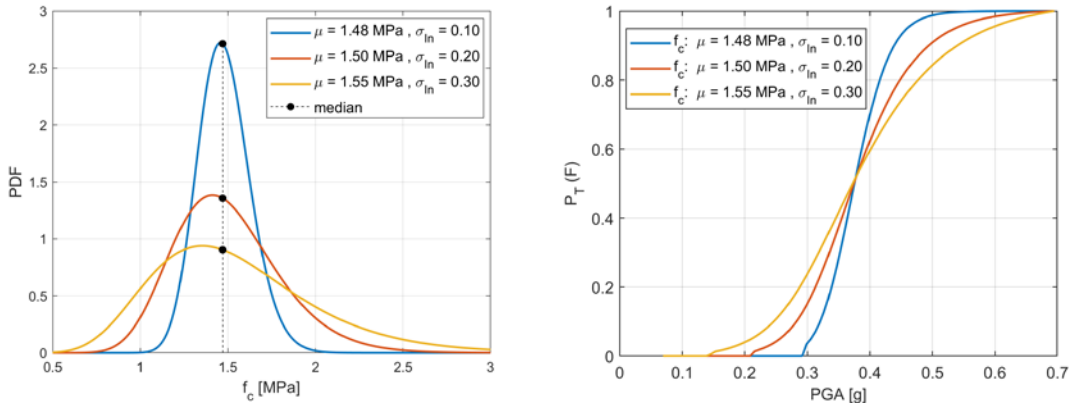

(a) (b)

Figure 5.26 – (a) PDFs of masonry compressive strength, characterized by the same median value and (b) the corresponding fragility curves.

Table 5.9 – PGA corresponding to the reach the probability of failure of 5%

PGA [g]	A	B	C
DL3	0.21	0.26	0.31

- *Different damage levels*

As mentioned before, the proposed procedure allows the incorporation of different damage levels. Three of them are identified in this work (§5.2.3) and herein reported in terms of fragility curves for the different level of uncertainties considered (*Case* 1, *Case 2* and *Case 3*). Specifically, in Figure 5.27 are represented DL3 with solid line, DL2 with dotted one and DL1 with point-dotted one. The results highlight the effect of different damage levels which provoke a shift of the fragility curve without significant variations in terms of dispersion.

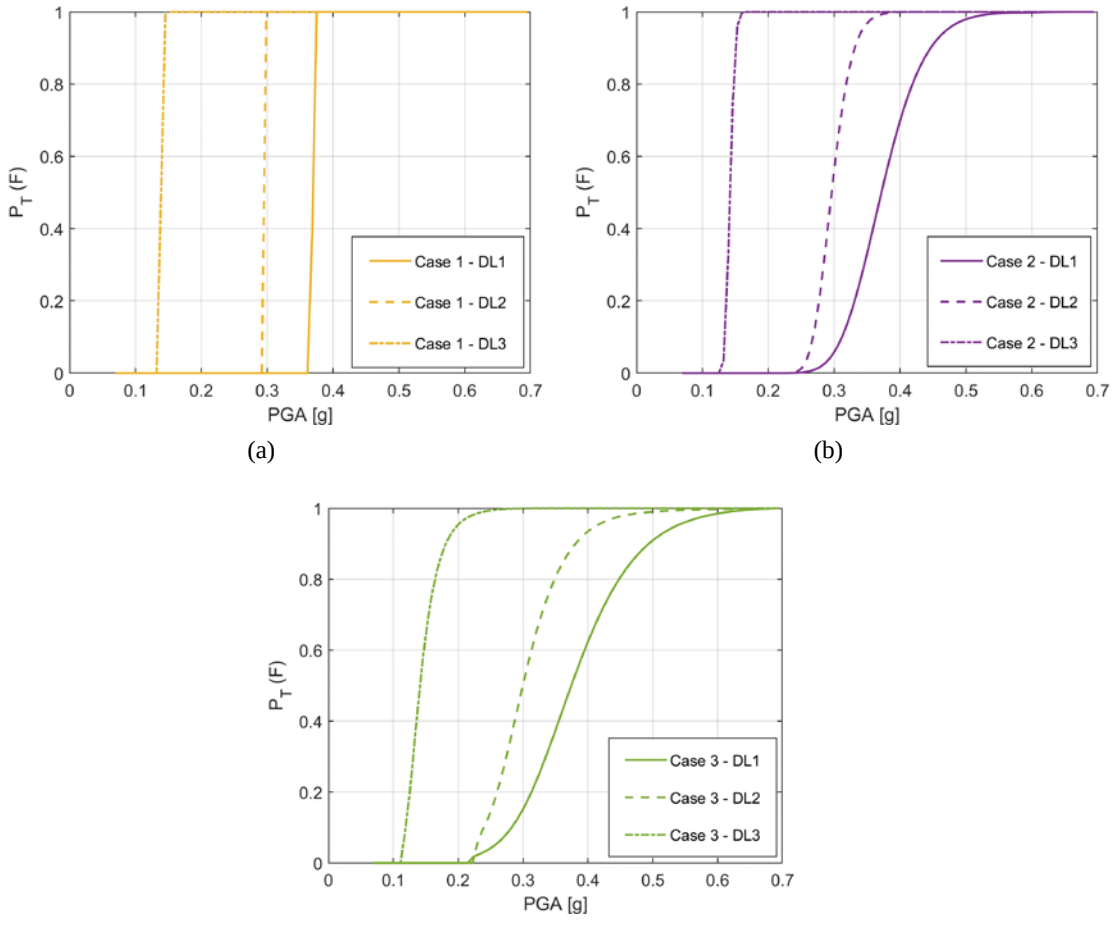

Figure 5.27 – Fragility curves related to the damage levels considered (DL1, DL2 and DL3) and for (a) Case 1, (b) Case 2, and (c) Case 3.

Observing the results of Table 5.10, which reports, also in this case the PGA values corresponding to 5% of probability of failure, the discrepancy among the three selected damage levels gradually decrease for lower values of PGA. This result seems to identify for the higher level of PGA (corresponding to a severe damages) the more relevant role of the uncertainties introduced in the

methodology; and confirms that the first damage level (corresponding to the displacements exceed the elastic limit state) is almost insensitive to variation of the nonlinear model parameters.

Table 5.10 – PGA corresponding to the reach the probability of failure of 5%.

PGA [g]	DL1	DL2	DL3
Case 1	0.13	0.29	0.36
Case 2	0.13	0.25	0.30
Case 3	0.11	0.23	0.26

5.4. Conclusions

In this chapter, a procedure has been proposed for incorporating structural modelling uncertainties into the probabilistic assessment of seismic vulnerability of historic masonry towers. The results have been presented through the definition of fragility curves, by evaluating the effect of different sources of uncertainties and different damage levels. Indeed, this work was motivated by the scarcity of researches specifically addressed to the derivation of fragility curves for masonry constructions by incorporating the uncertainties in the structural modelling parameters.

The proposed procedure has allowed to include the available experimental data in a Bayesian procedure, to improve the FE-model prediction in both linear and nonlinear field. The results have been based of nonlinear static analyses of a reference masonry tower, considered to be representative of a large number of other case studies. In this way, despite the quantitative results have been referred to the considered specific case, qualitative considerations could be easily extended to other similar structures. In particular:

- incorporating modelling uncertainties increases the dispersion of the fragility curve,
- the effect of incorporating modelling uncertainties is greater for higher levels of PGA,
- when the modelling parameters are more uncertain, the dispersion of the fragility curve increases,
- neglecting the effects of modelling uncertainties seems to be not conservative, giving rise to lower values of PGA.

These considerations point more generally to the need of appropriately characterization and propagation of the uncertain structural parameters both for linear and nonlinear model; since modelling uncertainties may have a large effect on the seismic vulnerability prediction.

The discussion thus far has focused on the uncertainties related to the structural parameters; however, for a comprehensive assessment of the seismic risk, the uncertainties related to the seismic hazard must to be considered, as carried out in the next chapter.

Chapter 6

Seismic risk assessment

The assessment of robust reliability takes into account the uncertainties from structural modelling in addition to the uncertain excitation, which can occurred during the lifetime of a structure as seismic loads [63]. In this framework, the comprehensive definition of the seismic risk can be reached through the cost estimation chain, proposed by PEER Centre [138] and summarized in Figure 6.1.

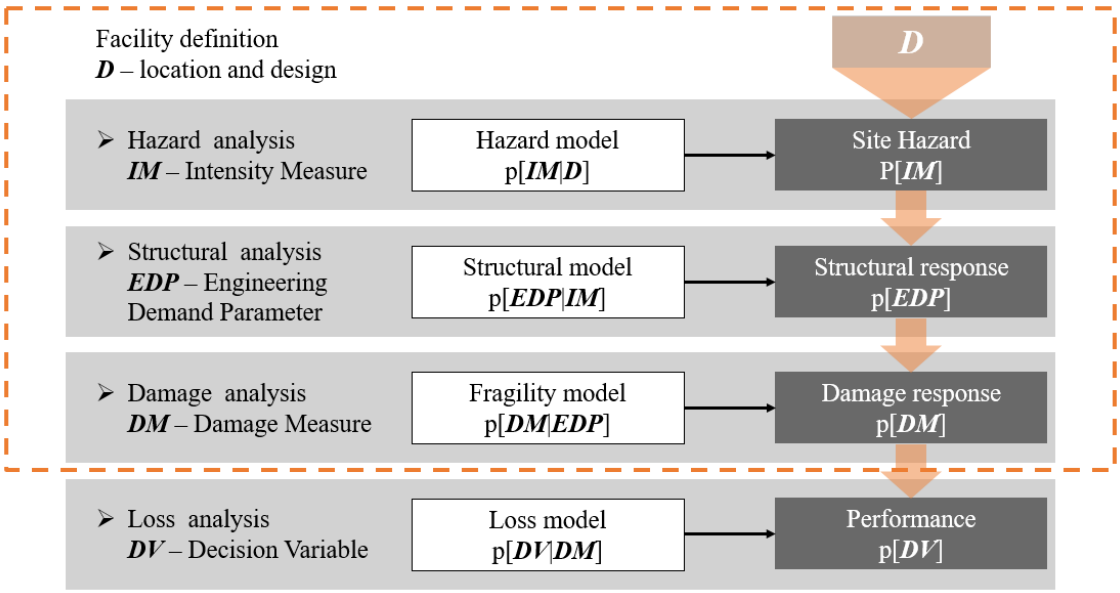

Figure 6.1 - PEER chain in which the rings considered in this work are highlighted.

The approach starts with the ground motion *Intensity Measure*, by defining in a probabilistic frame the main features of the seismic hazard affecting the structural response. Then, the

Engineering Demand Parameters are defined in order to synthetize the structural response, calculated by simulations of the building against seismic action. These parameters are next related to the *Damage Measure*, which provide the structural damage on the structure. Finally, given a detailed probabilistic description of damage, the procedure translates this quantity into losses and then allows risk management decisions [138]. The approach underlines the uncertainties in all the phases of the risk assessment, providing an effective tool for integrating data and models in different fields.

Some recent works proposed the effect of the uncertainties on engineering demand parameters for common reinforced concrete and steel structures [84,139–144] but only a few papers deal with the probabilistic vulnerability assessment of masonry buildings [145–147]. As far as historic masonry towers are concerned, several studies proposed their seismic risk assessment, although rarely with probabilistic procedure [18,57,91].

The present dissertation aims to cover this gap of knowledge for historic masonry towers, by dealing with, in a simplified manner, the first three steps of the cost estimation chain (Figure 6.1), in order to conclude the methodology proposed in this dissertation through a quantitative assessment of the seismic risk.

6.1. Methodology

The PEER methodology can be expressed as a triple integral based on the total probability theorem, as stated in Eq. (58). The costs, usually termed Decision Variable (*DV*), are assessed by deconvoluting the structural Damage Measure (*DM*), the Engineering Demand Parameters (*EDP*), and the ground-motion Intensity Measure (*IM*) as intermediate variables [138,148].

$$\upsilon(\boldsymbol{DV}) = \iiint G(\boldsymbol{DV}|\boldsymbol{DM})\,|dG(\boldsymbol{DM}|\boldsymbol{EDP})|\,|dG(\boldsymbol{EDP}|\boldsymbol{IM})|\,|d\lambda(\boldsymbol{IM})| \tag{58}$$

where, $G(\boldsymbol{X}|\boldsymbol{Y})$ represents the complementary cumulative probability function of $\boldsymbol{X}$ conditioned on a given level of $\boldsymbol{Y}$ and $\lambda(\boldsymbol{IM})$ is the mean annual rate of exceeding, given $\boldsymbol{IM}$.

6.1.1. Assumptions and application

The same concepts can be applied for historic masonry towers; by employing the PEER procedure to evaluate the effect in terms of seismic risk of the different sources of uncertainties introduced in the methodology illustrated in the previous chapters. In particular, in this application the term $\boldsymbol{DV}$ is neglected, because no information are available on the definition of the cost estimation; the integral of Eq. (58), become:

$$v(\boldsymbol{DM}) = \iint G(\boldsymbol{DM}|\boldsymbol{EDP}) \; |dG(\boldsymbol{EDP}|\boldsymbol{IM})| \; |d\lambda(\boldsymbol{IM})| \tag{59}$$

Moreover, $\int G(\boldsymbol{DM}|\boldsymbol{EDP})|dG(\boldsymbol{EDP}|\boldsymbol{IM})|$ can be considered as the seismic vulnerability assessment obtained in the previous chapter. Specifically, the assessment of seismic risk process can be represented through logical elements studied in a probabilistic framework. In order to carry out this process for the considered masonry tower, Figure 6.2 introduces some assumptions.

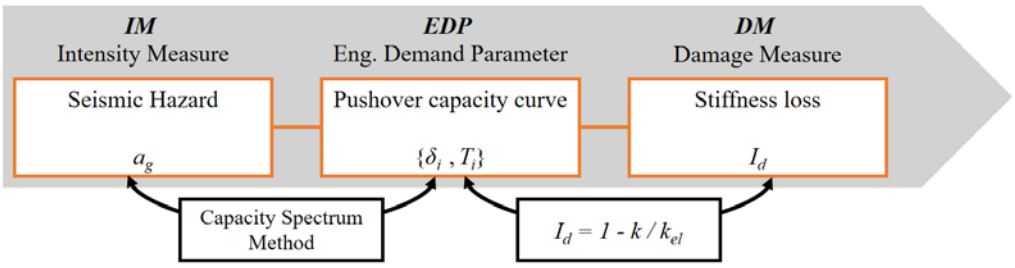

Figure 6.2 – Flowchart of the procedure with the assumptions related to the application on historic masonry towers.

$\boldsymbol{IM}$ is considered as peak bedrock acceleration a_g, including the record-to-record variability in the seismic response spectra; $\boldsymbol{EDP}$ is represented by the pushover curve, *i.e.* the displacement of the control point and the corresponding base shear for each step of the analysis, and $\boldsymbol{DM}$ is evaluated as the damage index $\boldsymbol{I_d}$, obtained directly from the pushover curve as function of the ratio between its tangent and elastic stiffness (§5.2.3). Thus, this index is a measure of the structural damage and ranges from zero (undamaged structure) to one (collapsed structure):

$$\boldsymbol{I_d} = 1 - \frac{k}{k_{el}}$$

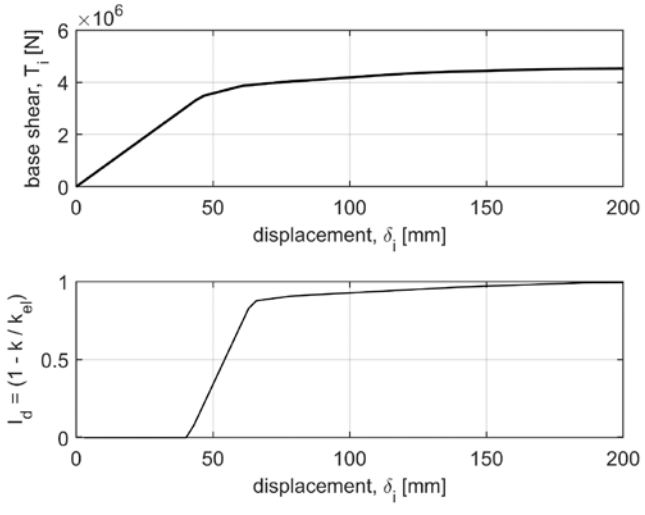

Figure 6.3 – Pushover curve and the corresponding damage index I_d.

After these considerations, the seismic risk assessment as function of the damage index I_d, can be calculate through the following integral:

$$\upsilon(I_d) = \int G(I_d|a_g)\ |d\lambda(a_g)| \tag{60}$$

where $G(I_d|a_g)$ is the probability of exceedance of a certain I_d, given the peak bedrock acceleration a_g, and $\lambda(a_g)$ is the mean annual rate of exceeding of the peak bedrock acceleration a_g. Below, these two terms are shown with specific regard to the reference case considered:

- the first term $G(I_d|a_g)$ for $I_d = 1$, represents the fragility curve obtained in Chapter 5, related to DL3, and reported for the sake of clarity in Figure 6.4.

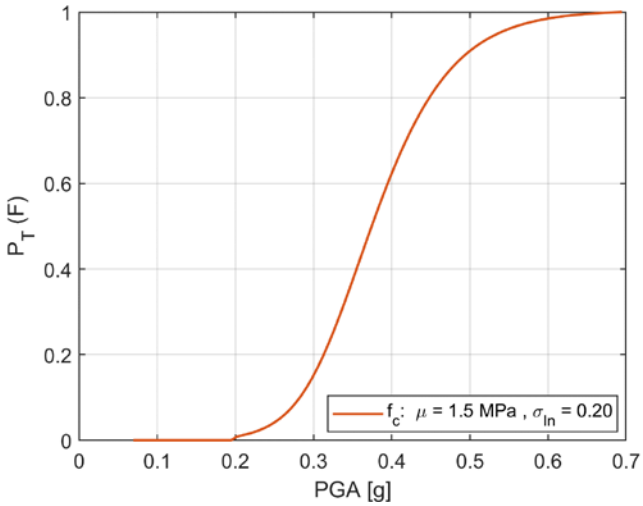

Figure 6.4 - Fragility curve for I_d = 1 (DL3).

- the second term $\lambda(a_g)$ includes the seismicity of the investigated area. The peak bedrock acceleration a_g and the relationship between this parameter and the return period T_R has been obtained by the data available on Italian Building Code [113]. Specifically, Eq. (61) reports the definition of the probability of exceedance P_{VR} for the considered reference life V_R (50 years), as a function of the return period T_R. The values of P_{VR} are defined in the Italian Building Code [113] for four typology of Limit States, as reported in Table 6.1. Other values of P_{VR} can be calculated by using Eq. (61) with all the values of T_R supplied in [113].

$$T_R = -\frac{V_R}{\ln(1-P_{VR})} \rightarrow -\frac{V_R}{T_R} = \ln(1-P_{VR}) \rightarrow P_{VR} = 1 - e^{-\frac{V_R}{T_R}} = 1 - e^{-\lambda V_R} \tag{61}$$

Table 6.1 – Limit states supplied in Italian building code and corresponding P_{VR} and T_R , for $V_R = 50$ years.

Typology of Limit State		P_{VR}	T_R
Operational	SLO	81%	30
Damage	SLD	63%	50
Life Safety	SLV	10%	475
Collapse Prevention	SLC	5%	975

The seismic hazard curve is thus obtained through interpolation of these values as a function of a_g; indeed, the Italian Building Code associates for each return period a corresponding value of a_g, dependent on the site location.

For the sake of clarity, two seismic hazard curves are considered for the next comparisons (Figure 6.5): the first is related to San Gimignano (seismic zone III, $0.05 < a_g \leq 0.15$), where the reference tower is located, and the second is related to Norcia (seismic zone I, $a_g > 0.25$), where the last seismic events occurred.

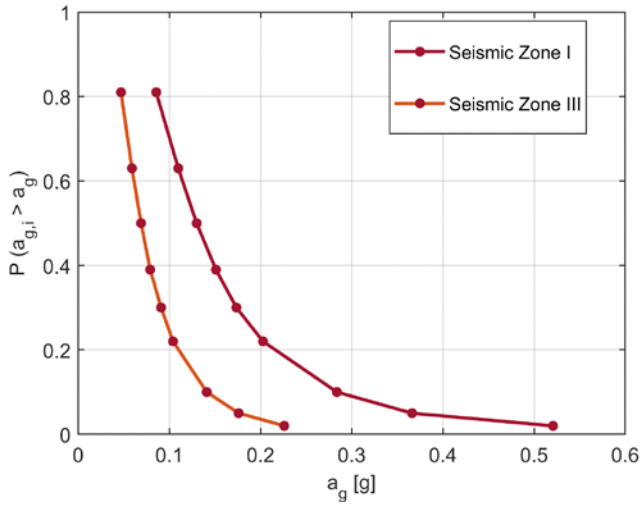

Figure 6.5 – Hazard curve for two seismic areas.

Note that, a_g is the acceleration of peak on rigid ground ($S = 1$, and $PGA = S \cdot a_g = a_g$) and, in the following, this will be referred to as PGA.

6.2. Applications

The seismic risk of the masonry tower considered as reference case, is evaluated of providing a quantitative assessment of the sources of uncertainty introduced in the methodology proposed in this dissertation. In order to achieve this purpose, Eq. (60) is applied for the cases analysed in §5.3, and here synthetically reported for the sake of clarity:

- *Case 1*: deterministic assessment of constitutive parameters of both linear and nonlinear model, based on the knowledge of experimental natural periods.
- *Case 2*: deterministic assessment of constitutive parameters of linear model based on the knowledge of experimental natural periods, probabilistic evaluation of the constitutive parameters of nonlinear model.
- *Case 3*: Bayesian updating of constitutive parameters of linear model based on the knowledge of experimental natural periods, probabilistic evaluation of the constitutive parameters of nonlinear model.

Through the comparison among these selected cases, the role of the uncertainties related to the parameters of linear model (specifically the elastic modulus E and the restraint conditions h), is highlighted together with the uncertainties of the nonlinear model (in particular the compressive strength of the plastic model of the masonry f_c). The same comparison is carried out for the three damage levels introduced in §5.2.3: DL1, DL2 and DL3.

In this respect, Figure 6.6 and Figure 6.7 show the seismic hazard for two representative seismic zones together with the seismic vulnerability of the masonry tower express in terms of fragility curves for the selected cases.

In particular, Figure 6.6 reports this representation related to the ultimate damage level DL3 and some considerations can be drawn. The low seismic hazard of San Gimignano (seismic zone III) does not allow to quantify the risk for the cases selected, which are characterized by a capacity PGA higher than the demand PGA corresponding to the return periods provided by Italian Building Code. As far as the seismic hazard of Norcia (seismic zone I) is concerned, taking into account a reference life of 50 years, the *Case 1* reaches a seismic risk equal to 2.9 %, the *Case 2* equal to 3.5 % and the *Case 3* equal to 4.1 %, as reported in Table 6.2. These values reveal that the uncertainties on the nonlinear model seem to have more effect compared to the uncertainties on the linear model, this confirm the relevant role of the masonry compressive strength definition. In any case, the limited knowledge on both linear and nonlinear models, represented by a probabilistic assessment of the constitutive model parameters, produces an increment of the seismic risk. Notice that, these considerations are referred to the three specific cases considered, which are characterized by the same median values of geometrical and mechanical parameters

(Table 5.7), obtaining the 50% of the population of towers collapsed for the same level of PGA. These comparisons aim to quantify the effects in terms of seismic risk of the various sources of uncertainities, rather than determine the most conservative case. Indeed, to achieve this latter goal additional deterministic cases must be considered in order to represent other possible model choices.

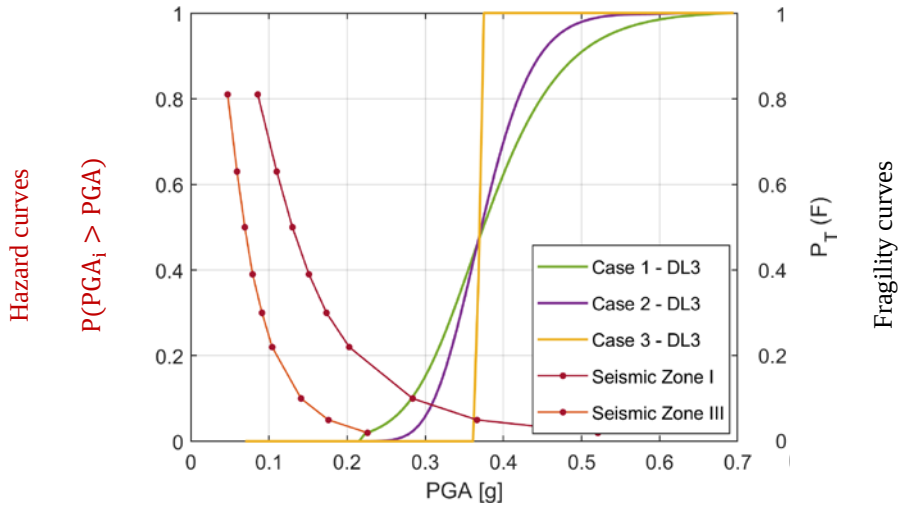

Figure 6.6 – Fragility curves related to DL3 and hazard curves.

Table 6.2 – Seismic risk assessment for DL3.

$v(\bar{I}_d)$	Seismic Zone I (Norcia)	Seismic Zone III (San Gimignano)
$\bar{I}_d$	DL3	DL3
Case 1	2.9 %	-
Case 2	3.5 %	-
Case 3	4.1 %	-

The discussion so far focused on the case related to the ultimate damage level; the same comparisons can be applied to the other two damage levels previously considered. In this respect, Figure 6.7 shows the same representation of the Figure 6.6 including the vulnerability assessment of all the considered damage levels. Specifically, the solid lines represent DL3, the dotted line DL2 and the point-dotted line DL1. In addition to the previous considerations, Figure 6.7 and Table 6.3 underline that the uncertainties (related to the constitutive parameters both linear and nonlinear model) have less relevance on DL1 and DL2 compared to DL3.

This aspect is particularly evident for DL1. Indeed, the achievement of this damage level is almost insensitive to variation of the nonlinear model parameters. This fact is also confirmed by the

negligible discrepancy between the risk related to *Case 1* and *Case 2*, for whose the only difference is on the compressive strength of the masonry, considered in the first case with a unique value and in the second case with a probability distribution. For this specific damage level, the seismic risk ranges from 43.6 % to 43.4 % for Norcia and from 8.5 % to 8.6 % for San Gimignano. Instead, considering the Case 3, for which also the parameters of the linear model are represented with probability distributions, the risk increases up to 44.4 % for Norcia and to 9.3 % for San Gimignano.

The discrepancies of the seismic risk values related to the two seismic zones considered, underline the great relevance of the seismic hazard for low levels of PGA. This effect appears less evident for higher levels of PGA, usually corresponding to severe damage of a construction, for which the uncertainties related to the structural parameters gain much relevance.

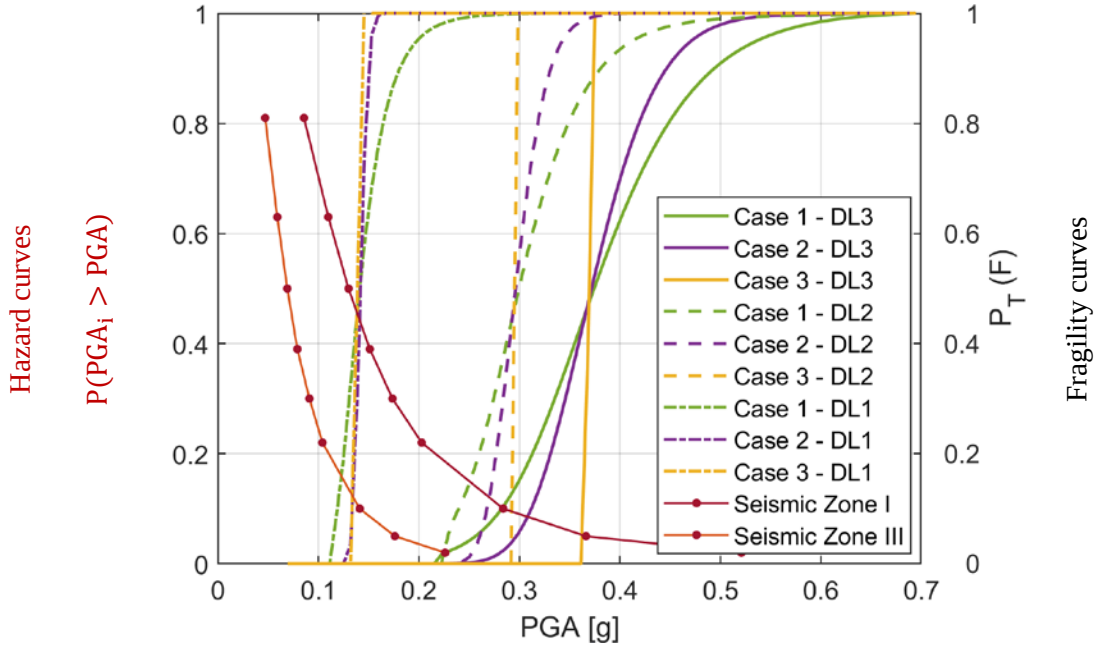

Figure 6.7 – Fragility curves related to DL1, DL2 and DL3 with the hazard curves.

Table 6.3 – Seismic risk assessment for DL1, DL2 and DL3.

$v(\bar{I}_d)$	Seismic Zone I (Norcia)			Seismic Zone III (San Gimignano)		
$\bar{I}_d$	DL1	DL2	DL3	DL1	DL2	DL3
Case 1	43.6 %	7.3 %	2.9 %	8.5 %	-	-
Case 2	43.4%	7.6 %	3.5 %	8.6 %	-	-
Case 3	44.4 %	8.9 %	4.1 %	9.3 %	-	-

6.3. Conclusions

In this chapter, the expected performance of a masonry tower subjected to earthquake hazard has been defined. The quantitative results obtained in terms of seismic risk, are specifically related to the reference case study. However, the methodology can be easily extended to other historic masonry towers; indeed, the procedure has general soundness, providing a useful tool applicable also to other structural typologies.

The methodology divides the seismic risk assessment process into logical elements that have been studied and managed in the previous chapters of this dissertation. The definition of a ground motion intensity measure has been the first step and, in this respect, the peak ground acceleration PGA was selected because of this parameter is strongly related to the structural damage, is easily to measure, and at least in linear field, is proportional to the horizontal loads generated during a seismic event. Moreover, despite the prediction of a seismic event is infeasible, probabilistic prediction of the PGA measure related to a certain area is provided by Italian Building Code. After, the results of the Chapter 5 have been used in order to take into account the seismic vulnerability of masonry tower, considering different assumptions on the modelling uncertainties. Eventually, the convolution between the seismic hazard at the site, and the seismic vulnerability of the towers, has allowed the seismic risk definition.

In this framework, two main sources of uncertainties were taken into account: the first related to the characterization of the earthquake ground motion, and the second related to the simulation of the structural response, through the employment of models that represent the elastic and inelastic behaviour of the tower. The effect of these uncertainties has been evaluated in terms of seismic risk assessment, thus obtaining the following considerations:

- the probabilistic assessment of some constitutive parameters of both linear and nonlinear model gives rise to a relevant variation of the seismic risk, which increases (for *Case 2* and *Case* 3) respect to the deterministic mean structure (*Case 1*). This effect is more evident for severe damages of the tower (higher level of PGA),
- for low levels of PGA, the uncertainties related to the seismic hazard are more relevant compared to those related to the modelling assumptions. Indeed, these latter uncertainties acquire importance for high levels of PGA.

As final remark, the cases analysed and the results proposed, demonstrate that comprehensive assessment of seismic risk of historic masonry towers requires careful propagation of modelling uncertainties, accurate definition of damage states and appropriate probabilistic framework.

Chapter 7

Conclusions and future developments

The present dissertation has dealt with the role of uncertainties in the seismic risk assessment of historic masonry towers. The main purpose of the work was to provide a general framework for a robust measure of the seismic vulnerability of historic masonry towers, through the definition of fragility curves by including a Bayesian methodology for updating its reliability using dynamic experimental data. The research was motivated by the relevance of an improved knowledge of the seismic response of historic masonry towers, which incorporates the uncertainties related to the structural model with those related to the seismic hazard; a further motivation of the research was due to the scarcity of researches specifically addressed to the derivation of fragility curves as a measure of the seismic vulnerability of these structures. Indeed, for seismic risk assessment on a large scale, fragility information can represent an useful tool: however, the most comprehensive procedures for this aim, such as HAZUS (FEMA) [149] or Risk-UE [150], do not currently explicitly define the application to masonry tower structures, although they represent a structural typology widespread in Italian and European territory.

The proposed framework has been composed by three connected phases: a) Bayesian updating, b) seismic vulnerability, and c) seismic risk, which correspond, respectively, to Chapter 4, 5 and 6 of the present dissertation. This framework has been aimed to provide the seismic response assessment of masonry towers, taking into account both the available experimental data and the different sources of uncertainties involved in the process. However, to reach this aim, a preliminary step (Chapter 3) has been useful in order to identify, from the scientific literature, the experimental data usually collected for these structures, thus obtaining a general framework easily

applicable for other similar researches, which handles and combines all the available additional information.

The results have been referred to the Becci tower (San Gimignano, Italy), considered as reference case, representing a typological example of tower house and showing a regular geometry, which allows to extend the qualitative results to other case studies. It is worth repeating that the present work has required numerous hypothesis, considered one of the possible choices among many other valid alternatives. However, the aim to provide an effective reference case for the assessment of the proposed methodology has been reached, in order to evaluate the role of the uncertainties in the seismic risk assessment process.

In particular, the *Bayesian updating* has been used to improve the numerical model by using experimental dynamic data. The methodology allows for the explicit treatment of the uncertainties arising from both measurement noise and modelling errors by providing a probabilistic description of the structural models of masonry tower.

This updated model has been employed for the *seismic vulnerability* assessment, and in this second phase, also the additional uncertainties related to the constitutive parameters of the nonlinear model have been incorporated. The results provide the definition of the fragility curves in terms of the conditional exceedance probability of the selected seismic intensity measure (*i.e.* PGA), taking into account different uncertainty levels of the structural model parameters.

The quantification of these uncertainties has been evaluated in terms of *seismic risk*, introducing the additional variability due to the seismic hazard.

The results obtained can be summarized through the following general considerations:

- the probabilistic assessment of some constitutive parameters of both linear and nonlinear model gives rise to a relevant variation of the seismic risk, which increases respect to the deterministic mean structure. This effect is more evident for severe damage levels of the tower (higher level of PGA) and reveals, for the considered cases, which to neglect the effects of modelling uncertainties seems to be not conservative, obtaining lower risk values,
- for low levels of PGA, the uncertainties related to the seismic hazard are more relevant compared to whose related to the modelling assumptions. Indeed, these latter uncertainties acquire importance for high levels of PGA,
- the dispersion of the fragility curves is strictly related to the damage levels and the uncertainties of the modelling parameters.

The cases analysed and the results proposed, confirm that the crucial points for obtaining a more reliable picture of the structural safety of historic masonry towers, are related to careful propagation of modelling uncertainties, to accurate definition of damage states and to appropriate probabilistic framework.

In this respect, significant advances have been reached in the scientific literature for reinforced concrete constructions and some masonry ordinary buildings, but no comparable results are currently available for historic masonry towers. This aspect makes the proposed framework a useful tool for the seismic risk assessment of masonry towers and provides opportunities for future researches, which could include the following aspects:

- *Improvements of the assumptions*

Additional analyses can be performed of evaluating the effect of alternative assumptions, *e.g.*, in terms of: definition of damage levels, typology of analysis, modelling of the masonry. Indeed, these assumptions may have a relevant role on the final results; making necessary additional comparisons in order to provide more general and comprehensive considerations.
In this regard, the specific choice of the structural analyses has made possible to highlight simple bending damage mechanisms at the base of the model, but relevant improvements could be reached through a specific identification of other common cracking patterns, such as those near the top, as it usually occurs for slender bell cells.

- *Structural health monitoring*

The proposed methodology could be used during structural health monitoring to update measures of structural safety that could be changing due to deterioration or damage induced by severe environmental effects such as earthquakes. Indeed, structural monitoring through dynamic identification has been widely used as an effective technique for health status assessment of cultural heritage buildings, also for masonry towers, particularly susceptible to vibrations. In this respect, the damage identification represents a challenging issue for cultural heritage preservation. Indeed, still a number of issues are open to properly detect the variation of the dynamic characteristics and its meaning on the structural properties of the tower.

- *Confidence factors*

The uncertainties in the seismic risk assessment of masonry buildings have been usually taken into account by reducing material strength, according to a selected level of knowledge, by means the application of confidence factors. This approach for historic masonry constructions, proposed by several building codes, has considerable limitation, such as the lack of proper consideration of experimental data. In this framework, the results of the seismic vulnerability assessment, proposed in this dissertation in terms of fragility curves, could be used in order to fill this gap of knowledge related to the confidence factors definition for historic masonry towers.

- *Validation of the methodology*

As previously demonstrated, the focus of this thesis was on the role of the uncertainties in the seismic risk assessment of historical masonry towers, and the main attractive results are represented by quantification of the effect of the many uncertain parameters in the achievement of a certain damage level. In this respect, the results themselves can be considered as a guidance in the identification of the uncertain parameters affecting the final result in terms of seismic risk. Nevertheless, the application of the proposed methodology to a collapsed or strongly damaged tower, due to the seismic action, could represent an important validation of the methodology and a proof of the right numerical modelling strategies.

REFERENCES

[1] Lucchesi M, Pintucchi B. A numerical model for non-linear dynamic analysis of slender masonry structures. Eur J Mech A/Solids 2007;26:88–105. doi:10.1016/j.euromechsol.2006.02.005.

[2] Betti M, Galano L, Vignoli A. Finite element modelling for seismic assessment of historic masonry buildings. Earthquakes Their Impact Soc., 2016. doi:10.1007/978-3-319-21753-6_14.

[3] Leftheris BP, Stavroulaki ME, Sapounaki AC, Stavroulakis GE. Computation mechanics for heritage structures. Southampto. 2006.

[4] Corradi M, Borri A, Vignoli A. Strenghtening techinques tested on masonry structures struck by the Umbra-Marche earthquake of 1997-1998. Constr Build Mater 2002;16:229–39.

[5] Binda L, Saisi A, Tiraboschi C. Investigation procedures for the diagnosis of historic masonries. Constr Build Mater 2000;14:199–233. doi:10.1016/S0950-0618(00)00018-0.

[6] Lourenço PB. Computations on historic masonry structures. Prog Struct Engng Mater 2002;4:301–19. doi:10.1002/pse.120.

[7] Lourenço PB, Krakowiak KJ, Fernandes FM, Ramos LF. Failure analysis of monastery of Jero nimos, Lisbon: How to learn from sophisticated numerical models. Eng Fail Anal 2007;14:280–300.

[8] Lourenço PB, Pina-Henriques J. Validation of analytical and continum numerical methods for estimating te compressive strength of masonry. Comput Struct 2006;84:1977–89.

[9] DPCM. Direttiva del Presidente del Consiglio dei Ministri per la valutazione e riduzione del rischio sismico del patrimonio culturale con riferimento alle norme techinche per le costruzioni di cui al decreto del Ministero delle infrastrutture e dei trasporti de 2011:G.U. 26/2/2011, No. 47 (In Italian).

[10] Lourenço PB. Assessment, diagnosis and strengthening of Outeiro Church, Portugal.

Constr Build Mater 2005;19:634–45.

[11] Romera LE, Hernandez S, Reinosa JM. Numerical characterization of the structural behaviour of the Basilica of Pilar in Zaragoza (Spain) Part 1: Global and local models. Adv Eng Softw 2008;39:301–14.

[12] Betti M, Vignoli A. Modelling and analysis of a Romanesque chirch under earthquake loading: assessment of seismic resistance. Eng Struct 2008;30:352–67.

[13] Taliercio A, Binda L. The Basilica of San Vitale in Ravenna: investigation on the current structural faults and their mid-term evolution. J Cult Herit 2008;8:99–118.

[14] Betti M, Bartoli G, Orlando M. Evaluation study on structural fault of a Reinassance Italian Palace. Eng Struct 2010;32:1801–13.

[15] Casolo S, Milani G. Simplified out-of-plane modelling of three-leaf masonry walls accounting for the material texture. Constr Build Mater 2013;40:330–51. doi:10.1016/j.conbuildmat.2012.09.090.

[16] Casolo S. A three-dimensional model for vulnerability analysis of slender medieval masonry towers. J Earthq Eng 1998;2:487–512. doi:10.1080/13632469809350332.

[17] Cerioni R, Brighenti R, Donida G. Use of incompatible displacement modes in a finite element model to analyse the dynamic behaviour of unreinforced masonry panels. Comput Struct 1995;57:47–57.

[18] Giannini R, Pagnoni T, Pinto PE, Vanzi I. Risk analysis of a medieval tower before and after strengthening. Struct Saf 1996;18:81–100. doi:10.1016/0167-4730(96)00007-0.

[19] Modena C, Valluzzi MR, Tongini Folli R, Binda L. Design choices and intervention techniques for repairing and strengthening of the Monza cathedral bell tower. Constr Build Mater 2002;16:385–95.

[20] Acito M, Bocciarelli M, Chiesi C, Milani G. Collapse of the clock tower in Finale Emilia after the May 2012 Emilia Romagna earthquake sequence: numerical insight. Eng Struct 2014;72:70–91.

[21] Tiberti S, Acito M, Milani G. Comprehensive FE numerical insight into Finale Emilia Castle behavior under 2012 Emilia Romagna seismic sequence: Damage causes and seismic vulnerability mitigation hypothesis. Eng Struct 2016;117:397–421. doi:10.1016/j.engstruct.2016.02.048.

[22] Salvatore W, Bennati S, Della Maggiora M. On the collapse of a masonry tower subjected to earthquake loadings. Adv Earthq Eng 2003;13:141–55.

[23] Casolo S, Milani G, Uva G, Alessandri C. Comparative seismic vulnerability analysis on ten masonry towers in the coastal Po Valley in Italy. Eng Struct 2013;49:465–90. doi:10.1016/j.engstruct.2012.11.033.

[24] Pintucchi B, Zani N. Effectiveness of nonlinear static procedures for slender masonry towers. Bull Earthq Eng 2014;12:2531–56. doi:10.1007/s10518-014-9595-z.

[25] Bongiovanni G, Clemente P, Buffarini G. Analysis of the Seismic Response of A Damaged Masonry Bell Tower. Proc 12th World Conf Earthq Eng Auckland, New Zeal 2000;Paper No.:2–9.

[26] Bonato P, Ceravolo R, De Stefano A, Molinari F. Cross-Time Frequency Techniques for

the Identification of Masonry Buildings. Mech Syst Signal Process 2000;14:91–109. doi:10.1006/mssp.1999.1273.

[27] Ivorra S, Pallarés FJ. Dynamic investigations on a masonry bell tower. Eng Struct 2006;28:660–7. doi:10.1016/j.engstruct.2005.09.019.

[28] Bartoli G, Betti M, Spinelli P, Tordini B. An " innovative " procedure for assessing the seismic capacity of historical tall buildings : the " Torre Grossa " masonry tower 2006.

[29] Cosenza E, Iervolino I. Case Study: Seismic Retrofitting of a Medieval Bell Tower with FRP. J Compos Constr 2007;11:319–27. doi:10.1061/(ASCE)1090-0268(2007)11:3(319).

[30] Peña F, Lourenço PB, Mendes N, Oliveira D V. Numerical models for the seismic assessment of an old masonry tower. Eng Struct 2010;32:1466–78. doi:10.1016/j.engstruct.2010.01.027.

[31] Ivorra S, Cervera JR. Analysis of the dynamic actions when bells are swinging on the bell tower of Bonreposi Mirambell Church (Valencia, Spain). 3rd Int. Semin. Hist. Constr., Guimarães, Portugal: 2001.

[32] Bennati S, Nardini L, Salvatore W. Dynamic Behavior of a Medieval Masonry Bell Tower. Part II: Measurement and Modeling of the Tower Motion. J Struct Eng 2005;131:1647–55. doi:10.1061/(ASCE)0733-9445(2005)131:11(1647).

[33] Gentile C, Saisi A. Ambient vibration testing of historic masonry towers for structural identification and damage assessment. Constr Build Mater 2007;21:1311–21. doi:10.1016/j.conbuildmat.2006.01.007.

[34] Júlio ENBS, da Silva Rebelo CA, Dias-da-Costa DASG. Structural assessment of the tower of the University of Coimbra by modal identification. Eng Struct 2008;30:3468–77. doi:10.1016/j.engstruct.2008.06.001.

[35] Bayraktar A, Türker T, Sevim B, Altunişik AC, Yildirim F. Modal parameter identification of Hagia Sophia bell-tower via ambient vibration test. J Nondestruct Eval 2009;28:37–47. doi:10.1007/s10921-009-0045-9.

[36] Casciati S, Al-Saleh R. Dynamic behavior of a masonry civic belfry under operational conditions. Acta Mech 2010;215:211–24. doi:10.1007/s00707-010-0343-4.

[37] Ramos LF, Marques L, Lourenço PB, De Roeck G, Campos-Costa A, Roque J. Monitoring historical masonry structures with operational modal analysis: Two case studies. Mech Syst Signal Process 2010;24:1291–305. doi:10.1016/j.ymssp.2010.01.011.

[38] Ivorra S, Pallarés FJ, Adam JM, Tomás R. An evaluation of the incidence of soil subsidence on the dynamic behaviour of a Gothic bell tower. Eng Struct 2010;32:2318–25. doi:10.1016/j.engstruct.2010.04.007.

[39] Carone AS, Foti D, Giannoccaro NI, Nobile R. Non-desctructive characterization and dynamic identification of an hisotrical bell tower 2013;1:1–16.

[40] Pieraccini M, Dei D, Betti M, Bartoli G, Tucci G, Guardini N. Dynamic identification of historic masonry towers through an expeditious and no-contact approach: Application to the "Torre del Mangia" in Siena (Italy). J Cult Herit 2014;15:275–82. doi:10.1016/j.culher.2013.07.006.

[41] Lancellotta R, Sabia D. Identification Technique for Soil-Structure Analysis of the

Ghirlandina Tower. Int J Archit Herit 2015;9:391–407. doi:10.1080/15583058.2013.793438.

[42] Ferraioli M, Mandara A, Miccoli L. Dynamic identification and seismic safety of masonry bell towers 2010.

[43] Ceriotti M, Mottola L, Picco GP, Murphy a. L, Guna S, Corra M, et al. Monitoring heritage buildings with wireless sensor networks: The Torre Aquila deployment. 2009 Int Conf Inf Process Sens Networks 2009:277–88. doi:10.1145/1602165.1602191.

[44] Russo G, Bergamo O, Damiani L, Lugato D. Experimental analysis of the "Saint Andrea" Masonry Bell Tower in Venice. A new method for the determination of "Tower Global Young's Modulus E." Eng Struct 2010;32:353–60. doi:10.1016/j.engstruct.2009.08.002.

[45] Colapietro D, Fiore A, Netti A, Fatiguso F, Marano GC, Fino M De, et al. Dynamic Identification and Evaluation of the Seismic Safety of a Masonry Bell Tower in the South of Italy 2013:12–4.

[46] Gentile C, Saisi A. Operational modal testing of historic structures at different levels of excitation. Constr Build Mater 2013;48:1273–85. doi:10.1016/j.conbuildmat.2013.01.013.

[47] Bartoli G, Betti M, Giordano S. In situ static and dynamic investigations on the " Torre Grossa" masonry tower. Eng Struct 2013;52:718–33. doi:10.1016/j.engstruct.2013.01.030.

[48] Diaferio M, Foti D, Giannocaro NI. Non-destructive characterization and identification of the modal parameters of an old masonry tower. EESMS 2014 - 2014 IEEE Work Environ Energy Struct Monit Syst Proc 2014:57–62. doi:10.1109/EESMS.2014.6923265.

[49] Bassoli E, Vincenzi L, Bovo M, Mazzotti C. Dynamic identification of an ancient masonry bell tower using a MEMS-based acquisition system. 2015 IEEE Work Environ Energy, Struct Monit Syst EESMS 2015 - Proc 2015:226–31. doi:10.1109/EESMS.2015.7175882.

[50] Gentile C, Guidobaldi M, Saisi A. Structural health monitoring of a historic masonry tower. 2015 IEEE Work Environ Energy, Struct Monit Syst Proc 2015:168–73. doi:10.1109/EESMS.2015.7175872.

[51] Ubertini F, Cavalagli N, Materazzi AL, Ubertini F, Comanducci G, Cavalagli N. Automated post-earthquake damage detection in a monumental bell tower by continuous dynamic monitoring Vibration-based structural health monitoring of a historic bell-tower using output-only measurements and 2017. doi:10.1177/1475921716643948.

[52] Bartoli G, Betti M, Pintucchi B. Effects of damage on dynamic modal properties of masonry towers. XVII Convegno ANIDIS - L'ingegneria sismica Ital., 2017.

[53] Gentile C, Saisi A, Cabboi A. One-year dynamic monitoring of a masonry tower. Struct Anal Hist Constr 2012;3:1–8. doi:10.1051/matecconf/20152405003.

[54] Castellazzi G, D'Altri AM, de Miranda S, Ubertini F. An innovative numerical modeling strategy for the structural analysis of historical monumental buildings. Eng Struct 2017;132:229–48. doi:10.1016/j.engstruct.2016.11.032.

[55] Ceravolo R, Pistone G, Zanotti Fragonara L, Massetto S, Abbiati G. Vibration-Based monitoring and diagnosis of cultural heritage: a methodological discussion in three

examples. Int J Archit Herit 2016;10:375–95.

[56] Baraccani S, Palermo M, Silvestri S, Gasparini G, Trombetti T. SSHM and DSHM for a better knowledge and risk prevention of historical buildings: two cases of the two towers in Bologna and the Cathedral in Modena. Int. Work. Environ. energy Struct. Monit. Syst., 2015.

[57] Marra AM, Salvatori L, Spinelli P, Bartoli G. Incremental Dynamic and Nonlinear Static Analyses for Seismic Assessment of Medieval Masonry Towers 2016:1–10. doi:10.1061/(ASCE)CF.1943-5509.0001022.

[58] Gentile C, Saisi A, Cabboi A. One-year dynamic monitoring of a masonry tower. Struct Anal Hist Constr 2012. doi:10.1051/matecconf/20152405003.

[59] Salvatori L, Marra AM, Bartoli G, Spinelli P. Probabilistic seismic performance of masonry towers: General procedure and a simplified implementation. Eng Struct 2015;94:82–95. doi:10.1016/j.engstruct.2015.02.017.

[60] Rota M, Penna A, Magenes G. A methodology for deriving analytical fragility curves for masonry buildings based on stochastic nonlinear analyses. Eng Struct 2010;32:1312–23. doi:10.1016/j.engstruct.2010.01.009.

[61] Collins JD, Hart GC, Hasselman TK, Kennedy B. Statistical identification of structures. AIAA J 1974;12:185–90.

[62] Beck JL, Katafygiotis LS. Updating models and their uncertainties. i: Bayesian statistical framework. J Eng Mech 1998.

[63] Papadimitriou C, Beck JL, Katafygiotis LS. Updating robust reliability using structural test data. Probabilistic Eng Mech 2001;16:103–13. doi:10.1016/S0266-8920(00)00012-6.

[64] Beck JL, Au SK. Bayesian Updating of Structural Models and Reliability using Markov Chain Monte Carlo Simulation. J Eng Mech 2002;128:380–91. doi:10.1061/(ASCE)0733-9399(2002)128:4(380).

[65] Cheung SH, Beck JL. Simulation with Application to Structural Dynamic Models with Many Uncertain Parameters 2009;135:243–55.

[66] Cheung SH, Bansal S. A new Gibbs sampling based algorithm for Bayesian model updating with incomplete complex modal data. Mech Syst Signal Process 2017;92:156–72. doi:10.1016/j.ymssp.2017.01.015.

[67] Goller B, Schu??ller GI. Investigation of model uncertainties in Bayesian structural model updating. J Sound Vib 2011;330:6122–36. doi:10.1016/j.jsv.2011.07.036.

[68] Vanik M., Beck JL, Au SK. Bayesian probabilistic approach to structural health monitoring. J Eng Mech 2000;126:738–45.

[69] Green PL, Cross EJ, Worden K. Bayesian system identification of dynamical systems using highly informative training data. Mech Syst Signal Process 2015;56:109–22. doi:10.1016/j.ymssp.2014.10.003.

[70] Giannini R, Sguerri L, Paolacci F, Alessandri S. Assessment of concrete strength combining direct and NDT measures via Bayesian inference. Eng Struct 2014;64:68–77. doi:10.1016/j.engstruct.2014.01.036.

[71] Ramos LF, Miranda T, Mishra M, Fernandes FM, Manning E. A Bayesian approach for

NDT data fusion: The Saint Torcato church case study. Eng Struct 2015;84:120–9. doi:10.1016/j.engstruct.2014.11.015.

[72] Jalayer F, Iervolino I, Manfredi G. Structural modeling uncertainties and their influence on seismic assessment of existing RC structures. Struct Saf 2010;32:220–8. doi:10.1016/j.strusafe.2010.02.004.

[73] Bracchi S, Rota M, Magenes G, Penna A. Seismic assessment of masonry buildings accounting for limited knowledge on materials by Bayesian updating. Bull Earthq Eng 2016;14:2273–97. doi:10.1007/s10518-016-9905-8.

[74] Structures E, Mishra S, Technologies A. Hurricane loss estimation in wood-frame buildings using Bayesian model updating : Assessing uncertainty in fragility ... 2017. doi:10.1016/j.engstruct.2016.12.063.

[75] Choe D, Gardoni P, Asce M, Rosowsky D, Asce M. Closed-Form Fragility Estimates , Parameter Sensitivity , and Bayesian Updating for RC Columns 2007;133:833–43.

[76] Kouris LAS. Seismic fragility curves for timber-framed masonry structures based on empirical damage data. Int J Sustain Mater Struct Syst 2016;2:233. doi:10.1504/IJSMSS.2016.078715.

[77] Zhong J, Gardoni P, Rosowsky D. Bayesian updating of seismic demand models and fragility estimates for reinforced concrete bridges with two-column bents. J Earthq Eng 2009;13:716–35. doi:10.1080/13632460802421334.

[78] Bakhshi A, Asadi P. Probabilistic evaluation of seismic design parameters of RC frames based on fragility curves. Sci Iran 2013;20:231–41. doi:10.1016/j.scient.2012.11.012.

[79] Porto F, Tecchio G, Dona M. Seismic fragility curves of as-built single-span masonry arch bridges ` 1 • 2016. doi:10.1007/s10518-016-9931-6.

[80] Matos JC, Cruz PJS, Valente IB, Neves C., Moreira VN. An innovative framework for probabiulistic-based structural assessment with an application to existing reinforced concrete structures. Eng Struct 2016;111:552–64.

[81] Au SK, Beck JL. A new adaptive importance sampling scheme for reliability calculations. Struct Saf 1999;21:135–58. doi:10.1016/S0167-4730(99)00014-4.

[82] Ã IP, Amarchinta HK, Grandhi R V. A Bayesian approach for quantification of model uncertainty. Reliab Eng Syst Saf 2010;95:777–85. doi:10.1016/j.ress.2010.02.015.

[83] Rota M, Penna A, Strobbia C. Typological Fragility Curves From Italian Earthquake Damage Data. … Conf Earthq … 2006:3–8.

[84] Liel AB, Haselton CB, Deierlein GG, Baker JW. Incorporating modeling uncertainties in the assessment of seismic collapse risk of buildings. Struct Saf 2009;31:197–211. doi:10.1016/j.strusafe.2008.06.002.

[85] Zonta D, Pozzi M. Managing the Historical Heritage Using Distributed Technologies 2008. doi:10.1080/15583050802063691.

[86] Beconcini ML, Croce P, Marsili F, Muzzi M, Rosso E. Probabilistic reliability assessment of a heritage structure under horizontal loads. Probabilistic Eng Mech 2016;45:198–211. doi:10.1016/j.probengmech.2016.01.001.

[87] Miranda TFS. Geomechanical parameters evaluation in underground structures : artificial

intelligence, bayesian probabilities and inverse methods. Dep Civ Enginnering 2007;{PhD} thes.

[88] Conte JP, Astroza R, Ebrahimian H. bayesian methods for nonlinear system identifications of civil structures. MATEC web Conf., 2015.

[89] Marsili F, Friedman N, Croce P, Formichi P, Landi F. On Bayesian Identification Methods for the Analysis of Existing Structures The Bayesian Approach to the stochastic Inverse Problem 2016:21–3.

[90] Mishra M, Ramos L, Miranda T. Bayesian approach to fuse NDT data to find Dynamic Elastic Modulus of granite Stone. 9th Int Mason Conf 2014 Guimarães 2014:3–9.

[91] Salvatori L, Marra AM, Bartoli G, Spinelli P. Probabilistic seismic performance of masonry towers: General procedure and a simplified implementation. Eng Struct 2015;94:82–95. doi:10.1016/j.engstruct.2015.02.017.

[92] Campostrini GP, Taffarel S, Bettiol G, Valluzzi MR, Da Porto F, Modena C. A Bayesian approach to rapid seismic vulnerability assessment at urban scale. Int J Archit Herit 2017;3058:1–11. doi:10.1080/15583058.2017.1370506.

[93] Milani G, Casolo S, Naliato A, Tralli A. Seismic Assessment of a Medieval Masonry Tower in Northern Italy by Limit, Nonlinear Static, and Full Dynamic Analyses. Int J Archit Herit 2012;6:489–524. doi:10.1080/15583058.2011.588987.

[94] Bartoli G, Betti M, Monchetti S. Seismic Risk Assessment of Historic Masonry Towers : Comparison of Four Case Studies 2016:1–16. doi:10.1061/(ASCE)CF.1943-5509.0001039.

[95] Faccio P, Podestà S, Saetta A. Venezia, Campanile della Chiesa di Sant'Antonio, Esempio 5. Linee guid, 2009.

[96] Rainieri C, Fabbrocino G. Estimating the elastic period of masonry towers. Conf Proc Soc Exp Mech Ser 2012;5:243–8. doi:10.1007/978-1-4614-2425-3_22.

[97] Shakya M, Varum H, Vicente R. Predictive Formulation for the Estimation of the Fundamental Frequency of Slender Masonry Structures 2011;3058:3–5. doi:10.1080/15583058.2014.951796.

[98] Fabbrocino F. Estimation of the natural periods of existing masonry towers through empirical procedure 2016;2:250–61.

[99] Giorgi L, Matracchi P. Architectural Evolution : Modifications , Alterations , and Restorations through Centuries 2014:1–10. doi:10.1061/(ASCE)CF.1943-5509.0001014.

[100] Tucci G, Bonora V, Ph D. Towers in San Gimignano : Metric Survey Approach 2018;31. doi:10.1061/(ASCE)CF.1943-5509.0001085.

[101] Pieraccini M, Dei D, Mecatti D, Parrini F. Dynamic testing of historic towers using an interferometric radar from an unstable measurement position. J Nondestruct Eval 2013;32:398–404. doi:10.1007/s10921-013-0193-9.

[102] Pieraccini M. Extensive Measurement Campaign Using Interferometric Radar n.d.:1–7. doi:10.1061/(ASCE)CF.1943-5509.0000987.

[103] Lunedei E, Peruzzi G, Albarello D. Ambient Vibrations in Seismic Studying the Unesco Cultural Heritage Site of San Gimignano (Italy) n.d.:3–5.

[104] Donà C, De Maria A. Manuale delle murature storiche - Analisi e valutazione del comportamento strutturale - schede operative per gli interventi di restauro strutturale. DEI, Tipografia del Genio Civile, Roma; 2011.

[105] Manfredi G, Dolce M. The state of earthquake engineering research in Italy: The ReLUIS-DPC 2005-2008 project. Dipartimento della Protezione Civile, Roma (in Italian); 2009.

[106] Tomaszewska A, Szymczak C. Identification of the Vistula Mounting tower model using measured modal data. Eng Struct 2012;42:342–8.

[107] Kohan PH, Nallim LG, Gea SB. Dynamic characterization of beam type structures: Analytical, numerical and experimental applications. Appl Acoust 2011;72:975–81. doi:10.1016/j.apacoust.2011.06.007.

[108] Ceroni F, Pecce M, Manfredi G. Seismic Assessment of the Bell Tower of Santa Maria Del Carmine: Problems and Solutions. J Earthq Eng 2009;14:30–56. doi:10.1080/13632460902988968.

[109] Zonta D, Zanon P, Toffaletti MMS. Aggiornamento della vulnerabilità sismica della Torre Civica di Portogruaro basato su misure vibrazionali 2004.

[110] Valluzzi MR, Porto FDA, Casarin F, Monteforte N. A contribution to the characterization of masonry typologies by using sonic waves investigations Résumé Keywords Masonry and building typologies 2009.

[111] Castellacci I, Spinelli P, Vignoli A, Galano L. Caratterizzazione dinamica del campanile della pieve di San Cresci a Macioli nei pressi di Pratolino, comune di Vaglia, e progetto di miglioramento sismico. Boll Degli Ing 2007;10:21–3.

[112] Abruzzese D, Vari A. Vulnerabilità sismica di torri medievali in muratura 2004.

[113] NTC Norme Tecniche per le Costruzioni. D.M. del ministero delle infrastrutture e dei trasporti del 14/01/2008. Nuove norme tecniche per le costruzioni 2008:G.U. 04/02/2008, No. 29 (In Italian).

[114] NCSE Norma de Construcciòn Sismorresistente - Parte General y Edificaciòn 2002:Madrid, Spain (in Spanish).

[115] L. S. Katafygiotis; J. L. Beck. Updating models and their uncertainies II: model identifiability. J Eng Mech 1998;124(4):463–7. doi:10.1061/(ASCE)0733-9399(1998)124:4(455).

[116] Ivorra S, Brotóns V, Foti D, Diaferio M. A preliminary approach of dynamic identification of slender buildings by neuronal networks. Int J Non Linear Mech 2016;80:183–9. doi:10.1016/j.ijnonlinmec.2015.11.009.

[117] CNR Consiglio Nazionale delle Ricerche. Istruzioni per la valutazione affidabilistica della sicurezza sismica di edifici esistenti 2013.

[118] Madiai C, Renzi S, Ph D, Vannucchi G. Geotechnical Aspects in Seismic Soil – Structure Interaction of San Gimignano Towers : Probabilistic Approach 1999:1–14. doi:10.1061/(ASCE)CF.1943-5509.0001041.

[119] Casolo S, Diana V, Uva G. Influence of soil deformability on the seismic response of a masonry tower. Bull Earthq Eng 2017;15:1991–2014. doi:10.1007/s10518-016-0061-y.

[120] Da Porto F, Guidi G, Garbin E, Modena C. In-plane behaviour of clay masonry walls:

Experimental testing and finite-element modeling. J Struct Eng 2010;136:1379–92.

[121] Gambarotta L, Lagomarsino S. Damage models for the seismic response of a brck masonry shear walls. Part I: the mortar joint model and its application. Earthq Eng Struct Dyn 1997;26:423–39.

[122] ANSYS Inc. ANSYS manual 1998.

[123] Drucker D, Prager W. Soil mechanics and plastic analysis or limit deisgn. Q Appl Math 1952;10:157–65.

[124] Valente M, Milani G. Seismic assessment of historical masonry towers by means of simplified approaches and standard FEM. Constr Build Mater 2016;108:74–104. doi:10.1016/j.conbuildmat.2016.01.025.

[125] Zucchini A, Lourenço PB. A micro-mechanical model for the homogenisation of masonry. Int J Solids Struct 2007;39:3233–55.

[126] Cividini A. Constitutive behaviour and numerical modelling. Compr Rock Eng n.d.;1:395–426.

[127] William KJ, Warnke ED. Constitutive model for the triaxial behaviour of concrete. Int. Assoc. Bridg. Struct. Eng., Bergamo, Italy: 1975.

[128] Chiostrini S, Galano L, Vignoli A. In situ shear and compression tests in ancient stone masonry walls of Tuscany, Italy. ASTM J Test Eval 2003;31:289–304.

[129] Casolo S, Milani G, Uva G, Alessandri C. Comparative seismic vulnerability analysis on ten masonry towers in the coastal Po Valley in Italy. Eng Struct 2013;49:465–90. doi:10.1016/j.engstruct.2012.11.033.

[130] Casolo S, Uva G. Seismic vulnerability assessment of masonry towers: full nonlinear dynamics vs pushover analyses. COMPDYN, ECCOMAS Themat. Conf. Comput. methods Struct. Dyn. Earthq. Eng., 2011.

[131] Freeman SA, Nicoletti JP, Tyrell JV. Evaluations of existing buildings for seismic risk - a case study of Puget Sound Naval Shipyard, Bremerton, Washington. 1st U.S. Natl. Conf. Earthq. Eng. EERI, 1975, p. 113–22.

[132] Freeman SA. Development and use of capacity spectrum method. 6th U.S. Natl. Conf. Earthq. Eng., Seattle: 1998.

[133] Isukapalli SS, Roy A, Georgopoulos PG. Stochastic response surface methods (SRSMs) for uncertainty propagation: Application to environmental and biological systems. Risk Anal 1998;18:351–63. doi:10.1111/j.1539-6924.1998.tb01301.x.

[134] Youn BD, Choi KK. A new response surface methodology for reliability-based design optimization. Comput Struct 2004;82:241–56. doi:10.1016/j.compstruc.2003.09.002.

[135] Yang M, You H, Jia X, Wang D. An Effective Method to Extract Probability Distribution of Circuit Performance Modeled by Quadratic Response Surface Model. 2008 Int Symp Inf Sci Eng 2008:600–3. doi:10.1109/ISISE.2008.212.

[136] Gupta S, Manohar CS. An improved response surface method for the determination of failure probability and importance measures. Struct Saf 2004;26:123–39. doi:10.1016/S0167-4730(03)00021-3.

[137] Zheng Y, Das PK. Improved response surface method and its application to stiffened plate reliability analysis. Eng Struct 2000;22:544–51. doi:10.1016/S0141-0296(98)00136-9.

[138] Moehle J, Deierlein GG. A framework methodology for performance-base earthquake engineering. 13th World Conf. Earthq. Eng., 2004.

[139] Porter KA, Beck JL, Shaikhutdinov R V. Sensitivity of building loss estimates to major uncertain variables. Earthq Spectra 2002;18:719–43. doi:10.1193/1.1516201.

[140] Ibarra LF, Krawinkler H. Global Collapse of Frame Structures under Seismic Excitations. Evaluation 2005:1–301. doi:10.1002/eqe.

[141] Lee TH, Mosalam KM. Seismic demand sensitivity of reinforced concrete shear-wall building using FOSM method. Earthq Eng Struct Dyn 2005;34:1719–36. doi:10.1002/eqe.506.

[142] Baker JW, Cornell CA. Uncertainty propagation in probabilistic seismic loss estimation. Struct Saf 2008;30:236–52. doi:10.1016/j.strusafe.2006.11.003.

[143] Vamvatsikos D, Fragiadakis M. Incremental dynamic analysis for estimating seismic performance sensitivity and uncertainty. Earthq Eng Struct Dyn 2010;39:141–63.

[144] Dolsek M. Incremental dynamic analysis with consideration of modelingg uncertainties. Earthq Eng Struct Dyn 2009;38:805–25.

[145] Asteris PG. On the Structural Analysis and Seismic Protection of Historical Masonry Structures. Open Constr Build Technol J 2008;2:124–33. doi:10.2174/1874836800802010124.

[146] Barbieri G, Biolzi L, Bocciarelli M, Fregonese L, Frigeri A. Assessing the seismic vulnerability of a historical building. Eng Struct 2013;57:523–35. doi:10.1016/j.engstruct.2013.09.045.

[147] Asteris PG, Chronopoulos MP, Chrysostomou CZ, Varum H, Plevris V, Kyriakides N, et al. Seismic vulnerability assessment of historical masonry structural systems. Eng Struct 2014;62–63:118–34. doi:10.1016/j.engstruct.2014.01.031.

[148] Cornell CA. Hazard analysis, ground motions and probabilistic assessment for PBSD. Int. Work. performance-bades Des., Bled, Slovenia: 2004.

[149] FEMA. HAZUS, earthquakes loss estimation methodology 1999.

[150] RISK-UE. The European risk-Ue project: an advanced approach to earthquake risk scenarios n.d.